UNIVERSIDAD AUTÓNOMA DE MADRID

Programa de Doctorado en Biociencias Moleculares

MOLECULAR MECHANISMS THAT PREVENT DNA RE-REPLICATION

Sergio Muñoz Sánchez

Doctoral thesis

Madrid, 2017

DEPARTMENT OF MOLECULAR BIOLOGY
FACULTY OF SCIENCES
UNIVERSIDAD AUTÓNOMA DE MADRID

MOLECULAR MECHANISMS THAT PREVENT DNA RE-REPLICATION

Sergio Muñoz Sánchez
Graduate in Biochemistry

Thesis Director: Dr. Juan Méndez Zunzunegui
Centro Nacional de Investigaciones Oncológicas (CNIO)

Madrid, 2017

cnio
Centro Nacional
de Investigaciones
Oncológicas

El abajo firmante, **Juan Méndez Zunzunegui**, Investigador responsable del Grupo de Replicación de DNA, Programa de Oncología Molecular, Centro Nacional de Investigaciones Oncológicas (CNIO),

CERTIFICA:

Que D. **Sergio Muñoz Sánchez**, Licenciado en Bioquímica por la Universidad Autónoma de Madrid (UAM) y estudiante de Doctorado en el programa de Biociencias Moleculares de dicha Universidad, ha realizado bajo mi dirección la Tesis Doctoral que lleva por título: "**Molecular mechanisms that prevent DNA re-replication**". Considero que esta Tesis reúne todos los requisitos necesarios para su presentación y defensa en la UAM.

En Madrid, 28 de marzo de 2017

Juan Méndez, PhD

tel +34 917 328 000 ext 3490
fax +34 917 328 033
jmendez@cnio.es

FINANCIACIÓN

La investigación ha sido financiada por los siguientes proyectos del Ministerio de Economía y Competitividad: Consolider CSD2007-00015, BFU2010-21467, BFU2013-49153-P, así como una beca del Plan de Formación de Personal Investigador (FPI).

AGRADECIMIENTOS

En primer lugar quiero dar las gracias Juan Méndez. Gracias por acogerme en tu grupo, por la supervisión del trabajo científico, por las discusiones y las conversaciones (científicas o no), por los consejos, por la ayuda en las presentaciones, en la redacción de artículos y la propia tesis, por lo aprendido durante estos años, por el tiempo dedicado y el apoyo prestado. Gracias.

En segundo lugar quiero agradecérselo a todos los compañeros y amigos con los que he compartido este tiempo; tanto del grupo de Replicación como del grupo de Dinámica Cromosómica. Quiero agradeceros vuestra ayuda y apoyo, vuestras aportaciones y todo lo que he aprendido de vosotros. Pero también quiero agradeceros las risas, los buenísimos momentos y todo lo que he disfrutado junto a vosotros. Karol, Sara, Marcos, Dani, Sabe, Silvia, Silvana, Blanca, Miguel, Alek, Magali, Carmen, Miry, Ana, Sam, María y todos los demás; gracias a vosotros, acudir cada mañana al laboratorio siempre fue un placer, nunca una obligación. Sinceramente, no imagino mejor grupo de compañeros que vosotros.

En especial quiero dar las gracias a tres personas porque, además de todo lo dicho, han trabajado directamente en los proyectos aquí expuestos. A Sabela Búa, por todo el trabajo con los ratones de CDC6 y CDT1. Un proyecto que hemos compartido y desarrollado en estrecha colaboración. Tu trabajo ha sido esencial e imprescindible. A Sara Rodríguez, por enseñarme la técnica de las fibras de ADN y porque aquí se muestran experimentos que has cuantificado personalmente (mas todos en los que has ayudado, los que has supervisado, comprobado y recomprobado, y porque sin tu ayuda aquí no habría fibras). Pero también quiero agradecerte todos esos consejos valiosísimos que me han permitido seguir avanzando. Y a Daniel González, que en el proyecto de RAD51, también has resultado fundamental ayudándome con los experimentos, ejecutando personalmente varios de ellos y en definitiva participando activamente en la realización de este trabajo.

Quiero darle las gracias a Ana Losada, también he aprendido mucho este tiempo gracias a ti. Como con Juan, siempre he valorado mucho tu opinión y tus consejos, que realmente me han ayudado durante este periodo y seguro me seguirán ayudando.

A las Unidades Técnicas del CNIO, Microscopía Confocal, Citometría, Animales Transgénicos, Patología Comparada y al equipo del Animalario. También ellos forman parte de esta tesis. Especialmente a aquellos con los que he trabajado más directamente: Jesús, Ximo, Manu y Diego de Confocal, por los *screenings* y las cuantificaciones. Miguel Ángel, Ultan y Lola de Citometría, por los ciclos y los *sortings*. María y Alba de Histopatología; a María por su enorme trabajo realizado con las tinciones y sus cuantificaciones, a Alba por la precisa descripción histológica. A Soraya del Animalario, por cuidar de nuestros ratones. También he de dar las gracias al Dr. Patrick Sung de la Universidad de Yale, que nos facilitó amablemente los mutantes de RAD51.

Personalmente, quiero agradecérselo a mis amigos. Primero a mis amigos de toda la vida, Sorry, Esther, Topo, Alba, Pablo y Lerma. Muchas gracias por estar ahí, por vuestro apoyo constante y vuestra amistad. A todos los demás, que pese a haberos conocido después, sois igual de importantes, igual de necesarios, igualmente amigos. A mis amigos de la universidad, a todos ellos, pero especialmente a Miguel y Elena que han tenido que soportar algunas de las penas de esta tesis, gracias por escucharme.

A toda mi familia. Por vuestro apoyo y vuestro cariño. Por estar conmigo, antes, ahora y siempre. Por ser como sois. Por ser parte de mi.

A las cuatro personas más importantes de mi vida, mi hermano, mis padres, y mi mujer. A mi hermano; mi mejor amigo y compañero. Por los ánimos y la comprensión, por preocuparte por mí, por ser un buen hermano. Gracias tío. A mis padres; mi ejemplo, y mi soporte. Gracias por enseñarme a pensar, a trabajar y a esforzarme. Por no dejar que me rinda, por aguantarme, valorarme y apoyarme. Por quererme. Esto es para vosotros.

Y a Blanquita. Mi preciosa, mi alegría y mi amor. Te quiero. Sin ti nada sería posible. Gracias por estar a mi lado, gracias por ayudarme y darme fuerzas, por aceptarme, por entenderme, por hacerme mejor. Gracias por compartir tu vida conmigo. Contigo todo merece la pena. Gracias.

A Blanquita.
A mis padres y mi hermano.

ABSTRACT

PRESENTACIÓN

ABSTRACT

DNA replication must be precisely regulated to ensure faithful inheritance of genetic information. In mammalian cells, the process of genomic duplication starts from thousands of replication origins. During G1, the Origin Recognition Complex (ORC), CDC6 and CDT1 proteins cooperate to engage the MCM helicase complex at the origins. This process is called 'origin licensing' and renders cells competent to initiate DNA replication in the subsequent S phase. After the S phase starts, initiator proteins are inhibited to prevent origin re-licensing and reactivation. If this control is overridden, cells undergo aberrant DNA re-replication, which causes DNA damage, genomic instability and even cell death. The effects of DNA re-replication have been mainly studied in cells in culture, but not in mammalian organisms *in vivo*.

In the first part of this Thesis we have studied the consequences of CDC6 and CDT1 deregulated expression in mice. We have identified a limiting role for CDC6 in origin licensing and activity. We have also found that both CDC6 and CDT1 need to be overexpressed in combination to induce re-replication in primary MEFs and adult tissues. Highly proliferative cells, including embryonic stem cells and hematopoietic precursors showed a marked susceptibility to CDT1 overexpression, which correlated with high expression of endogenous CDC6. In the mouse, DNA re-replication caused severe tissue dysplasias that become lethal in less than 2 weeks.

In the second part of the Thesis we have carried out a genetic screening to find new mechanisms that control the extent of re-replication caused by origin refiring. We have identified FBH1 and RAD51 as members of a new pathway that limits this aberrant process. RAD51 binds to chromatin in S phase and acts as a molecular brake to hinder progression of re-replication forks. This role depends on the binding of RAD51 to DNA around the origins but is independent of homologous recombination. Finally, we have found that MRE11 nuclease might be also involved in this process by catalyzing the resection of re-replicated DNA.

PRESENTACIÓN

A fin de asegurar la transmisión del material genético, la replicación del DNA está regulada de manera precisa para que ocurra una única vez en cada ciclo celular. En células de mamífero, la duplicación comienza en miles de puntos del genoma conocidos como 'orígenes de replicación'. En la fase G1, las proteínas iniciadoras ORC, CDC6 y CDT1 cooperan para 'cargar' la helicasa MCM en los orígenes, un proceso conocido como "licenciamiento". Tras el inicio de la fase S, estas proteínas son inhibidas para evitar la reactivación de orígenes que conduce a la re-replicación, un proceso aberrante que causa daños en el DNA, inestabilidad genómica y muerte celular. Los efectos de la re-replicación han sido muy estudiados en sistemas celulares, pero no en organismos mamíferos *in vivo*.

En la primera parte de esta Tesis se han estudiado las consecuencias de la sobre-expresión de las proteínas CDC6 y CDT1 en ratones. Hemos encontrado un papel limitante de CDC6 en el licenciamiento y la actividad de los orígenes. También hemos encontrado que la desregulación conjunta de CDC6 y CDT1 induce re-replicación en células primarias y algunos tejidos adultos. En células con alta tasa de proliferación, como las células madre embrionarias y los precursores hematopoyéticos, la sobre-expresión de CDT1 es suficiente para causar re-replicación, probablemente debido a sus elevados niveles endógenos de CDC6. *In vivo*, la re-replicación causa displasias en varios tejidos y resulta letal en menos de dos semanas.

En la segunda parte de la Tesis se ha desarrollado un *screening* genético para detectar nuevos mecanismos que bloqueen la re-replicación. FBH1 y RAD51 han sido identificados como componentes de una nueva vía que limita dicho proceso. RAD51 se une a la cromatina durante la fase S y actúa como 'freno molecular' para bloquear la progresión de las horquillas re-replicadas. Este papel depende de la unión de RAD51 al DNA pero es independiente de la recombinación homóloga. Además, la nucleasa MRE11 podría estar implicada en esta vía a través de la resección del DNA re-replicado.

TABLE OF CONTENTS

TABLE OF CONTENTS

ABBREVIATIONS

ABBREVIATIONS

Aph	Aphidicolin
ARS	Autonomously-replicating sequences
Asyn	Asynchronous
ATRi	ATR inhibitor
BIR	Break-induced replication
BM	Bone marrow
BrdU	5-bromo-2'-deoxyuridine
C1	CDT1
C6	CDC6
CDK	Cyclin-Dependent Kinase
ChIP	Chromatin immunoprecipitation
CldU	5-Chloro-2'-deoxyuridine
CMG	CDC45-GINS-MCM
Ctrl	Control
DAPI	4',6-diamidino-2-phenylindole
DDK	Dbf4-Dependent Kinase
DDR	DNA damage response
DDT	DNA damage tolerance
DMBA	7,12-dimethylbenz[α] anthracene
dNTP	Deoxyribonucleotide triphosphate
DSBs	Double strand breaks
dsDNA	double strand DNA
Dox	Doxycycline
EdU	5-Ethynyl-2'-deoxyuridine

ESCs	Embryonic stem cells
esiRNA	Endoribonuclease-prepared siRNAs
FA	Fanconi Anaemia
FACS	Fluorescence activated cell sorting
FBS	Foetal bovine serum
FC	Fold change
FL	Foetal liver
FR	Fork rate
G4	G-quadruplexes
GI	Gastrointestinal
H&E	Haematoxylin and Eosin
HR	Homologous recombination
HSCs	Hematopoietic stem cells
HTM	High-throughput microscopy
HU	Hydroxyurea
ICL	Inter-strand crosslink
IdU	5-Iodo-2’-deoxyuridine
IF	Immunofluorescence
IHC	Immunohistochemistry
IOD	Inter-origin distance
IP	Immunoprecipitation
iPOND	isolate proteins on nascent DNA
MEF	Mouse embryonic fibroblast
NAHR	Non-allelic homologous recombination
NER	Nucleotide excision repair

NHEJ	Non-homologous end-joining
ns	non significant
o/e	overexpression
PFA	Paraformaldehyde
PI	Propidium iodide
preIC	pre-Initiation complex
preRC	pre-Replicative complex
R26	Rosa 26 locus
RS	Replicative stress
rtTA	tetracycline-responsive element
RT-qPCR	Retrotranscription and quantitative PCR
shRNA	short hairpin RNA
siRNA	short interfering RNA
SNS	Short nascent strands
SSA	Single strand annealing
ssDNA	single strand DNA
Tg	Transgenic
Thy	Thymidine
TLS	Translesion synthesis
TMRE	Tetramethylrhodamine ethyl ester
TPA	12-O-tetradecanoylphorbol 13-acetate
TS	Template switching
UTR	Untranslated region
UV	Ultraviolet
WT	Wild type

INTRODUCTION

INTRODUCTION

DNA replication and replication origins

Proliferating cells duplicate their entire genome during the S phase of the cell cycle before each mitotic division. In eukaryotes, the process of genomic duplication starts from thousands of points in the genome called **replication origins**. A precise regulation over origin activity is required to maintain genomic stability and to ensure the faithful transmission of genetic information. Deregulated DNA replication has been linked to DNA damage, genomic instability and cancer (reviewed by Arias and Walter 2007; Blow and Gillespie, 2008; Hills and Diffley, 2014; Muñoz and Mendez, 2016).

Whereas in the budding yeast *Saccharomyces cerevisiae* replication origins are defined by specific, autonomously-replicating sequences (ARS) in the DNA, in higher eukaryotes, origins are rather defined by chromatin states and/or epigenetic marks (reviewed by Fragkos et al, 2015; Prioleau and MacAlpine, 2016). Origins may contain G-rich sequences (Cayrou et al, 2011; 2012; Besnard et al 2012) capable of forming G-quadruplexes (G4) that could influence nucleosome positioning (Cayrou et al; 2015) and/or be specifically recognized by **initiator proteins** (Hoshina et al, 2013; Keller et al, 2014).

Replication origin activation is also related to gene transcription (Cadoret et al, 2008). Indeed, replication origins have been identified at CpG islands and other gene regulatory elements with open chromatin structure. Several studies have shown a high correlation between replication origins and DNase I-accesible chromatin. Actually, it has been suggested that the strongest origins, i.e. those with higher probability of firing or those that are conserved in different cell types, are located at CpG islands and open chromatin structures (Cadoret et al, 2008; Miotto et al, 2016; Sequeira-Mendes et al, 2009; Besnard et al, 2012). In addition, replication origins and their surroundings are enriched in epigenetic marks corresponding to open chromatin, such as H3K9ac, H3K4me3, H3K79me2 and H3K20me2 (Fu et al 2013; Picard et al, 2014). It has been proposed that tethering the PR-Set7 methyltransferase to DNA is sufficient to define a new origin (Tardat et al, 2010). In contrast, other epigenetic marks such as H4 acetylation are not sufficient to define an origin, but could be related to origin efficiency (Miotto and Struhl, 2010).

Spatially, replication origins are organized in higher structures called "**replication factories**" (Nakamura et al, 1986; Jackson and Pombo, 1998; reviewed by Berezney et al, 2000). A replicon is defined as the length of DNA that is duplicated from a single origin, although other origins may exist and remain silent. Replication factories harbour a cluster of origins that activate synchronously (Huberman and Riggs, 1968; Berezney et al, 2000) and they can be visualized as discrete foci in the nucleus by the detection of nucleotide analogues incorporated onto newly synthesized DNA (Stubblefield, 1975). The cohesin complex plays a role in stabilizing the DNA loops between adjacent origins in a replication factory (Guillou et al, 2010). Organization of replication origins in factories facilitates their simultaneous activation and their regulation under special stress situations (see below).

Origin activation

Activation of replication origins is tightly regulated to ensure that DNA is copied only once in each cell cycle. Origins are activated in two steps. First, an "**origin licensing**" step in G1 that consists in the loading of proteins with helicase activity onto the DNA. This is followed by "**origin firing**" in S phase that involves the activation of the helicase and initiation of DNA synthesis (Fig 1; reviewed in Deegan and Diffley, 2016).

Origin Licensing

Eukaryotic origins are recognized by initiator proteins called **ORC** (Origin Recognition Complex), **CDC6** (Cell Division Cycle 6) and **CDT1** (Cdc10-Dependent Transcript 1), whose function is to attract and engage the **MCM2-7** (Mini-Chromosome Maintenance) hexameric complex with the DNA. The resulting structure is referred to as **pre-replicative complex** (pre-RC). MCM2-7 forms the core of the replicative helicase, which will be activated in S phase (reviewed by Deegan and Diffley, 2016) (Fig 1).

ORC is a hexameric AAA+ ATPase that binds to origins during the entire cell cycle (Bell and Stillman, 1992). It works as a platform for the binding of CDC6, another AAA+ ATPase (Speck et al 2005). At least in yeast, CDT1, a protein with a chaperone function, binds to MCM2-7 to form a heptameric complex (Takara and Bell, 2011). ORC and CDC6 cooperate to recruit CDT1-MCM2-7 to origins to form the pre-RC in a reaction dependent on their ATPase activities (Randell et al, 2006).

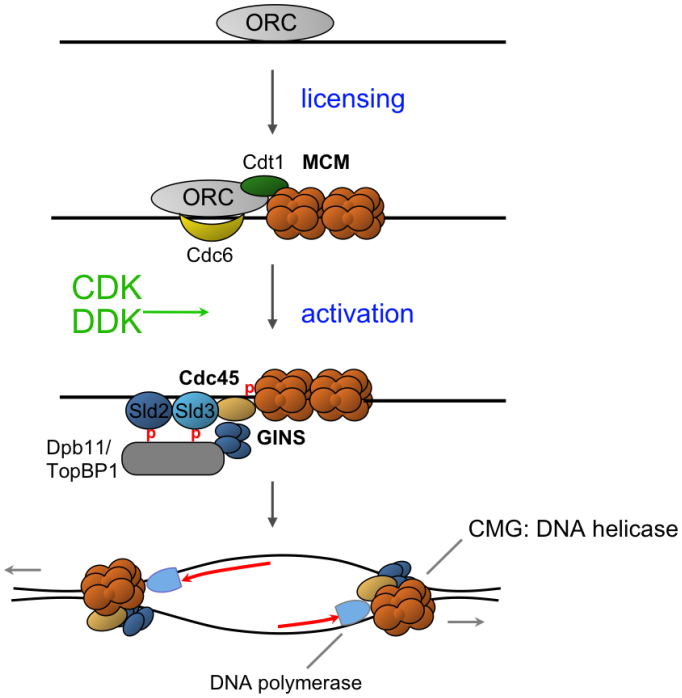

FIGURE 1. Replication origin activation pathway. In the G1 phase, ORC, CDC6 and CDT1 cooperate to load a double MCM complex hexamer. At S phase, CDK and DDK activities phosphorylate different proteins (Sld2, Sld3, TopBP1 and MCMs) to promote the loading of CDC45 and GINS complex, activating the CMG helicase. The binding of polymerases and accessory components configure the replisome to initiate bidirectional DNA replication.

MCM2-7 complex is a ring-shaped planar heterohexamer in which each subunit contains an N-terminal interacting domain and a C-terminal AAA+ ATPase domain. The ATPase sites are configured at the interphase between two subunits, one of them providing the Walker A and B motifs to bind ATP and the other one providing an "Arginine finger" element required for ATP hydrolysis (Fletcher et al, 2003; Costa et al 2013; Li et al, 2015). MCM2-7 is loaded in an inactive form as a double head-to-head hexamer that encircles dsDNA (Ervin et al, 2009; Remus et al, 2009). The interphase between the MCM2 and MCM5 subunits configures a steric gate to open and close the MCM2-7 complex around dsDNA (Samel et al, 2014). Then, DNA and ATP binding may induce structural changes to promote a closer conformation (Hesketh et al, 2015; Boskovic et al, 2016). Interestingly, MCM complexes can translocate passively on the DNA and move away from the origins (Powel et al, 2015).

The multi-step pathway of MCM loading has been recently investigated in detail (Fernández-Cid et al, 2013; Frigola et al, 2013; Coster et al, 2014; Kang et al, 2014; Yeeles et al, 2015). It starts with the formation of an OCCM (ORC-CDC6-CDT1-MCM) complex (Fernández-Cid et al, 2013). If any component of this complex is missing or if ORC has been inactivated, CDC6 ATPase activity induces complex disassembly (Frigola et al, 2103). However, if the complex is formed correctly, ORC and CDC6 ATPase activities promote CDT1 release and the formation of the OCM

(ORC-CDC6-MCM) complex (Fernández-Cid et al, 2013). It has also been proposed that ATP hydrolysis by MCM complex leads to CDT1 release (Coster et al, 2014; Kang et al, 2014). Loading of the second MCM hexamer is less well understood but it requires the interaction between CDC6 and MCM3 (Frigola et al; 2013) as well as a second molecule of CDC6 (Ticau et al, 2015).

Origin Firing

At the onset of S-phase, CDK (Cyclin-Dependent Kinase) and DDK (Dbf4-Dependent Kinase) activities promote the binding of CDC45 and GINS proteins to MCMs, forming the CMG (CDC45-GINS-MCM) holo-enzime. CMG is the active helicase that unwinds DNA, a necessary step to initiate bidirectional replication from each origin (Tognetti et al, 2014; Fig 1). At least in yeast, additional factors are needed to activate the helicase: Sld2, Sld3/7, Dpb11, DNA polymerase ε and Mcm10 (Yeeles et al, 2015). Sld2 and Sld3 are the only essential targets of CDKs and their phosphorylation promotes their binding to Dpb11 (Tanaka et al, 2007; Zegerman and Diffley, 2007). Sld2 phosphorylation promotes GINS and Polε recruitment to the origin (Muramatsu et al; 2010) while Sld3 facilitates Cdc45 binding to MCM2-7 (Nakajima et al, 2002; Tanaka et al, 2010). This regulation is maintained in higher eukaryotes through RecQL4, Treslin and TopBP1, the Sld2, Sld3 and Dpb11 homologues, respectively (Sangrithi et al, 2005; Im et al, 2009; Kumagai et al, 2010; 2011; Boos et al, 2011). In turn, the main target for DDK seems to be the MCM complex (Sheu and Stillman, 2006). Phosphorylation of MCM2, 4 and 6 appear to be necessary to activate the complex (Francis et al, 2009; Sheu and Stillman, 2010). Regarding MCM10, its precise biochemical activity is not clear but it facilitates Polα association with the replisome and DNA unwinding (Kanke et al 2012; van Deursen et al 2012).

DNA synthesis initiates with the assembly of the ‘replisome’ complex (Fig 2) and the establishment of two ‘replication forks’ that move bidirectionally from each origin. The replisome is composed by multiple proteins including three DNA polymerases (α, δ, and ε), the processivity factor PCNA (Proliferating Cell Nuclear Antigen), Ctf4 and the so-called ‘replication pausing complex’ (Tipin, Tim1, And1 and Claspin) that tethers the DNA polymerases to the helicase (Gambus et al, 2006; 2009; Errico et al, 2009).

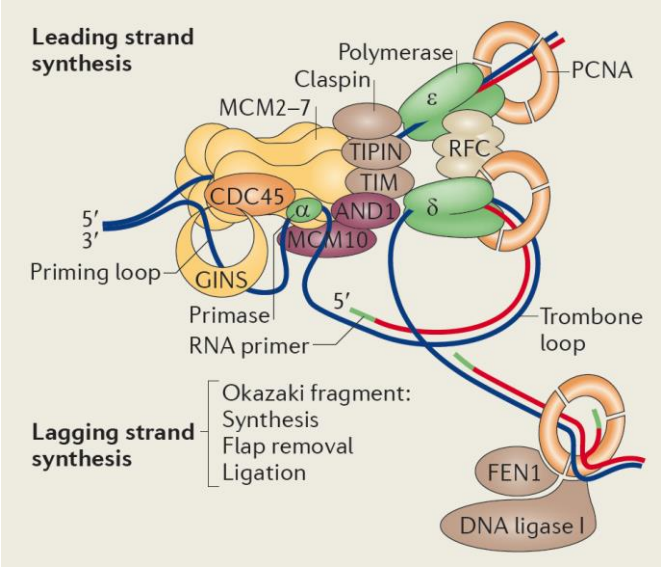

FIGURE 2. Structure of eukaryotic replisome (taken from *Alabert & Groth. 2012).* CMG complex, DNA polymerases, PCNA, Replication Factor C (RFC) and the replication pausing complex (Tipin, Tim1, And1 and Claspin) are shown.

Origin activation: once and only once in each cell cycle

Origin licensing and firing are separated in two different phases to ensure a single round of DNA replication in each cell cycle (reviewed in Arias and Walter, 2007). During S phase, origin licensing is inhibited because the same signals that promote origin activation inhibit the activity of initiator proteins (Fig 3A). In this way, origin relicensing is prevented during S and G2 phases. Cell cycle oscillations of CDK activity are a key component of this strategy, and additional mechanisms reinforce this control (see below). The ubiquitin ligase APC (Anaphase Promoting Complex) and its cofactors Cdc20 and Cdh1 target cyclins for degradation providing a window of low CDK activity in G1 that allows the licensing of all potential origins (Fig 3B). Following APC inactivation, CDK activity is increased in S phase, promoting both origin firing and initiator proteins inhibition (Fig 3A, B).

The inability to assemble new pre-RC during S phase represents a risk if replication forks are paused, blocked or inactivated in any way. For this reason, G1 cells license an excess of replication origins that remain in a ‘dormant’ state (Ge et al. 2007; Ibarra et al. 2008). Activation of these dormant origins is likely the main mechanism to restore replication after fork stalling in higher eukaryotes (Petermann and Helleday, 2010). This and other mechanisms will be presented in more detail in the section “Replication stress”.

If origins could be relicensed during S or G2, when origin firing is favoured, relicensed origins would easily be reactivated, giving rise to partial **DNA re-replication**.

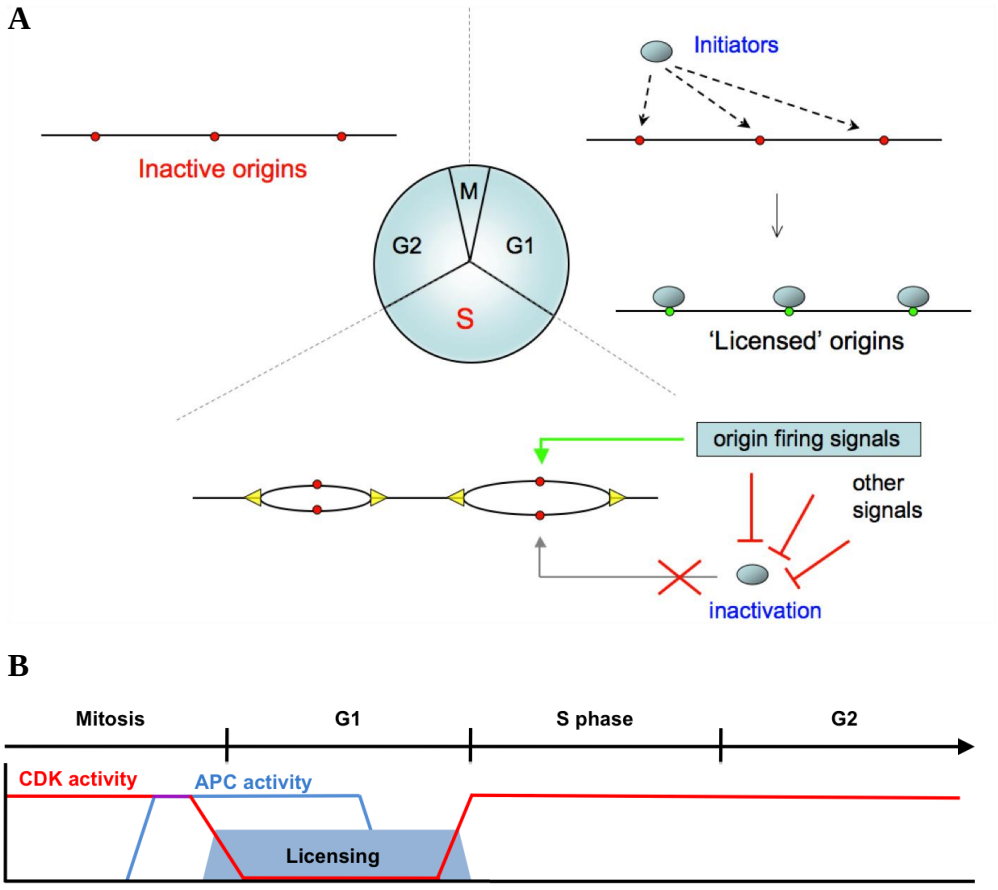

FIGURE 3. Strategy to impede origin relicensing. A. During G1 phase, initiator proteins are active and license replication origins. At S phase, origin firing signals, especially CDK activity, inhibit initiator proteins. This mechanism ensures that after a replication origin is fired, it cannot be activated again until the next cell cycle. Regulation of origin licensing and firing restricts replication to once per cell cycle. **B.** CDK oscillations and APC activity configure a "window of opportunity" for origin licensing.

DNA re-replication

Re-replication has been detected in several eukaryotic organisms when one or more components of pre-RC are deregulated (Nguyen et al, 2001; Vaziri et al, 2003; Melixetian et al, 2004; Green et al, 2006; Sugimoto et al, 2009). It leads to replication stress (RS) and DNA damage, monitored by single strand DNA accumulation (Melixetian et al, 2004; Zhu and Dutta, 2006; Liu et al, 2007; Neelsen et al, 2013) and DNA double strand breaks (DSBs) (Zhu and Dutta, 2006; Lovejoy et al, 2006; Davidson et al, 2006; Neelsen et al, 2013). Activation of the G2/M checkpoint prevents cells with re-replicated DNA from entering mitosis and abrogation of the checkpoint results in cell death, probably due to mitotic catastrophe (Melixetian et al, 2004; Zhu et

al, 2004; Zhu and Dutta, 2006; Lin and Dutta 2007; Liu et al 2007). Re-replicated cells could activate the apoptotic program from G2 when p53 is functional (Vaziri et al, 2003). BRCA1 and several components of the Fanconi Anemia (FA) pathway are necessary to activate the checkpoint in response to re-replication (Zhu and Dutta, 2006). In yeast, the checkpoint response is rad9-dependent and mrc1-independent, suggesting that DSBs rather than ssDNA exposure is the main signal that activates the pathway (Archambault et al, 2002; Green and Li, 2005). In contrast, in mammalian cells, ATR and CHK1 are activated before ATM and CHK2 in response to RS (Liu et al 2007; Neelsen et al 2013). In fact, depletion of the ATM branch had no effect over re-replication-induced G2 arrest (Lin et al, 2006). These results indicate that ATR pathway is the main signal to activate the cellular response to DNA re-replication in mammals (Fig 4).

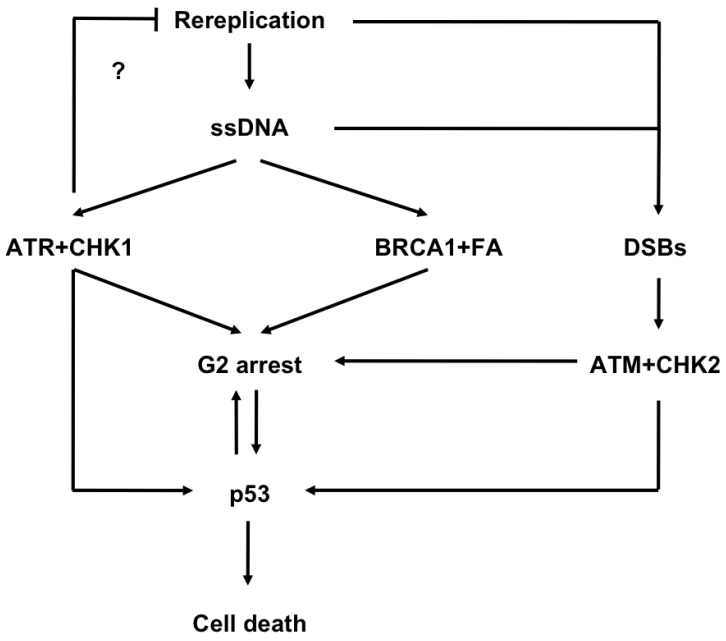

FIGURE 4. Cellular responses to re-replication. Re-replication promotes ssDNA accumulation and DSBs that activate ATR, FA and ATM pathways. Checkpoint activation promotes G2 arrest and eventually, cell death. ATR activation might also restrict re-replication.

Whether ATR activation is simply the consequence of DNA damage or the ATR pathway regulates the extension of re-replication and its eventual repair is a matter of debate. On one hand, when origin licensing is disrupted by overexpression of CDT1, ATR prevents re-replication extension in some cell lines (Liu et al 2007). On the other hand, blocking cells in G2 may facilitate the reactivation of replication origins, giving rise to higher levels of re-replication (Klotz-Noack et al 2012). In a situation of developmentally-controlled re-replication such as that occurring in *Drosophila* ovarian

follicle cells, checkpoint activation is required to allow the progression of re-replicated forks (Alexander et al, 2015).

Two models have been proposed to explain how re-replication induces DNA DSBs. The first model was proposed in *Xenopus* egg extracts and it implies head-to-tail collisions between the two consecutive forks established from the same origin (Davidson et al, 2006) (Fig 5). The model explains the presence of DNA fragments after several rounds of re-replication (Davidson et al, 2006) but it implies that re-replicated forks progress at a faster pace than regular forks, which needs to be formally demonstrated. The second model suggests that in conditions of deregulated origin licensing, the first round of replication leaves small sections of ssDNA that are converted in DSBs at the passage of the second fork on the same template (Fig 5). This model is supported by electron microscopy analyses of re-replicated forks (Neelsen et al, 2013). How re-replication promotes the accumulation of ssDNA gaps remains to be characterized. These models are not mutually exclusive. In addition, it has been proposed that DSBs could arise when re-replicated tracks copy through immature Okazaki fragments (Zhu and Dutta, 2006b; Liu et al, 2007) but this possibility has not been experimentally addressed.

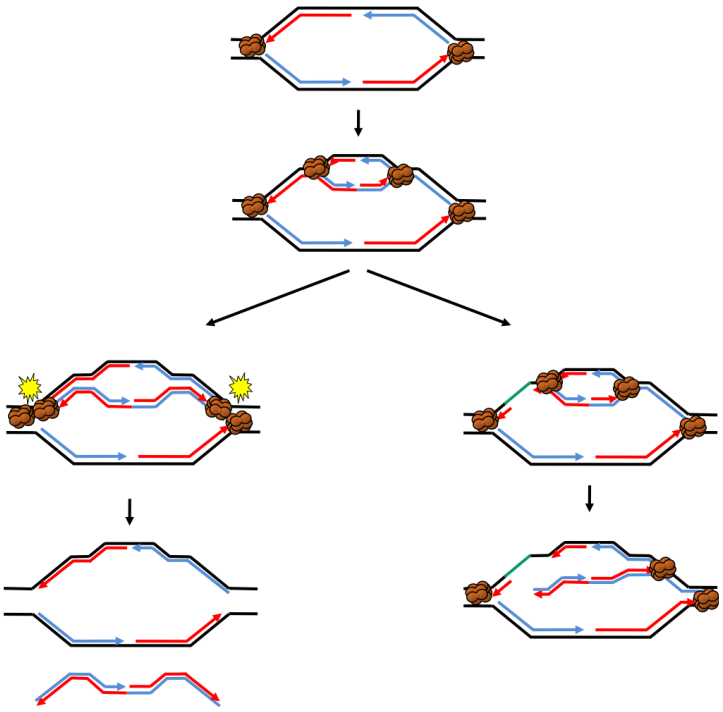

FIGURE 5. Models to explain re-replication-induced DSBs.
Left branch: If re-replicated forks progress faster than regular ones, they eventually collide. Head-to-tail fork collisions results in DSBs.
Right branch: Deregulation of origin licensing induces accumulation of ssDNA in the first round of replication. When re-replicated tracks progress through these ssDNA gaps, forks collapse into DSBs.

In yeast, origin reactivation can lead to re-replication-induced gene amplification by non-allelic homologous recombination (NAHR; Green et al, 2010; Finn and Li, 2013). In this system, re-replicated forks are prone to break, and any partial homology between the two ends may be sufficient to induce recombination via single strand annealing (SSA; Finn and Li, 2013). This could be a specific feature of yeast, as only a fraction of the genome is re-replicated upon licensing deregulation (Tanny et al, 2006). Recently, sequences called re-initiation promoters have been identified that dictate which origins could be relicensed and which could not (Richardson and Li; 2014). The presence of re-replication-prone origins in yeast could contribute to re-replication-induced gene amplification. In addition, re-replication of centromeres in budding yeast induces chromosome segregation problems and causes aneuploidy (Hanlon and Li, 2014).

In mammalian cells, DNA re-replication appears to be spread throughout the genome (Klotz-Noack et al, 2012) and it could also drive chromosomal rearrangements and genomic instability, as observed upon CDT1 deregulation (Lovejoy et al 2006; Liontos et al, 2007). Cells derived from CDT1-transgenic p53-null mice show aneuploidy (Seo et al, 2005). A closer relationship between re-replication and genomic instability has been established recently in a subset of p53-null tumours with high p21 expression. These cells accumulate pre-RC proteins and display DNA re-replication and genomic instability (Galanos et al, 2016). Mitotic conflicts derived from re-replication could underlie the increase in genomic instability.

Mechanisms that control re-replication

In yeast, CDK activity is the main regulator of origin licensing (Fig 3). Phosphorylation of Cdc6, Orc2 and Orc6 inhibits their licensing activity. After the G1-S transition, CDK activity also promotes Cdc6 destruction and the translocation of Cdt1-MCM2-7 complexes to the cytoplasm (reviewed in Arias and Walter, 2007). These mechanisms prevent origin re-licensing.

In higher eukaryotes, CDK activity regulates ORC1 chromatin binding (Li et al 2004), as well as CDC6 nuclear-cytosolic translocation (Saha et al 1998; Petersen et al 1999; Jiang et al, 1999). This regulation appears to be restricted to soluble CDC6 (Alexandrow and Hamlin, 2004) because a fraction of CDC6 remains bound to

chromatin during S, G2 and M phases (Mendez and Stillman, 2000). CDKs also phosphorylate CDT1 to promote its degradation via SCF^{Skp2} after G1 (Liu et al 2004).

In addition, other mechanisms control the stability of preRC components throughout the cell cycle. A fraction of ORC1 subunit is degraded after S phase through SCF^{Skp2} (Mendez et al, 2002), while other fraction remains on chromatin during the entire cell cycle (Okuno et al, 2001). Despite this regulation, individual ORC1 overexpression does not induce re-replication in human cells (Sugimoto et al, 2009).

CDC6 is targeted for proteolysis by at least three E3 ubiquitin ligases: APC/C^{Cdh1} at the exit from mitosis (Petersen et al 2000), CRL4-Cdt2 during S phase (Clijsters et al, 2014), and $SCF^{Cyclin\ F}$ from S phase to mitosis (Walter et al, 2016; Fig 6). APC/C-dependent destruction is important to limit CDC6 levels in quiescent cells. Phosphorylation of CDC6 by Cdk2-Cyclin E stabilizes the protein to allow origin licensing during cell cycle re-entry (Mailand and Diffley, 2005). CDC6 overexpression induces limited re-replication in tumoral cells (Vaziri et al 2003; Liontos et al, 2007), but elimination of $SCF^{Cyclin\ F}$-dependent CDC6 regulation only results in re-replication when CDT1 activity is also deregulated (Walter et al, 2016).

CDT1 stability is also controlled by three ubiquitin ligases: APC/C^{Cdh1} at mitotic exit (Sugimoto et al, 2008), Cul4-Ddb1-Cdt2 in S phase and SCF^{Skp2} from S phase to mitosis (Nishitani et al, 2006; Fig 6). Cul4-Ddb1-Cdt2 regulation is restricted to S phase because it relies on CDT1 binding to PCNA (Arias and Walter, 2006; Senga et al, 2006) while SCF^{Skp2} could act during G2 and mitosis because it relies on phosphorylation of CDT1 Cy motif by CDK activity (Liu et al, 2004). Deregulation of CDT1 has a major impact on DNA replication, at least in tumoral cell lines. CDT1 overexpression is sufficient to promote extensive re-replication (Vaziri et al, 2003; Liontos et al, 2007; Teer and Dutta, 2008). Expression of mutant versions of CDT1 that impair the interactions with Cdh1, PCNA or Skp2 also induces re-replication to different extents (Sugimoto et al, 2008; Arias and Walter, 2006; Takeda et al, 2005). In addition, cell lines resistant to CDT1 overexpression are sensitized when ATR is interfered (Liu et al 2007). Intriguingly, in non-cancerous cell lines CDT1 overexpression does not boost extensive origin refiring (Sugimoto et al, 2009).

Several pre-RC components, including CDC6 and CDT1, are degraded in the presence of DNA damage (Mendez et al, 2002; Hu et al, 2004; Duursma and Agami, 2005; Higa et al, 2006; Senga et al, 2006; Hall et al, 2007), probably to prevent origin relicensing when the DNA damage checkpoint inhibits CDK activity to block cell cycle progression (Arias and Walter, 2007; Hall et al, 2008).

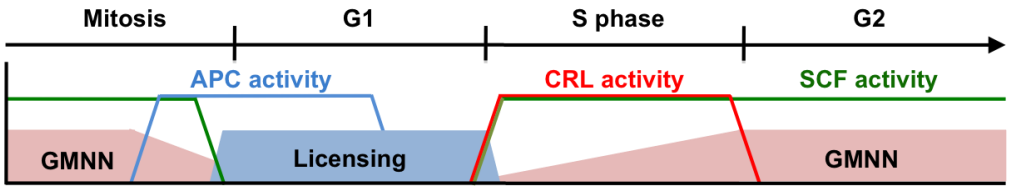

FIGURE 6. Regulation of re-replication through GMN and ubiquitin ligases. GMN binds and inhibit CDT1 from S phase to late mitosis. Ubiquitin ligases target preRC proteins for degradation in different phases of cell cycle. APC complex (blue) is active from late mitosis to G1. CRL complexes (red) are active during S phase whereas SCF complexes perform their activity from S phase to the end of G2. See text for details.

CDT1 protein is also regulated by the binding of a small inhibitor called Geminin (GMN), which prevents CDT1 activity between S and M (Fig 6; Wohlschlegel et al, 2000). Hence, GMN depletion causes DNA re-replication in many cancer cell lines (Melixetian et al, 2004; Klotz-Noack et al, 2012) but not in primary cell lines (Zhu and DePamphilis, 2009). Interestingly, GMN also facilitates origin licensing in G1 by protecting a fraction of CDT1 from degradation during G2 and M phases (Ballabeni et al, 2004). Finally, epigenetic modifications may also participate in re-replication control, as histone methyltransferases PRset7 and DOT1L are necessary to impede origin reactivation (Tardat et al, 2010; Fu et al 2013).

Animal models for the study of DNA re-replication

Most of the available information about the control of DNA re-replication has been derived from cultured cell lines. In invertebrates, it has been shown that DNA over-replication has lethal consequences during embryonic development in *C. elegans* and *D. melanogaster* (Zhong et al, 2003; Thomer et al, 2004). Regarding mammalian organisms, no mouse models have been described in which the consequences of DNA over-replication could be studied *in vivo*. It is worth noting that several mouse models have been developed to investigate the opposite situation, i.e. insufficient origin licensing and activity. Mouse strains with partial MCM deficiency undergo genomic instability, haematopoietic defects and are prone to cancer (e.g. Shima et al, 2007; Pruitt

et al, 2007; Kawabata et al, 2010; Alvarez et al, 2015). The potential oncogenic role of deregulated CDC6 and CDT1 has been individually addressed in mice (Búa et al, 2016; Seo et al, 2005), but no evidence of DNA re-replication was reported in these studies. Given the link between DNA re-replication and genomic instability, one of the objectives of this thesis has been the characterization of mouse models in which DNA re-replication could be induced in a controlled manner.

Prevalence of origin re-firing and extension of re-replicated DNA

In principle, re-replication is an aberrant process that should only be observed when the origin licensing process is deregulated. However, several evidences suggest that this process might be more prevalent than expected and that re-replication might also occur under physiological conditions (Green et al, 2006). A single ORC-Cdc6-Cdt1 complex can load multiple MCM complexes (Edwards et al, 2002; Bowers et al, 2004; Powell et al, 2015). When multiple MCM complexes are gathered around a single origin, there is a risk of re-activation in S phase. In human cells, it has been proposed that origins undergo several rounds of activation in S phase giving rise to small re-replicated DNA fragments, approximately 200 bp long (Gómez and Antequera, 2008). Up to 2.5% of ongoing forks detected in DNA fiber assays seem to arise from reactivated origins in control human cells, and their average extension is approximately 18 kb (Dorn et al, 2009). In addition, it has been reported that more than 5% of control G2 cells incorporate EdU (Walter et al, 2016).

The extension of re-replicated forks poses intriguing questions. For unknown reasons, re-replicated forks display less processivity and are prone to break (Green et al, 2006; Tanny et al, 2006; Finn and Li 2013). In yeast, regular forks are in charge of copying 100-200 kb of DNA (Dershowitz and Newlon, 1993; van Brabant et al, 2001), while re-replicated forks rarely travel longer than 30-35 kb from the origin (Nguyen et al, 2001). Comparative genomic hybridization (CGH) analysis in yeast shows no signs of re-replication 100-200 kb away from origins (Green et al, 2006).

These antecedents suggest that specific mechanisms may restrict the extension of re-replicated DNA after origin re-firing events caused by faulty licensing control. Part of this Doctoral thesis explores the relationship between DNA re-replication and several mechanisms that operate when the normal DNA replication process is perturbed. The

following Introduction sections are dedicated to fundamental aspects of RS and its crosstalk with origin activity.

Replication Stress

RS is defined as the slowing or stalling of replication forks during DNA synthesis (Zeeman and Cimprich, 2014). An immediate consequence of fork stalling is the exposure of stretches of ssDNA that are rapidly covered by RPA. The amount of RPA bound to ssDNA influences the strength of the cellular responses to RS (MacDougall et al, 2007). Not all interferences with DNA replication activate a RS response (Huang et al 2010) and we have recently suggested to extend the definition of RS to indicate that the extent and duration of fork slowing/stalling ought to be strong enough to activate a specific checkpoint response (Muñoz and Mendez, 2016). In the absence of an appropriate response, the replisome at the stalled fork is eventually dismantled and the failed replicative structure collapses into a DSB.

The possible causes and consequences of RS have been extensively discussed in recent reviews (Zeeman and Cimprich, 2014; Gaillard et al, 2015; Muñoz and Mendez, 2016). They include endogenous DNA damage as well as replication through DNA secondary structures, regions with DNA-bound non-histone proteins, fragile sites, centromeres, telomeres, topological conflicts and collisions with the transcriptional machinery. Exogenous genotoxic agents that induce DNA damage and/or affect the dNTP pool may also induce RS.

ATR (ataxia-telangiectasia mutated and RAD3-related) kinase is the main regulator of the cellular response to RS. It is activated by RPA-covered ssDNA (Cimprich and Cortez 2008) and phosphorylates multiple proteins, including the effector Chk1 kinase (Matsuoka et al. 2007). This pathway activates three responses: stabilization of stalled forks, inhibition of late origin firing, and inhibition of mitotic entry. Combined, these responses provide time to deal with the source of RS before the restart of DNA replication.

RS and origin activity

Dormant origins and the checkpoint response: "inhibit globally, activate locally"

When a stalled fork is unable to restart DNA synthesis, replication is normally "rescued" from a fork moving in the opposite direction (derived from an adjacent origin). The situation is more complicated when two forks moving towards each other are simultaneously stalled. Since the assembly of new replicative helicases on DNA is prevented during S phase, replication between the two stalled forks could be left incomplete and generate aberrant DNA intermediaries and anaphase bridges in mitosis, which in turn become chromosomal breaks (Liu et al, 2014). This problem is minimized by the licensing of multiple "dormant origins" in G1 (reviewed by Alver et al, 2014), which serve as a backup mechanism to reinitiate replication in response to stalled forks (Fig 7). Indeed, elimination of dormant origins by MCM downregulation sensitizes cells to drugs that challenge fork progression (Ge et al, 2007; Ibarra et al, 2008). In fact, Mcm4 hypomorphic cells display genomic instability even in the absence of exogenous replication challenges (Kawabata et al, 2010). Consistently, the lack of dormant origins in mouse models hypomorphic for different MCM subunits makes them cancer-prone (Pruitt et al, 2007; Shima et al, 2007; Bagley et al, 2012; Alvarez et al, 2015).

Cells must coordinate two different actions on replication origins in response to RS. On one hand, the checkpoint response should block late replication (i.e. late origins) until cells recover from RS. On the other hand, dormant origins should be activated to complete replication and maintain genome stability. As a solution to this paradox, it has been proposed that checkpoint proteins inhibit origin firing globally, while locally promoting backup origin activation around stalled forks (Fig 7; Ge and Blow, 2010; Yekerazee et al, 2013). The arrangement of groups of adjacent origins in replication factories (Jackson and Pombo 1998; Guillou et al, 2010; Aparicio et al, 2012) likely contributes to separate local and global effects.

At the mechanistic level, the ATR-CHK1 axis may inhibit global origin activity by targeting Sld3/Treslin and the Dbf4 subunit of the DDK kinase (Fig 7; Costanzo et al, 2003; Syljuasen et al. 2005; Maya-Mendoza et al, 2007; Lopez-Mosqueda et al, 2010; Zegerman and Diffley 2010; Guo et al, 2015). In contrast, how dormant origins are activated locally is still a matter of investigation. It has been proposed that following MCM2 phosphorylation by ATR at stalled forks, Polo kinase (PLK1) promotes CDC45

loading at nearby dormant origins, leading to their activation (Trenz et al, 2008). Moreover, PLK1 modulates claspin levels (Mainland et al 2006; Peschiaroli et al 2006), which may restrict CHK1 activity nearby stalled forks. FANCI protein, a member of the FA DNA repair pathway, has been recently related to dormant origin activation, although the precise mechanism remains unclear (Chen et al, 2015).

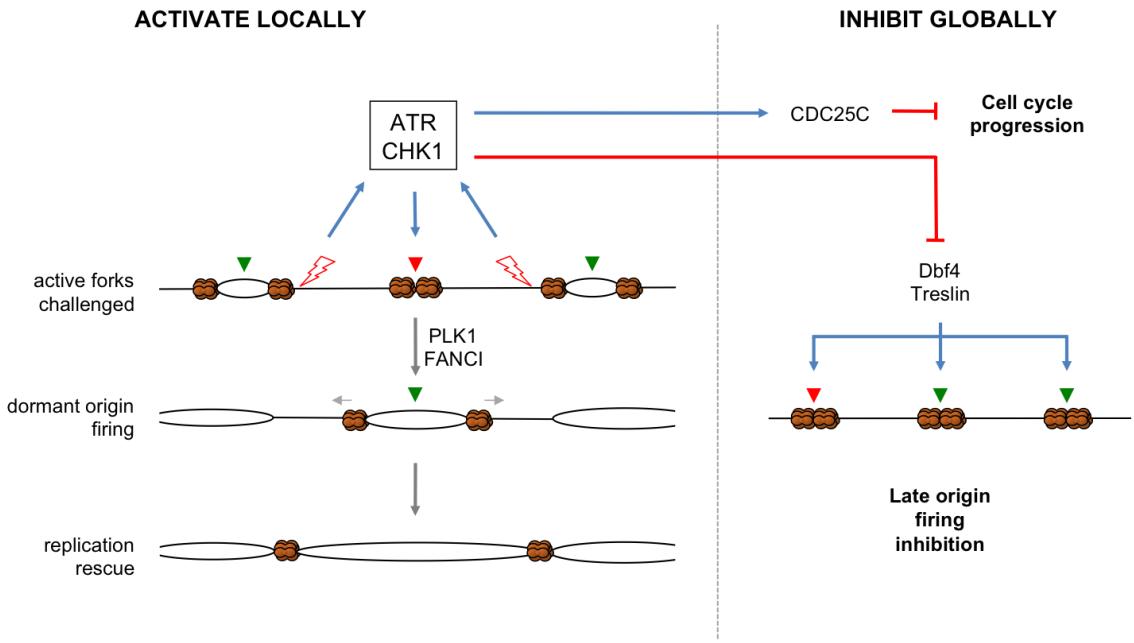

FIGURE 7. Dormant origin activation. Upon RS, dormant origins can be activated to rescue replication. The ATR and CHK1 pathway plays a dual role in this process. Inhibition of CDKs impedes activation of late replication origins through Dbf4 and Treslin. However, near the stalled forks, they promote dormant origin firing through FANCI and PLK1 activity. See text for details.

RS and aberrant origin firing

Deregulated origin activity is also a cause of RS. Origin over-usage leads to an accumulation of active forks that might reduce the pool of dNTPs or other limiting replisome components such as RPA (Bester et al, 2011; Toledo et al, 2013). In addition, it increases the chance of collisions with the transcription machinery (Jones et al, 2013). Notably, oncogene activation unbalances the licensing process (Eckholm-Reed et al, 2004) and has a direct effect in origin firing. It has been proposed that the DNA damage and senescence response induced by oncogenes are the result of aberrant origin activity at early stages of cancer development (Halazonetis et al, 2008; Hills and Diffley, 2014).

DNA replication restart at stalled forks

Fork stability, remodelling and restart

The replisome proteins and the structure of the fork itself must be stabilized in response to RS. Early studies postulated that the yeast orthologues of ATR and CHK1 (Mec1 and Rad53) were needed to maintain a stable replisome at stalled forks (Lopes et al 2001; Tercero and Diffley 2001; Cobb et al, 2003; Katou et al, 2003). However, more recent studies showed that replisomes are stably maintained at stalled forks in the absence of Mec1 and Rad53. Checkpoint phosphorylation of replisome components might be related to the control of replisome function rather than its stability (DePiccoli et al 2012).

Checkpoint activity could regulate fork remodelling into four-way junctions through a process called fork reversal (Fig 8). Reversed forks were initially described in checkpoint-deficient yeast strains subjected to RS and were considered an aberrant structure that would lead to fork breakdown and genome instability (Lopes et al 2001; Sogo et al; 2002). Nevertheless, recent data from human cells suggests that fork reversal is a transient physiological response that stabilizes the fork before DNA replication is resumed (reviewed by Neelsen and Lopes, 2015).

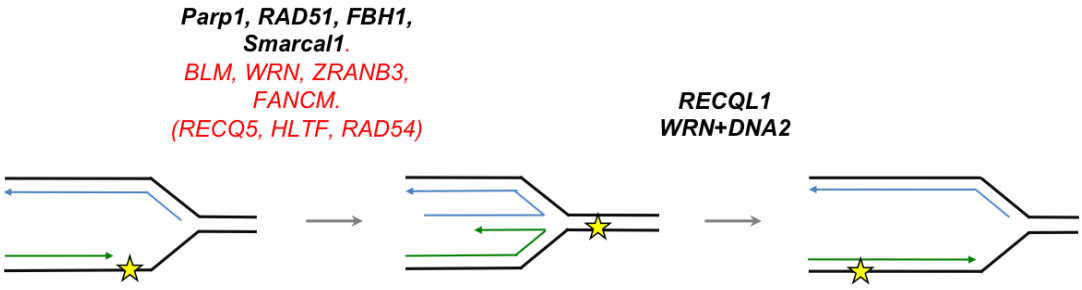

FIGURE 8. Proteins that mediate fork reversal. Proteins that perform this reaction *in vivo* are depicted in black. Proteins with fork remodelling activity *in vitro* that can promote fork restart *in vivo* are shown in red. In red brackets, proteins that catalyse fork reversal *in vitro*. RECQ1 and WRN-DNA2 mediate two independent mechanisms to remodel reversed structures into normal forks.

The process of fork reversal is mediated by different proteins, including FBH1 and SMARCAL1 helicases (Couch et al, 2013; Fugger et al, 2015) and Poly(ADP-ribose) polymerase (Ray Chaudhuri et al, 2012). Importantly, fork reversal is strictly dependent on RAD51 recombinase (Zellweger et al, 2015). Other helicases including BLM, WRN, RECQ5, RAD54, ZRANB3, HLTF or FANCM can reverse forks *in vitro* (reviewed by

Neelsen and Lopes, 2015). Amongst them, at least BLM, WRN, ZRANB3 and FANCM have been involved in fork restart (Davies et al, 2007; Ciccia et al, 2012; Yuan et al, 2012; Schwab et al, 2010; Sidorova et al, 2008).

Resumption of DNA synthesis from a regressed fork needs a second remodelling event that *in vivo* involves WRN. The mechanism is not completely understood but the ATPase activity of WRN, together with DNA2-mediated degradation of regressed arms, facilitates fork restoration (Thangavel et al, 2015). DNA2 activity is limited by BOD1L protein to avoid DNA over-resection (Higgs et al, 2015). A second mechanism to restore normal forks from regressed ones *in vivo* is catalyzed by RECQ1 helicase (Berti et al, 2013).

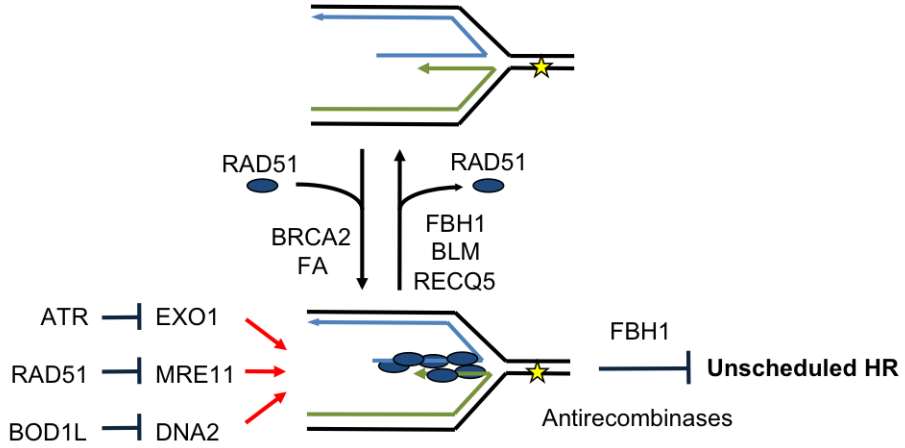

FIGURE 9. Fork stability after stalling. Stalled and reversed forks are susceptible to nuclease degradation. BRCA2 and FA proteins load RAD51 in these structures to protect them. ATR and BOD1L also contribute to fork stability by limiting EXO1 and DNA2 activities. FBH1, BLM, RECQ5 and other antirecombinases limit unscheduled HR.

Reversed forks also contribute to checkpoint activation because they resemble DSBs (Fugger et al 2015) and are therefore sensitive to nucleolytic degradation (Fig 9). Indeed, MRE11-dependent resection of DNA at stalled forks has been associated with genomic instability (Schlacher et al, 2011, 2012). FA proteins and BRCA2 promote RAD51 binding to stalled forks to counteract this degradation (Hashimoto et al, 2010; Schlacher et al, 2011, 2012; Fig 9). Other proteins involved in fork protection from MRE11 degradation are PARP1 (Ying et al, 2012), RAD51 paralogs (Somyajit et al, 2015), WRN (Su et al, 2014) and WRNIP1 (Leuzzi et al, 2016). In addition, ATR

activity prevents fork degradation by inhibiting EXO1 or CtIP exonucleases (El-Shemerly et al, 2008; Couch et al, 2013; Fig 9).

Although fork reversal might be part of RS response, reversed forks are recombinogenic structures (Cotta-Ramusino et al, 2005). Therefore, the homologous recombination (HR) pathway must be regulated to avoid negative consequences (Fig 9; Carr and Lambert, 2013). Control of RAD51 activity is a key step in this regard. RAD51 participates in both fork restart and recombination-mediated repair (Petermann et al, 2010). After short HU treatments, HR is inhibited and RAD51 may be involved in fork protection and DNA damage tolerance mechanisms. However, long HU treatment induces fork collapse and RAD51-mediated HR repair.

Several pathways may be involved in limiting HR in the RS response through RAD51 regulation (Fig 9). FBH1 displaces RAD51 filaments from ssDNA (Simandlova et al, 2013) and monoubiquitylates RAD51 to export it from the nuclei in response to HU (Chu et al, 2015). Other helicases such as BLM, RECQ5, FANCJ and RAD54 also displace RAD51 from DNA (Wu et al, 2001; Bugreev et al, 2007; Hu et al, 2007; Sommers et al, 2009; Shah et al, 2010), whereas RECQ1 and FANCM restrict HR by dissociating displacement loops (D-loops) (Bugreev et al, 2008; Rosado et al 2009).

Other mechanism to resume DNA replication

Eukaryotic cells have developed other mechanisms to complete replication in stress situations (Fig 10), which are not the focus of this doctoral thesis but are briefly described below.

DNA damage tolerance (DTT) mechanisms allow skipping DNA lesions during DNA replication. These lesions are then repaired post-replicatively, when two sister chromatids are available. There are two branches of DTT, translesion synthesis (TLS) and template switching (TS). The choice between them relies in the status of PCNA ubiquitylation (reviewed in Sale et al. 2012; Mailand et al, 2013). TLS is carried out by specialized DNA polymerases whose flexible active sites allow the insertion of nucleotides opposite damaged templates (reviewed by Lange et al, 2011; Sale et al. 2012; Fig 10A). TS is a recombination-related mechanism in which the stalled nascent DNA strand invades the sister chromatid to continue replication using undamaged newly synthesized strand as template (reviewed by Branzei, 2011; Fig 10B).

Stalled forks that could not be restarted are processed by structure-specific endonucleases such as Mus81-Eme1 (Hanada et al. 2006) that induce DSBs. These collapsed forks are repaired by HR. In the standard HR reaction at a DSB, the MRE11-RAD50-NBS1 (MRN) complex is recruited to the break and MRE11 performs DNA end resection. Then RAD52 and BRCA2 target RAD51 onto ssDNA and the RAD51-ssDNA filament invades the sister chromatid to generate a D-loop where DNA synthesis occurs. Other factors as RAD51AP1 or RAD54 support strand invasion and D-loop formation or dissociation. The final step may be carried out by different HR subpathways: synthesis-dependent strand annealing (SDSA), generation and resolution of double Holliday junctions, and break-induced replication (BIR; reviewed by Heller et al, 2010; Daley et al, 2013).

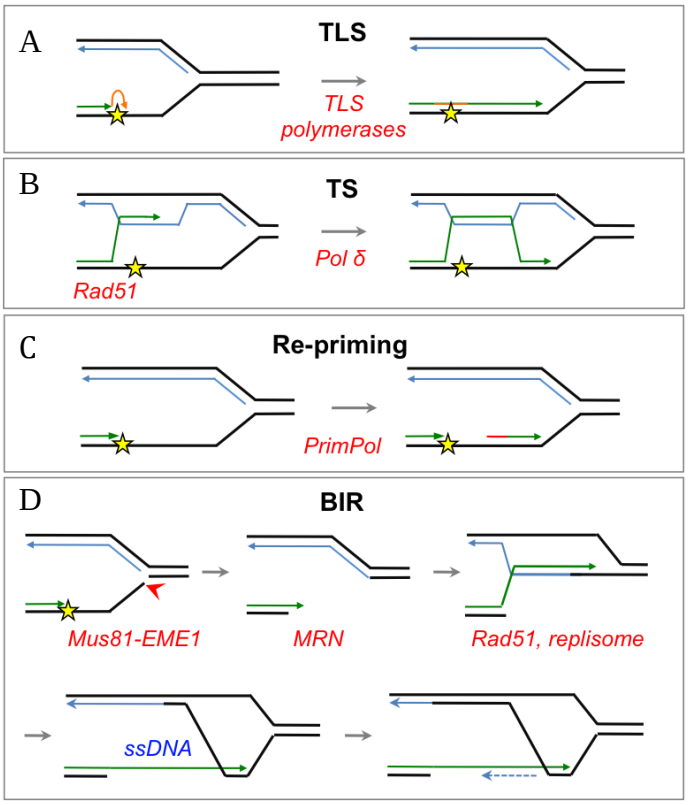

FIGURE 10. Mechanisms to resume DNA replication at stalled forks. A. TLS is performed by specialized polymerases that are able to synthesize DNA through damaged templates. **B.** TS is a recombination-related mechanism to bypass damaged templates. **C.** PrimPol promotes continuous DNA synthesis by repriming ahead of DNA lesions. **D.** Structure-specific endonucleases perform DSBs on stalled forks unable to restart. Collapsed forks are repaired through BIR. After resection, RAD51 catalyses strand invasion. Replication proceeds over hundreds of kilobases on the sister chromatid in a migrating bubble-like replication fork,.

Collapsed forks generate one-ended DSBs that are repaired by BIR (Costantino et al, 2014; Fig 10D). In yeast, Pif1 helicase cooperates with the HR machinery and replisome components to establish the migrating D-loop (Lydeard et al 2010; Wilson et al 2013). Replication proceeds for hundreds of kilobases (Davis and Symington 2004) via migrating bubble-like replication fork resulting in uncoupling leading and lagging

strands synthesis, ssDNA accumulation and a conservative inheritance of DNA (Saini et al 2013; Wilson et al 2013).

Whether any of the described mechanisms that remodel or repair stalled forks are also involved in the processing of re-replicated forks is one of the questions addressed in this doctoral thesis.

OBJECTIVES

OBJECTIVES

1. **Study the effects of Cdc6 and Cdt1 deregulated expression in primary mouse embryonic fibroblasts:** changes in cell cycle progression, dynamics of DNA replication and generation of DNA damage.

2. **Study the consequences of Cdc6 and Cdt1 deregulated expression during embryonic development and in adult mice, elucidating whether it leads to DNA re-replication *in vivo*.**

3. **Identification of cellular mechanisms that prevent DNA re-replication associated to origin reactivation.**

MATERIALS AND METHODS

MATERIALS AND METHODS

Mice procedures

Ethical statement

Mice were kept in the Animal Facility at CNIO in accordance with institutional policies and the 'Federation for Laboratory Animal Science Associations' (FELASA) guidelines. Animal procedures were approved by the Animal Experimental Ethics Committee of the Instituto de Salud Carlos III (Madrid, Spain).

Mice genotyping

Genotyping was performed by PCR analysis of genomic DNA isolated from tail clips following a standard protocol (Malumbres et al., 1997). Tails were lysed in PCR-K buffer (50 mM KCl, 1.5 mM MgCl2, 10 mM Tris-HCl pH 8.5, 0.01% gelatin, 0.45% NP-40, 0.45% Tween-20, 100 μg/mL proteinase K (Roche)) for 2 h at 55°C in agitation. Proteinase K was inactivated at 95°C for 15 min. PCR reactions were performed as follows: 2 μL of genomic DNA, 0.2 μL of Taq polymerase (Ecogen), 2.5 μL of 10X Taq reaction buffer (Ecogen), 1.5 μL of 50 mM MgCl2 (Ecogen), 1 μL of each primer from a 10 μM dilution in H20, 1 μL of 10 mM dNTPs (Fermentas), and H_2O to a final volume of 25 μL. The different primers used for mice genotyping are listed in Table 1.

Isolation of intestinal epithelium, bone marrow and fetal liver cells

The crypt-enriched fraction of intestinal cells was obtained following a described procedure (Sato and Clevers, 2013). E13.5 fetal livers or adult femur bone marrow (BM) were disaggregated in 2% FBS-RPMI by multiple passages through a 26G needle and filtered through a 70 μm strainer (BD Falcon). Fetal liver and BM cells were pulse-labelled *ex-vivo* with 10 μM BrdU for 30 min at 37^0 C. Afterwards cells were processed for flow cytometry analysis. A fragment of tissue was taken for subsequent genotyping.

RNA expression analysis

RNA isolation, retrotranscription and quantitative PCR (RT-qPCR)

Tissues or cell cultures were disrupted and homogenized in Trizol (Invitrogen) using a bead-beating system (Precellys). Total RNA was isolated according to manufacturer's instructions. Potential genomic DNA contamination was removed by DNaseI digestion (Roche). cDNA was obtained with Maxima First Strand cDNA kit (Thermo) according to the manufacturer's instructions. 1/100 cDNAs dilutions were used. qPCR was performed in triplicates using SYBR green-Real Time PCR master mix (Applied Biosystems). qPCR analyses were done in an Applied Biosystems 7900HT Fast Real Time PCR System equipment and analyzed with 7900HT Sequence Detection System (Applied Biosystems). Primers used for RT-qPCR analyses are shown in Table 2. Amplified fragments were quantified by $2^{\Delta\Delta Ct}$ method. Expression levels were normalized to GAPDH housekeeping gene.

Cell culture procedures

Primary Mouse Embryonic Fibroblasts (MEFs) isolation and culture

Mouse embryos were obtained at E12.5-14.5 days. Pregnant females were sacrificed by cervical dislocation and uterine horns were removed and transferred to a sterile PBS solution. In a laminar flow hood, embryos were removed from the uterus, fetal liver was excised and a fragment of tissue was taken for subsequent genotyping. The rest of embryonic tissue was minced and treated with 0.25% trypsin-EDTA (Sigma-Aldrich) for 20 min at 37°C. Cells were further disaggregated by pipetting, transferred to 9 mL medium (DMEM complete (Lonza), 20% FBS (Sigma-Aldrich), 10% penicillin/streptomycin solution (Invitrogen)), seeded in tissue culture plates and grown at 37°C and 5% CO2. Cells were expanded and frozen at passage 1 in 90% FBS, 10% dimethyl sulfoxide (DMSO, Sigma-Aldrich). Upon thawing, MEFs were cultured with medium supplemented with 10% FBS. All experiments with primary MEFs were performed at low passage number (≤ 4).

Generation of HCT116-shGMN cells

Stable HCT116-shGMN cell lines were obtained using a TRIPZ lentiviral vector carrying an inducible shRNA targeting the sequence 5'-TATGTAGTTATGTACTCTG-

3’ in the 3’ untranslated region (UTR) of GMN gene (GE Healthcare, USA). Lentiviruses were produced in 293T cells. HCT116 cells were infected twice and selected with 5μg/ml puromycin for 5 days. Resistant colonies were pooled and maintained in DMEM (Lonza) + 10% FBS (Sigma-Aldrich) + 10% penicillin/streptomycin ~~solution~~ (Invitrogen) + 0.5 μg/ml puromycin. Expression of GMN shRNA was induced with 2 μg/ml doxycyclin (Dox) for 3 days.

Genetic screening for factors modulating DNA re-replication

HCT-116 shGMN cells were cultured in μCLEAR bottom polylysine-treated 96-wells (Greiner Bio-One) in technical triplicates using medium supplemented with 2 μg/ml dox. Two controls (-dox and +dox) were seeded in every plate for normalization. 24 h after seeding. cells were transfected with individual esiRNA molecules (30 nM) from the designed esiRNA library (Sigma-Aldrich). Specific siRNAs against Luciferase (ctrl), Fbh1, Rad54 and Slx4 genes were added to the library. 72 h after seeding, cells were washed with PBS and fixed with PBS + 2% PFA for 10 min at RT. Cells were stained with 1 μg/ml DAPI (Sigma) in PBS for 3 min. Plates were analyzed in an Opera High-Content Screening System (PerkinElmer, USA) with an APO 20x, 0.7 NA water-immersion objective. Nuclei were segmented and area was evaluated with Acapella software 2.6 version (PerkinElmer, USA). >500 cells were quantified in each well. The median nuclear size in each well was quantified. Mean of control (-dox) medians was calculated and each well was normalized to this value.

siRNA and plasmid transfections

Transfections were carried out using Lipofectamine 2000 (Invitrogen) following manufacturer’s instructions. A single transfection was used for plasmids, and two transfectios for siRNA molecules (50 nM). A list of the siRNAs used can be found in Table 3.

Proliferation curves

Aliquots of 50,000 MEFs were seeded in 6-well plates in duplicates, harvested at the indicated time points and counted in a Neubauer hemocytometer.

Serum starvation and cell cycle re-entry

Cells were cultured to near 100% confluence in DMEN supplemented with 10% FBS. Then, to induce a G0 quiescent state, cells were serum starved cultured them in DMEN + 0.1% FBS for 72 hours. For cell cycle re-entry, cells were split and seeded at 50% confluence with DMEN supplemented with 20% FBS. At indicated time points, cells were pulse-labelled with 10μM BrdU pulse labelling for 30 min and harvested for ulterior analysis.

Cell cycle synchronization with thymidine

HCT116 cells were incubated in medium supplemented with 2.5 mM thymidine for 20 h to induce a G1/S block. Cells were washed and released in fresh medium for 7 h to obtain a population enriched in S+G2+M phases.

Preparation of whole cell extracts

Cells were trypsinized, collected by centrifugation (290 g/5 min), counted in a Neubauer hemocytometer, washed with PBS, lysed in Laemmli Sample Buffer (50 mM Tris-HCl pH 6.8, 10% glycerol, 3% SDS, 0.006% w/v bromophenol blue and 5% 2-mercaptoethanol) at 5000 cells/μL and sonicated using two pulses at 20% amplitude for 29 s (Branson Digital Sonifier).

Biochemical fractionation

Biochemical fractionations were performed as described (Méndez and Stillman, 2000). Briefly: Cells were resuspended at $2 \cdot 10^7$ cells/mL in buffer A (10 mM HEPES pH 7.9, 10 mM KCl, 1.5 mM MgCl2, 0.34 M sucrose, 10% glycerol, 1 mM DTT, 1 mM NaVO4, 0.5 mM NaF, 5 mM β- glycerophosphate, 0.1 mM PMSF), and incubated on ice for 5 min in the presence of 0.1% Triton X-100. Low- speed centrifugation (4 min/600 g/4°C) allowed the separation of the cytosolic fraction (supernatant) and nuclei (pellet). Nuclei were washed and subjected to hypotonic lysis in buffer B (3 mM EDTA, 0.2 mM EGTA, 1 mM DTT, 1 mM NaVO4, 0.5 mM NaF, 5 mM β- glycerophosphate, 0.1 mM PMSF, protease inhibitors cocktail) 30 min on ice. Nucleoplasmic and chromatin fractions were separated after centrifugation (4 min/600 g/4°C). Chromatin was resuspended in Laemmli Sample Buffer and sonicated twice for 29 seconds at 20% amplitude.

Immunoprecipitation and immunoblots

Cells were lysed in NP-40 buffer (150 mM NaCl, 1% NP-40, 50 mM Tris-HCl pH 8.0, 0.1 mM PMSF, Roche protease inhibitors) at $4x10^6$ cells/ml. Extracts were clarified by high-speed centrifugation (15 min/ 16000 g/ 4 C) and cleared with protein A agarose beads (Santa Cruz, USA) for 30 min. IPs were performed overnight with 3 μg of the indicated antibody. Protein A agarose beads were added to extracts and incubated for 1 h, collected by low-speed centrifugation (1 min/2500 g/4°C), washed and resuspended in Laemmli buffer.

SDS-polyacrylamide gels and immunoblotting were performed following standard protocols (Harlow and Lane, 2006). The primary antibodies used are listed in table 3. Horseradish peroxidase (HRP)-conjugated secondary antibodies (Amersham Biosciences) at 1:5000 dilution and ECL developing reagent (Amersham Biosciences) were used.

BrdU incorporation and flow cytometry

For BrdU incorporation and DNA content evaluation cells were pulse-labelled with 10 μM BrdU (Sigma) for 30 min before harvesting. Cells were fixed in 70% ethanol, treated with 2M HCl for 20 min, washed and incubated with FITC- conjugated anti-BrdU antibody (60 min/ 37C). To monitor DNA content, cells were stained overnight with 50 μg/ml propidium iodide (PI; Sigma) in PBS in the presence of 10 μg/ml RNase A (Qiagen).

For γH2AX detection, MEFs were harvested and fixed with 4% PFA (15 min/ RT) and permeabilized with 0.5% Triton-X100 in PBS (10 min/ 4C). Cells were incubated in blocking solution (1% bovine serum albumin in PBS; 0.05% Tween-20) for 15 min. Primary and secondary antibodies were incubated in blocking solution for 1 h at RT. DNA was stained with 5 μg/ml Hoestch 33342(Invitrogen) in PBS + 0,05 Triton X-100.

For apoptosis quantification, MEFs were harvested and incubated for 10 min at 37º C with 40 nM tetramethylrhodamine ethyl ester (TMRE, Sigma). Cells were then washed and resuspended in PBS. DAPI (Sigma) staining was used as viability dye. Flow cytometry was performed in a FACS Canto II cytometer (BD, San Jose, CA) and analyzed with FlowJo 9.4 (Tree Star, Ashland, OR).

For cell cycle phases sorting, MEFs were stained at 10^7 cells/ml with 5 μg/ml Hoestch 33342 (Invitrogen) for 30 min at 37ºC in DMEN + 10% FBS. Cells were washed and resuspended at 10^6 cells/ml in DMEN + 0.1% FBS. Cells were sorted by DNA content in a BD Influx sorter (BD, San Jose, CA) by the Cytometry Unit at CNIO.

Immunofluorescence

Cells were cultured in polylysine-treated coverslips. At harvesting time cells were fixed in 4% PFA (15 min/ RT) and permeabilized with 0.5% Triton-X100 in PBS (5 min/ RT). Coverslips were incubated in blocking solution (3% BSA or 5% normal donkey serum (Jackson ImmunoResearch) in PBS + 0.05% Tween 20) for 30 min. Primary and secondary antibody (1:200 dilution) incubations were performed in blocking solution for 1 h at RT. Nuclei were stained with 1 μg/ml DAPI (Sigma) in PBS for 1 minute. ProLong Gold antifade reagent was used as mounting media for IF. To visualize chromatin-bound proteins (MCMs, RPA, 53BP1, RAD51), cells were subjected to a pre-extraction step with 0.5% Triton X-100 in CSK buffer (10 mM PIPES pH 7.0, 0.1 M NaCl, 0.3 M sacarose and 3 mM MgCl2, 0.5 mM PMSF) prior to PFA fixation for 5 min at 4°C. Click-it chemistry EdU detection kit (Invitrogen) was used when indicated.

For AuroraB, pH3 and EdU stainings, images were acquired in a DM6000 B microscope (Leica microsystems, Germany). pH3- and EdU-double positive cells, G2 cells and mitotic index were scored manually. For RPA, 53BP1 and RAD51 stainings, images were captured in a SP2 (AOBS) confocal microscope (Leica microsystems, Germany). Image analysis was performed in the Confocal Microscoy Unit at CNIO. Pre-designed routines for foci or nuclei detection in Definiens Developer XD v2.5 software (Definiens, Germany) were used to evaluate either RPA or 53BP1 foci or RAD51 positive nuclei.

For microscopic analysis of colon sections, tissues were stained with 1 μg/ml DAPI (SIGMA). Samples were acquired on a TCS- SP5 (AOBS) Confocal microscope (Leica microsystems, Germany) with a 20 X HCX PL APO 0.7 N.A. dry Objective. Nuclei from Colon cripts were segmented and integral intensity was quantified by using Definiens Developer XD v2.5 software (Definiens, Germany). 312 crypt cells from 4

different colon areas were measured from each animal. 3 animals from each condition were evaluated.

When indicated, cells were cultured in μCLEAR bottom polylysine-treated 96-wells (Greiner Bio-One) in triplicates and analyzed in an Opera High-Content Screening System (PerkinElmer, USA) with an APO 20x, 0.7 NA water-immersion objective. Nuclei were detected with DAPI staining, and γH2AX or MCM intensities were measured within the nuclei mask using Acapella software (PerkinElmer, USA). For replication foci detection, HCT116 cells were pulse-labelled with 10 μM BrdU (Sigma) for 30 min previously to immunostaining. Foci detection routine was used to score BrdU foci number within each nucleus using the same software.

ssDNA detection with native BrdU staining

Cells were cultured in μCLEAR bottom polylysine-treated 24-wells (Greiner Bio-One) in triplicates. For nascent ssDNA (reversed forks) detection, cells were pulse-labeled with 10 μM BrdU (Sigma) for 10 min, washed, released in fresh medium and harvested at the indicated time points. For parental ssDNA detection, cells were pulse-labeled with 10 μM BrdU (Sigma) for 24 h, washed, released in fresh medium and harvested 24 h later. Immunodetection was conducted as described (Couch et al, 2013) with slight modifications. Cells were pre-extracted in CSK buffer + 0.5% Triton X-100 for 5 min at 4° C, fixed in 3% paraformaldehyde / 2% sucrose solution for 10 min at RT and blocked with 3% BSA in PBS + 0.05% Tween 20 15 min at RT. Cells were then incubated with mouse anti-BrdU antibody (BD Pharmingen; 1:50 dilution in blocking solution) for 60 min at 37 C followed by Alexa-488 goat anti-mouse (Invitrogen) secondary antibody (1:200 dilution in blocking solution) for 30 min at 37°C. Nuclei were stained with 1 μg/ml DAPI (Sigma).

Images were captured in Opera High-Content Screening System (PerkinElmer, USA) with an APO 20x, 0.7 NA water-immersion objective. Nuclei were segmented and BrdU intensity was assessed with Acapella software (PerkinElmer, USA).

Single-molecule analysis of DNA replication in stretched fibers

Exponentially growing cells were pulse-labeled with 50 μM CldU (20 min) followed by 250 μM IdU (20 min). Labeled cells were harvested and resuspended in cold PBS at

$0.25 \cdot 10_6$ cells/mL. 500 cells were lysed in 0.2 M Tris pH 7.4, 50 mM EDTA, 0.5% SDS 6 min at 30° C in a microscope slide into a humidity chamber. Slides were 15° tilted to stretch DNA fibers. DNA spreads were air-dried, fixed in cold 3:1 methanol: acetic acid for 2 min and refrigerated. Slides were treated with 2.5 N HCl for 30 min, washed 3 times with PBS and blocked in 1% BSA, 0.1% Triton X-100 in PBS for 1 h before incubation. For immunodetection of labeled tracks, fibers were incubated with primary antibodies for 1 h at RT and the corresponding secondary antibodies for 30 min at RT, in a humidity chamber. ProLong Gold antifade reagent (Invitrogen) was used as mounting media for IF. DNA was visualized with an anti-ssDNA antibody to assess fiber integrity.

To measure re-replicated tracks, cells were pulse-labeled with 50 μM CldU (120 min) followed by 250 μM IdU (30 min) as described (Neelsen et al, 2013). DNA fibers were incubated in stringency buffer (10 mM Tris-HCl pH 7.4; 0.4M NaCl; 0.2% Tween-20; 0.2% NP-40) for 10 min between incubations with primary and secondary antibodies (Dorn et al, 2009). Fiber images were obtained in a DM6000 B Leica microscope with an HCX PL APO 40x, 0.75 NA objective.

Fork progression rate was monitored in second-labeled (IdU) tracks. The length of 200-300 tracks was measured per condition using ImageJ software. Inter-origin distances (IODs) were measured between two contiguous origins in the same fiber. The lengths of 30-50 IODs were measured per condition. 500 total structures were measured to evaluate percentage of origin firing. 500 total green tracks were measured to evaluate percentage of re-replication. All re-replicated tracks found were measured to evaluate their length. The conversion factor used was 1 μm = 2.59 kb (Jackson and Pombo, 1998).

Histological analysis

Formalin-fixed tissue processing for histological analysis was done in the Histopathology Unit at CNIO. Tissue samples were fixed in 10% neutral buffered formalin (4% formaldehyde in solution), paraffin-embedded and cut at 3 μm, mounted in superfrost®plus slides and dried overnight. For different staining methods slides were deparaffinized in xylene and and re-hydrated through a series of graded ethanol until water. Consecutive sections were stained with hematoxylin and eosin (H&E) and

for immunohistochemistry an automated immunostaining platform was used (Ventana Discovery XT, Roche). Antigen retrieval was first performed with high or low pH buffer depending on the primary antibody (CC1m, Roche or RiboCC, Roche), endogenous peroxidase was blocked (peroxide hydrogen at 3%) and slides were then incubated with the appropriate primary antibody as detailed: rat monoclonal anti-p21 (291H; 1:10; Monoclonal Antibodies CNIO), rat monoclonal anti-p16 (327C; 1:10; Monoclonal Antibodies CNIO), rabbit polyclonal anti-Sox9 (1:800; Millipore, AB5535), rabbit monoclonal Ki67 (1:500; SP6; Master Diagnostica 000311OQD), rabbit polyclonal anti-Phospho Histone H3 (1/500; Millipore 06-570), rabbit polyclonal anti-Cleaved caspase 3 (1:750; Cell Signaling 9661) and mouse monoclonal anti-γH2AX (Millipore, 05-636; 1:100). After the primary antibody, slides were incubated with the corresponding secondary antibodies (rabbit anti rat, Vetor Labs) and visualization systems when needed (OmniRabbit, Ventana, Roche) conjugated with horseradish peroxidase. Immunohistochemical reaction was developed using using 3,30-diaminobenzidine tetrahydrochloride (DAB) as a chromogen (Chromomap DAB, Ventana, Roche or DAB solution, Dako) and nuclei were counterstained with Carazzi's hematoxylin. Finally, the slides were dehydrated, cleared and mounted with a permanent mounting medium for microscopic evaluation. Tissue slides were digitalized using a Mirax Scan or Axio Scan.Z1 scanners (Carl Zeiss, Germany) and images captured with the Zen Software (Zeiss). Image analysis and quantification was performed using AxioVision rel 4.6 digital image software (Carl Zeiss, Germany). Areas of positive staining were normalized to the total analyzed area. SOX9 positive nuclei were segmented after detection. CA3 and pH3 positive cells were scored manually.

Genome-wide data analyses

We analyzed available data in the NCBI Gene Expression Omnibus (GEO) database for ORC2 ChIP-Seq (GEO accession number GSE70165; Miotto et al, 2016) RAD51 ChIP-Seq (GEO accession number GSE91838) and short-nascent-strand (SNS) data (GEO accession number GSE46189; Picard et al, 2014). Data was analyzed with "Intersect intervals" tool from BEdTools package (Quinlan and Hall, 2010) in Galaxy website. The following requirements were used in overlap analyses: minimum overlap of 10% , reciprocal and unique overlap (-u).

Tables

Table 1. Primers for mice genotyping

Primer	Sequence	Locus
Col-A	GCACAGCATTGCGGACATGC	Col1A1
Col-B	CCCTCCATGTGTGACCAAGG	Col1A1
Col-C	GCAGAAGCGCGGCCGTCTGG	Col1A1
ROSA-1	GCGAAGAGTTTGTCCTCAACC	Rosa26
ROSA-2	GGAGCGGGAGAAATGGATATG	Rosa26
ROSA-3	AAAGTCGCTCTGAGTTGTTAT	Rosa26

Table 2. Primers for qPCR

Primer	Sequence	Gene
CDC6-Fw	ACACACTGTTTGAGTGGCCGT	mCdc6
CDC6-Rev	GCTTCAAGTCTCGGCAGAATTC	mCdc6
CDT1-Fw	TAGTACCCCAGATGCCAAGG	mCdt1
CDT1-Rev	GTAGGACAAGGCCTGGGAGA	mCdt1
GAPDH-Fw	TGAAGCAGGCATCTGAGGG	GAPDH
GAPDH-Rev	CGAAGGTGGAAGAGTGGGAG	GAPDH
FBH1-Fw	CCCACACCCACGTCTTCTAT	hFbh1
FBH1-Rev	ATGCCACTCTGATGGTTTCC	hFbh1
RAD54-Fw	TTTAATTAGCCGGTCCTCTCAA	hRad54
RAD54-Rev	ACTGCTGGATTTCCGTTTCCT	hRad54

Table 3. siRNAs

siRNA	Sequence	Gene
FBH1-1	GGGAUGUUCUUUUGAUAAAUU	hFbh1
FBH1-2	GUGCCUAUUUGGUGUAAGA	hFbh1
RAD51-1	GAGCUUGACAAACUACUUC	hRad51
RAD51-2	UCUUCCUGUUGUGACUGCCAGGAUA	hRad51
MUS81-1	CAGCCCUGGUGGAUCGAUA	hMus81
MUS81-2	CAUUAAGUGUGGGCGUCUA	hMus81
SMARCAL1-1	GCU UUGACCUUCUUAGCAA	hSmarcal1
SMARCAL1-2	AAGCAAGGCCCAUCCCAAA	hSmarcal1
RAD51AP1	GCAGUGUAGCCAGUGAUUA	hRad51AP1
RAD54	AAAUGCUUCAUGCUGACUGCUGUCC	hRad54

Table 4. Primary antibodies

Antibody	Use	Supplier	Ref/Catalogue #
hMCM2	WB	Méndez Lab	Ekholm-Reed et al, 2004
hMCM3	WB	Méndez Lab	Ekholm-Reed et al, 2004
mMCM3	WB, IF	Méndez Lab	Álvarez et al, 2015
hMCM4	WB	Méndez Lab	Ekholm-Reed et al, 2004
mMCM4	WB, IF	Méndez Lab	Bua et al, 2015
hMCM6	WB	Méndez Lab	Ekholm-Reed et al, 2004
mMCM6	WB	Méndez Lab	Bua et al, 2015
PSF2	WB	Méndez Lab	Aparicio et al, 2009
CDC45	WB	Méndez Lab	Aparicio et al, 2009
ORC1	WB	Méndez Lab	Mendez et al, 2002
ORC2	WB, IP	Méndez Lab	
CDC6	WB	Millipore	05-550
CDT1	WB	Millipore	07-1383
HA-TAG	WB	Cell Signaling	2367
FLAG-TAG	WB	Cell Signaling	2368
SMC1	WB	Bethyl	A300-055A
SMC1	WB	Losada Lab	Remeseiro et al, 2012
MEK2	WB	BD	610236
H3	WB	Abcam	ab1791
GMN	WB	Santa Cruz	sc-13015
BrdU-FITC conjugated	FACS	BD	556028
BrdU (CldU)	IF	Abcam	ab6326
BrdU (Idu)	IF	BD	347580
ssDNA	IF	Millipore	MAB3034
pSer10-h3	WB	Losada Lab	Kimura and Hirano, 2000
pSer10-H3	WB, IF	Abcam	ab14955
pSer10-H3	IHC	Millipore	06-570
γH2AX	WB, IF, IHC, FACS	Millipore	05-636
53BP1	IF	Novus Biologicas	NB-100-304
RPA	IF	Cell Signaling	2208
ps4/s8-RPA32	WB	Bethyl	A300-245A
pS345-CHK1	WB	Cell Signaling	2348
pS15-P53	WB	Cell Signaling	92845
pTyr15-CDK1	WB	Cell Signaling	9111
Cleaved Caspase-3	IHC	Cell Signaling	9661
Ki67	IHC	Master Diagnostica	0003110QD
p16	IHC	Monoclonal core unit CNIO	
p21	IHC	Monoclonal core unit CNIO	

SOX9	IHC	Millipore	AB5535
RAD51	WB, IF, IP	Santa Cruz	sc-8349
RAD51AP1	WB	Thermo Fisher	PA5-30395
SMARCAL1	WB	Millipore	ABE1836
MUS81	WB	Santa Cruz	MTA30 2G10/3
AURORA B	IF	BD	611082

Table 5. Secondary antibodies

Antibody	Use	Supplier	Ref/Catalogue #
Horseradish peroxidase–linked ECL anti-rabbit IgG	WB	GE Heathcare	NA934V
Horseradish peroxidase–linked ECL anti-mouse IgG	WB	GE Heathcare	NA931V
anti-rabbit IgG AF-488 (chicken)	IF	Invitrogen Molecular Probes	A21206
anti-rabbit IgG AF-594 (goat)	IF	Invitrogen Molecular Probes	A11012
anti-mouse IgG AF-488 (goat)	IF	Invitrogen Molecular Probes	A21121
anti-mouse IgG AF-594 (donkey)	IF	Invitrogen Molecular Probes	A21203
anti-mouse IgG2a AF-647 (goat)	IF	Invitrogen Molecular Probes	A201241
anti-rat IgG AF-594 (goat)	IF	Invitrogen Molecular Probes	A11007

RESULTS

RESULTS CHAPTER 1

Mouse models for CDC6 and/or CDT1 overexpression

Genetically engineered mouse strains that allow the inducible overexpression of Cdc6 or Cdt1 were generated in the laboratory as part of previous studies (S. Búa, Doctoral thesis, UAM 2013). These strains carried cDNAs encoding HA-tagged CDC6 protein or FLAG-tagged CDT1 protein at the Collagen 1 A1 (Col1A1) locus, under the control of a tetracycline-responsive element (TetO). The transactivator rtTA was *knocked-in* into the Rosa26 locus, and it requires the addition of tetracycline (or its derivative doxycycline, dox) to activate expression of the TetO-controlled transgene. This strategy allows ubiquitous overexpression of the transgene in a dox-dependent manner (Beard et al, 2006; Fig 11A, B). The resultant strains, named TetO-Cdc6 and TetO-Cdt1, could be crossbred to generate TetO-Cdc6+Cdt1 mice, which overexpress both transgenes in combination. The efficiency of Cdc6 and/or Cdt1 overexpression was evaluated in mouse embryonic fibroblast (MEFs) derived from each model (Fig 11C; S. Búa Doctoral thesis, UAM 2013). Exogenous proteins are overexpressed approximately 10- to 20-fold over endogenous levels after 24h of induction. These protein levels are similar to those reported in human cancer cells (5- to 20-fold; Tatsumi et al, 2006).

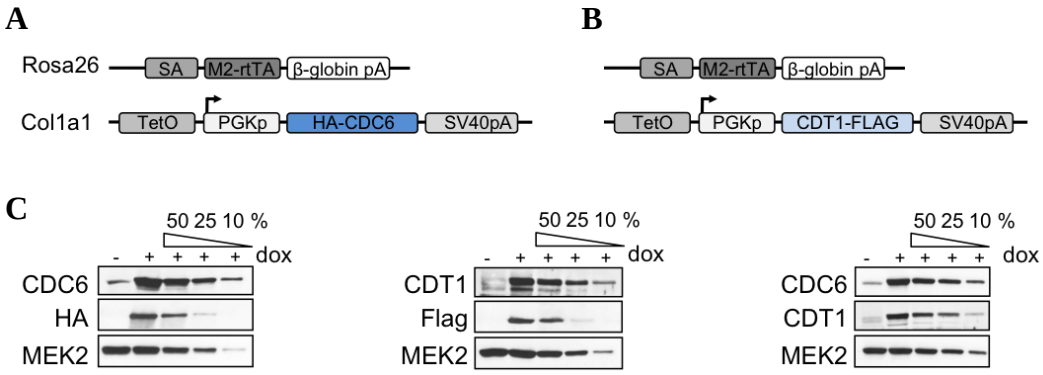

FIGURE 11. **A**. Schematic of the TetO-Cdc6 genetic design. Dox-responsive M2 rtTA is constitutively expressed from the Rosa26 promoter (R26p). HA-tagged Cdc6 cDNA is under the control of the rtTA-responsive operator (TetO) at the Col1A1 locus. pA, polyadenylation signal. **B.** Schematic for the TetO-Cdt1 genetic design, similar to that in (A), except that Cdt1 cDNA was tagged with FLAG. TetO-Cdc6+Cdt1 mice were obtained by crossbreeding TetO-Cdc6 and TetO-Cdt1 strains. **C.** Immunoblots showing expression levels of CDC6 and CDT1 proteins in MEFs derived from TetO-Cdc6 (left), TetO-Cdt1 (middle) and TetO-Cdc6+Cdt1 mice. In each case, endogenous protein levels are shown in lane 1. Lane 2 shows the levels in cells incubated with 1μg/ml dox for 24h. Lanes 3-5 show 50, 25 and 10% of the amount of sample loaded in lane 2. MEK2 levels are shown as loading control.

Exogenous HA-CDC6 and CDT1-FLAG are regulated as endogenous proteins

First, the dependency on dox for transgene expression was confirmed using antibodies to the HA and FLAG tags. Immunoblots in whole cell extracts from MEFs were negative for HA and FLAG signal in the absence of dox, indicating that the TetO system is not leaky (Fig 11C). In addition, CDC6 and CDT1 levels in transgenic MEFs not treated with dox were comparable to those in WT MEFs (Fig 12A), confirming that transgenes were only expressed upon dox addition.

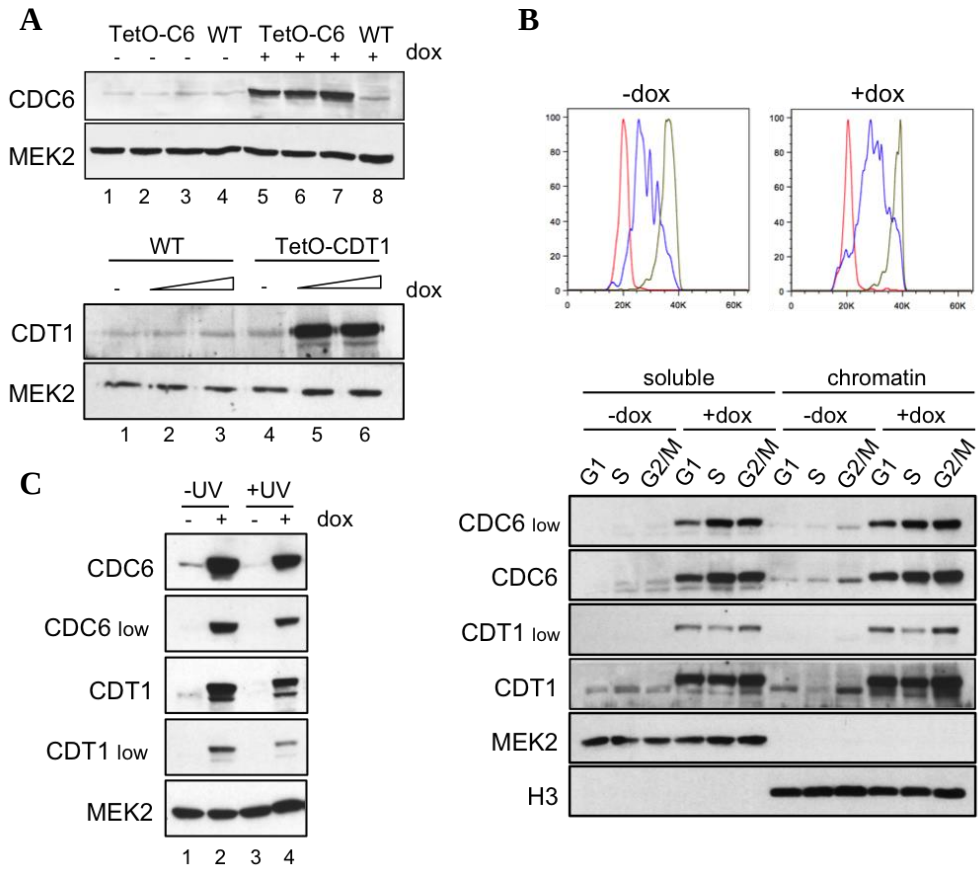

FIGURE 12. **A.** Immunoblots showing expression levels of CDC6 and CDT1 proteins in MEFs derived from TetO-Cdc6, TetO-Cdt1 and WT littermates. For TetO-Cdc6 model, 3 different clones are compared to one WT clone. Lanes 1 to 4 shown endogenous CDC6 levels in WT and Tg clones. Lanes 5 to 8 shows the levels in cells incubated with 1µg/ml dox for 24h. For TetO-Cdt1 model, one WT clone (lanes 1 to 3) is compared to 1 transgenic clone (lanes 4 to 6). Lanes 1 and 4 show endogenous CDT1 levels for WT and TetO-Cdt1 clones. Lanes 2 and 5 shows the levels in cells incubated with 1µg/ml dox for 24h. Lanes 3 and 6 shows the levels in cells incubated with 2µg/ml dox for 24h. MEK2 levels are shown as loading control. **B.** Upper panel: DNA content profiles of different fractions obtained after cell sorting of TetO-Cdc6+Cdt1 MEFs treated or untreated with dox for 24h. Lower panel: Immunoblot detection of the indicated proteins after biochemical fractionation of sorted cell fractions. Soluble and chromatin-bound fractions are shown. Soluble MEK2 and chromatin-bound H3 serve as fractionation controls. **C.** Immunoblot detection of CDC6 and CDT1 proteins after UV irradiation in TetO-Cdc6+Cdt1 MEFs. Lanes 1 and 2 show levels in control cells without UV pulse. Lanes 3 and 4 show protein levels 30 minutes after a 50J/m2 UV pulse. Lanes 2 and 4 are cells pre treated with dox for 24h. MEK2 levels are shown as loading control.

Next, several control experiments were performed to evaluate whether exogenous HA-CDC6 and CDT1-FLAG proteins are still subject to the control mechanisms that regulate their endogenous counterparts. First, we investigated the accumulation and chromatin-binding dynamics of exogenous proteins in the cell cycle. Control and dox-treated TetO-Cdc6+Cdt1 MEFs were sorted in G1, S and G2/M phases by DNA content and subjected to a biochemical fractionation. Exogenous proteins fluctuated in the cell cycle as their endogenous counterparts (Fig 12B). Both proteins distributed between in soluble and chromatin fractions and their association to chromatin was similar to the endogenous proteins. As expected, CDC6 was less abundant in G1 and remained bound to chromatin in S and G2/M phases (Fig 12B; Mendez and Stillman, 2000), whereas chromatin-bound CDT1 was degraded in S phase (Fig 12B; Nishitani et al, 2006). Next, we checked transgenic protein regulation upon DNA damage. As reported for endogenous proteins (Higa et al, 2006; Hall et al, 2007), overexpressed CDC6 and CDT1 were partially degraded in cells irradiated with UV (Fig 12C). These experiments show that even if they are expressed at higher levels, exogenous HA-CDC6 and CDT1-FLAG proteins are subject to regulatory mechanisms.

CDC6 overexpression enhances MCM chromatin loading

To test whether CDC6 or CDT1 overexpression could modify the amount of MCM complexes loaded onto DNA, biochemical fractionations were performed in TetO-Cdc6, TetO-Cdt1 and TetO-Cdc6+Cdt1 MEFs. As described in the initial characterization of these strains (S. Búa, Doctoral thesis, UAM 2013), CDC6 but not CDT1 overexpression was sufficient to increase the levels of chromatin bound-MCM complex (Fig 13A, lanes 7,8 and 9,10). Cooperation was not observed, since the combined overexpression of CDC6 and CDT1 did not further increase MCM loading (Fig 13A, lanes 8 and 12). This effect of HA-CDC6 protein was confirmed by immunofluorescence detection of chromatin-bound MCM3 protein (Fig 13B). These results suggest that CDC6 is a limiting factor for origin licensing.

The protein levels of other components of the licensing machinery or the CMG helicase remained constant after CDC6 or CDT1 overexpression (Fig 13C), indicating that MEFs do not respond to excessive origin licensing by downregulating pre-RC or CMG proteins or by upregulating the licensing inhibitor GMN.

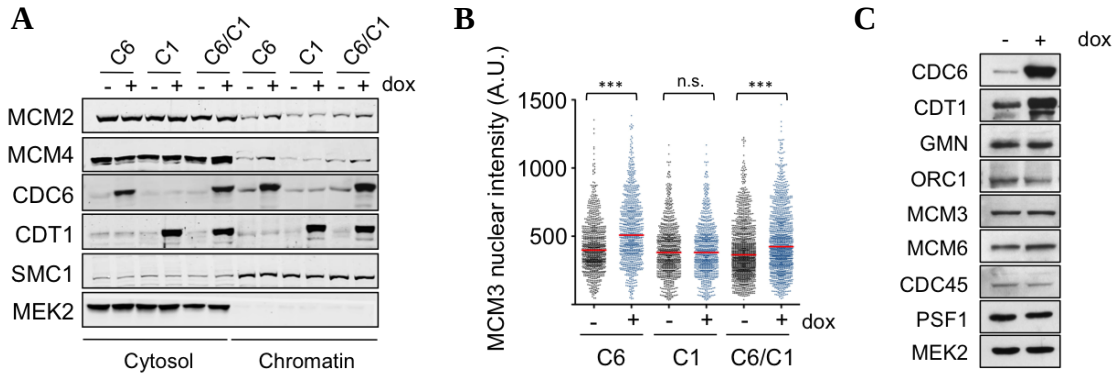

FIGURE 13. **A**. Immunoblot detection of the indicated proteins after biochemical fractionation of TetO-Cdc6 (C6), TetO-Cdt1 (C1) and TetO-Cdc6+Cdt1 (C6/C1) MEFs incubated with or without dox for 24 h. Soluble and chromatin-bound fractions are shown. Soluble MEK2 and chromatin-bound SMC1 serve as fractionation controls. **B.** High-throughput microscopy (HTM) acquisition of fluorescence intensity corresponding to chromatin-bound MCM3 protein in TetO-Cdc6 (C6), TetO-Cdt1 (C1) and TetO-Cdc6+Cdt1 (C6/C1) MEFs. Three separate experiments were conducted (>900 nuclei/condition) and a representative result is shown. p-values were calculated using Anova (Kruskal-Wallis test followed by Dunn's post-test; ***, p<0.001; n.s., not significant). **C.** Immunoblot detection of the indicated proteins in TetO-Cdc6+Cdt1 MEFs cultured in the presence of dox for 24h. MEK2 levels are shown as loading control. The experiment was conducted three times with similar results; one example is shown.

Combined CDC6 and CDT1 overexpression triggers re-replication in MEFs

To test the effects of CDC6 and CDT1 overexpression in primary cells, MEFs of the three genotypes were cultured in the absence or presence of dox. Incorporation of BrdU and cell cycle distribution were assessed by flow cytometry at different times (24, 48 and 72 hours). No defects in BrdU incorporation or cell cycle distribution were observed in TetO-Cdc6 and TetO-Cdt1 MEFs at any time point (Fig 14 and 15). In contrast, TetO-Cdc6+Cdt1 MEFs accumulated a population of BrdU-negative cells with DNA content >2C but <4C, consistent with partially re-replicated DNA (Fig 14, red gates). This population was increased by 5-fold in TetO-Cdc6+Cdt1 treated with dox for 24h. The percentage of cells undergoing re-replication was not as high after 72h (2.5-fold increase over control cells), but this could be explained by the high confluence of cells in the plate at this late time point, which slows down cell proliferation (Fig 14). Quantification of the cell cycle phases revealed a decrease in the percentage of G1 cells at 24h, (Fig 15). It should be noted that in primary MEF cultures, a small population of tetraploid cells frequently coexists with a majority of diploid cells. Importantly, Cdc6 and Cdt1 overexpression did not induce endoreplication that would result in tetraploidization, as the S and G2 phases of the tetraploid cell cycle were invariant in all strains independent of dox treatment (Fig 15).

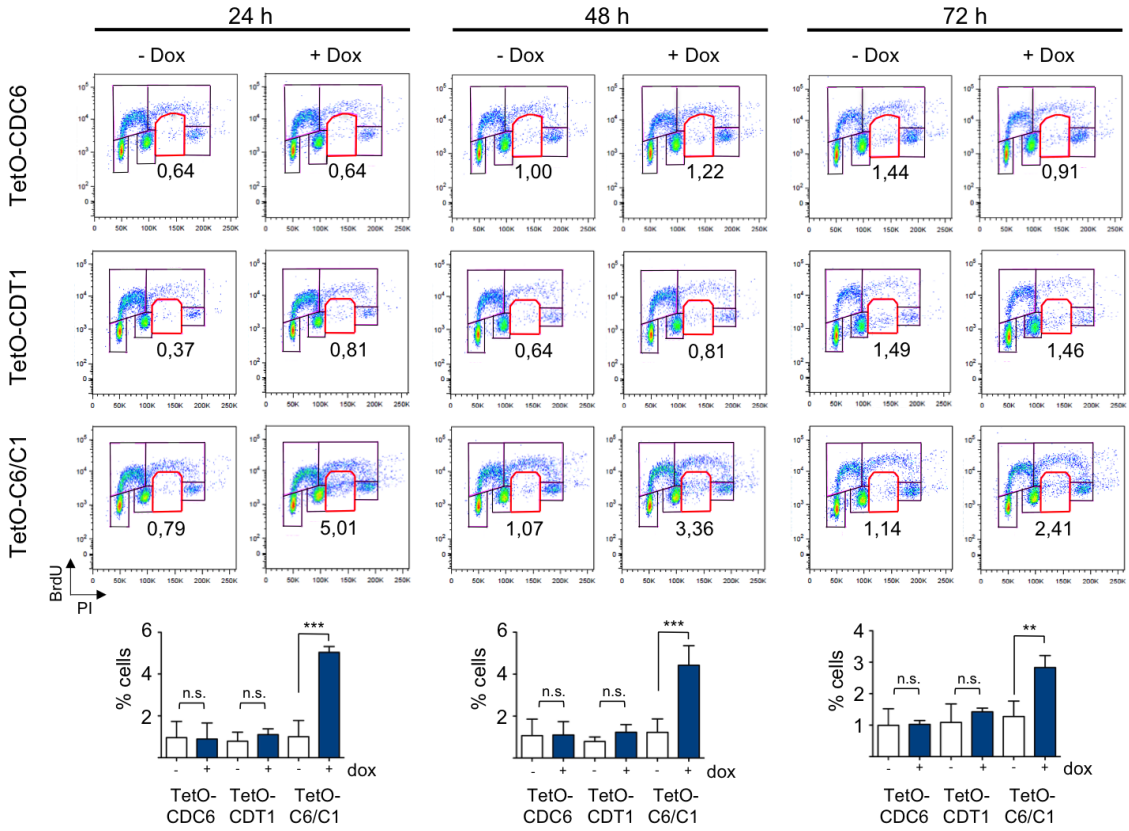

FIGURE 14. Flow cytometry graphs showing BrdU incorporation vs DNA content (propidium iodide, PI) in TetO-Cdc6, TetO-Cdt1 and TetO-Cdc6+Cdt1 MEFs grown in media with or without dox at 24, 48 and 72 hours. The red gate represents a population of cells displaying BrdU-negative cells with DNA content between 2C and 4C. Histograms show the percentage of cells within this gate (mean value and SD; n=3 assays in each case). Results were analyzed with one-way Anova and Bonferroni's post test; ***, $p<0.001$; n.s.= not significant.

To confirm the existence of re-replication upon combined (but not individual) CDC6 and CDT1 overexpression, we used an adaptation of the 'stretched DNA fibers' assay that allows the detection of origin refiring events. In this experiment, cells are pulse-labelled sequentially with two thymidine analogues that are later detected by immunofluorescence (Dorn et al, 2009; Neelsen et al, 2012). To maximize the chances of "capturing" events of origin refiring, cells were first pulsed with CldU (magenta) for 2 h and then with IdU (green) for 30 min. Active replication forks labelled at this time are observed as long magenta tracks followed by shorter green tracks. If an origin of replication were re-activated in any DNA region already replicated during the first pulse, a short green track would be found within the longer magenta track (Fig 16A). Using this technique, we found an increased percentage of re-replicated tracks only when CDC6 and CDT1 overexpression was combined (Fig 16A), confirming the necessary cooperation of both proteins to induce re-replication in primary cells.

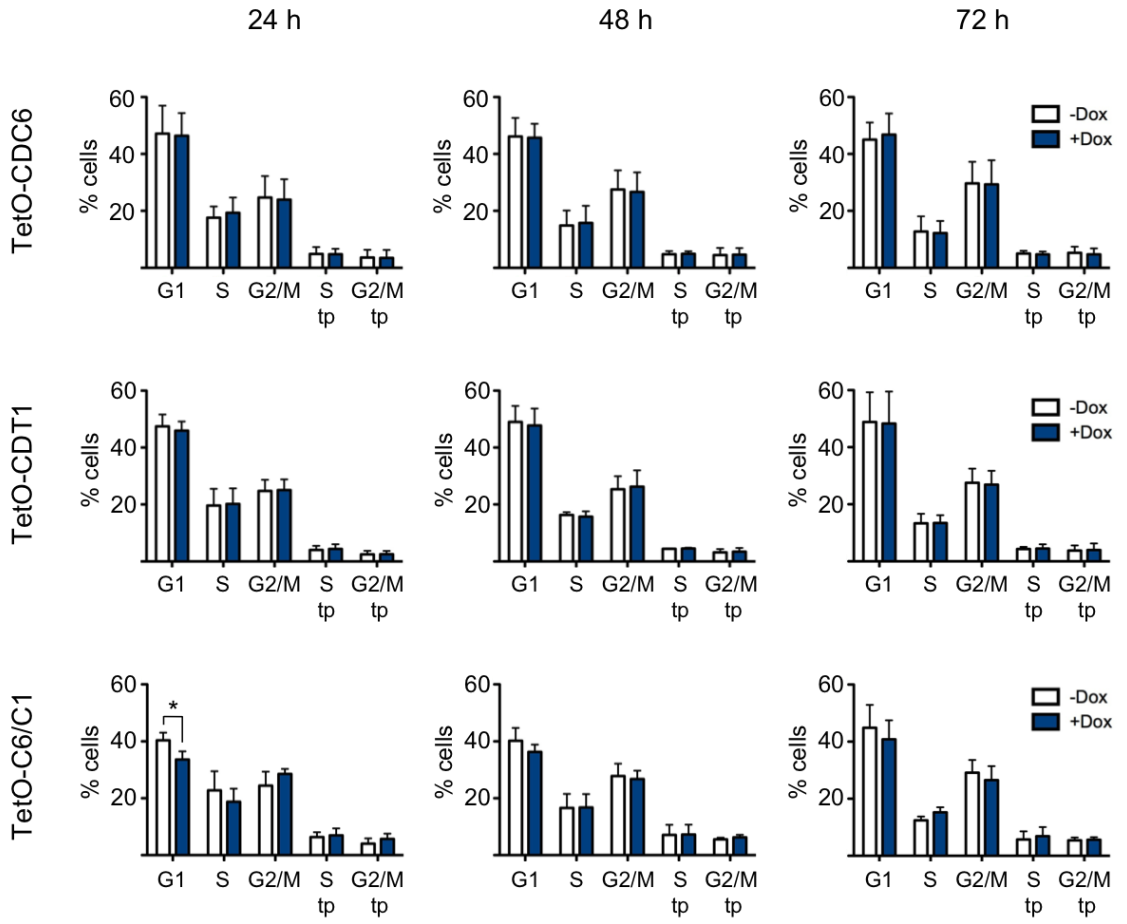

FIGURE 15. Cell cycle distribution assessed by DNA content of TetO-Cdc6, TetO-Cdt1 and TetO-Cdc6+Cdt1 MEFs cultured in the absence or presence of dox for 24, 48 and 72 h (n= 3 assays/strain). Histograms show the mean percentage values and SD of cells in each phase. White bars represent control MEFs, blue bars represent dox-treated MEFs. No statistically significant differences were detected between –dox and +dox growing conditions in any population, except when indicated. Results were analyzed with one-way Anova and Bonferroni's post test; *p<0.05; n.s.= not significant. tp=tetraploid.

It has been described that upon GMN depletion, re-replication mainly occurs from cells in the G2 phase of the cell cycle (Klotz-Noack et al, 2012). To check whether this is also the case after CDC6 and CDT1 overexpression, EdU incorporation was monitored in cells stained with anti-pSer10-H3. This antibody results in specific staining patterns in G2 and mitosis (Hendzel et al, 1997). In TetO-Cdc6+Cdt1 MEFs, a 3-fold increase in the percentage of cells positive for G2-specific pSer10-H3 and EdU incorporation was observed (Fig 16B). This result reflects the existence of unscheduled DNA replication during G2.

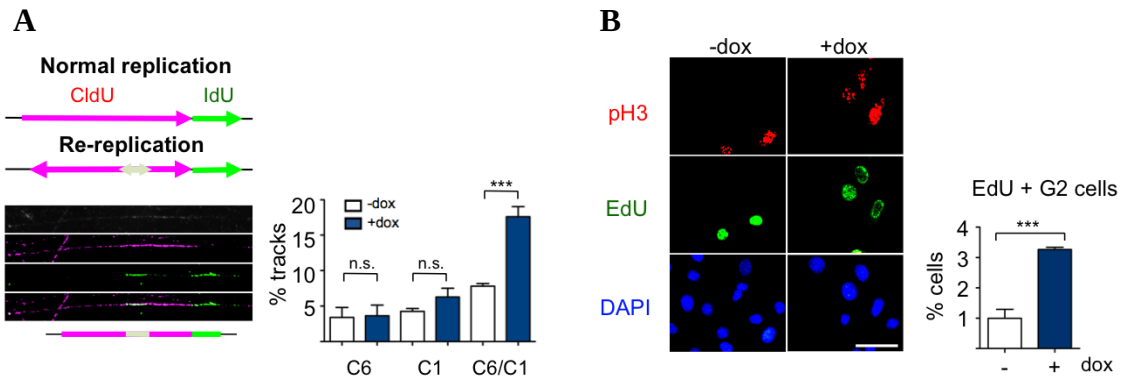

FIGURE 16. **A.** Detection of origin re-firing events using stretched DNA fibers. Cells are pulse-labelled consecutively with CldU (2h; magenta) and IdU (30 min; green). A normal fork results in a magenta-green track in the fibers, whereas a re-fired origin creates a short green track over a longer magenta track. Histogram shows the mean percentage values and SD of re-firing events (re-replicated tracks relative to the total number of green tracks) in TetO-Cdc6 (C6), TetO-Cdt1 (C1) and TetO-Cdc6+Cdt1 (C6/C1) MEFs grown in media with or without dox (n= 2 assays/condition; 488-532 green track measurements/ condition in each assay). One-way Anova followed by Bonferroni's post test was applied; ***p<0.001; n.s., not significant. **B.** Representative images of TetO-Cdc6+Cdt1 MEFs, pulse-labelled with EdU and immunostained for phosphorylated H3 (pH3). DNA was counterstained with DAPI. Histogram shows the mean percentage values and SD of cells positive for EdU and pH3 (n=4 assays. >500 cells/condition were scored in each case. Statistical significance was calculated using Student's t-test; ***, p<0.001).

Taken together, these results suggest that combined CDC6 and CDT1 overexpression induces partial DNA re-replication in primary MEFs.

CDC6 and CDT1 overexpression does not affect S phase entry from quiescence

To assess whether CDC6 and CDT1 deregulation would affect entry into S-phase in a context different from mitotic cell cycles, transgenic MEFs were driven to a G0 state by contact inhibition and serum starvation. After 72h in starvation, MEFs were released into normal medium in the absence or presence of dox, and BrdU incorporation was monitored at different time points (Fig 17A, 18A). CDC6 overexpression did not affect the dynamics of cell cycle re-entry, as previously described (S. Búa, Doctoral thesis, UAM 2013; Fig 17B). The same result was found after CDT1 overexpression (Fig 17C). The combined deregulation of CDC6 and CDT1 proteins neither affected the kinetics of S phase entry (Fig 18C, D) nor increased re-replication at noticeable levels (Fig 18C). It should be noted that HA-CDC6 protein was totally degraded, and CDT1-FLAG was downregulated in G0 (Figures 17D and 18B; Petersen et al, 2000; Sugimoto et al, 2008). The levels of both proteins progressively increased during cell cycle re-entry (Figures 17D, and 18B) and by 24h post-release their levels were similar to those of the asynchronous population. Re-replication was not observed in this experimental

setting, probably because of the limited time in which cells were exposed to high levels of CDC6 and CDT1. This result indicates that CDC6 and CDT1 are properly regulated during cell cycle exit and re-entry, and reinforces the notion that both are needed to promote DNA re-replication.

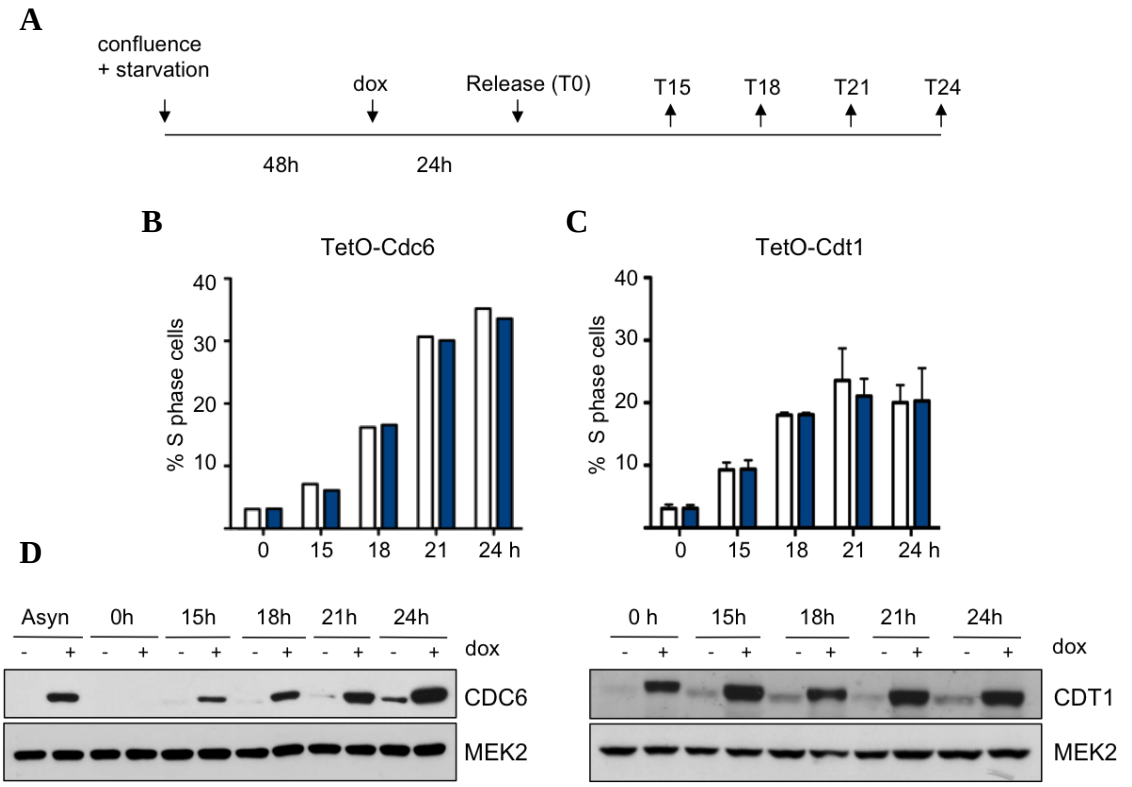

FIGURE 17. **A.** Schematic representation of serum starvation and cell cycle re-entry experiment. **B.** Quantification of TetO-Cdc6 BrdU-positive cells at indicated time points corresponding to MEFs growing in media with (blue bars) or without (white bars) dox. **C.** Same as in B for TetO-Cdt1 MEFs. Histograms show the mean percentage values and SD of BrdU-positive cells. No statistically significant differences were detected at any time point. (n=2 assays. Statistical significance was calculated using Student's t-test). **D.** Left, immunoblot detection of CDC6 in TetO-Cdc6 MEFs at the indicated time points. Right, immunoblot detection of CDT1 in TetO-Cdt1 MEFs at the indicated time points. MEK2 levels are shown as loading control.

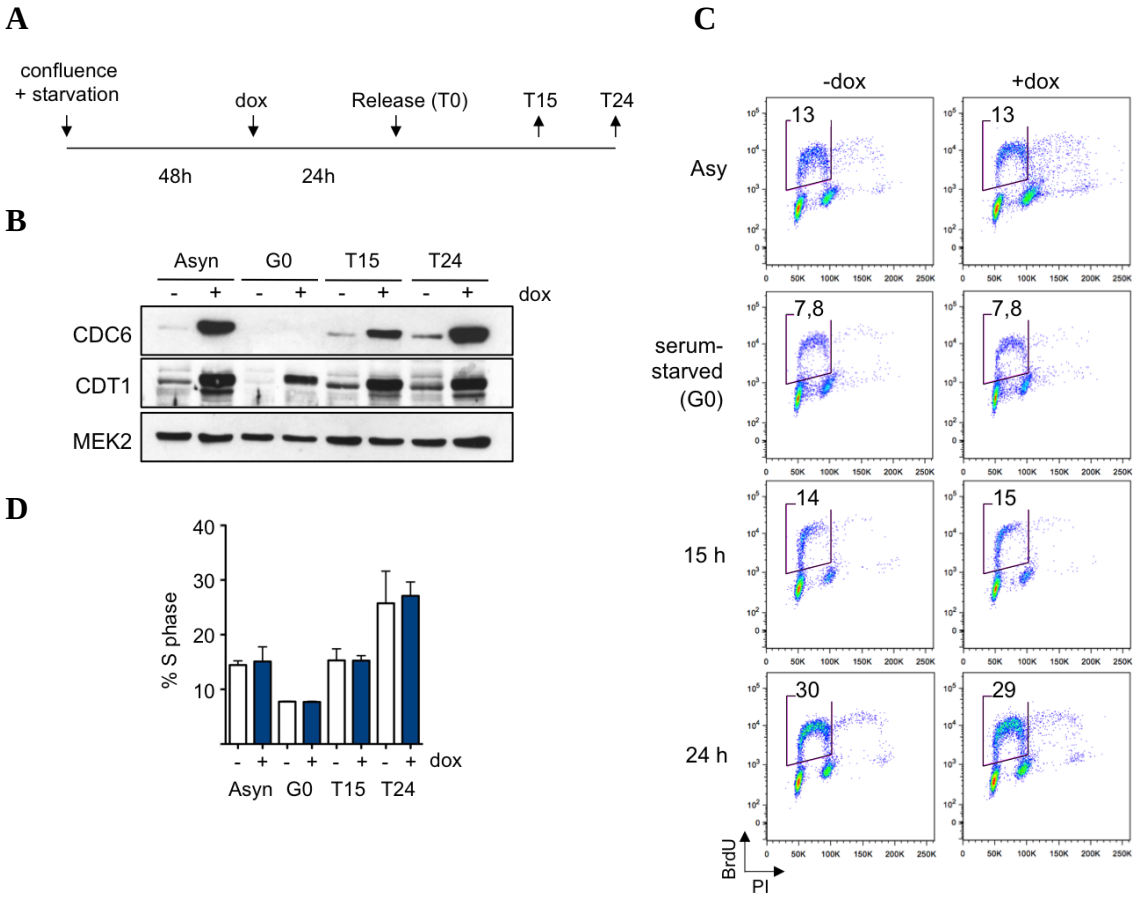

FIGURE 18. **A.** Schematic representation of serum starvation and cell cycle re-entry experiment. **B.** Immunoblot detection of CDC6 and CDT1 on TetO-Cdc6+Cdt1 MEFs at indicated time points growing in media with (+) or without (-) dox. MEK2 levels are shown as loading control. **C.** Flow cytometry graphs showing BrdU incorporation (FITC) vs DNA content (propidium iodide, PI) in TetO-Cdc6+Cdt1 MEFs grown in media with or without dox at indicated time points. Gates show BrdU positive S phase cells. **D.** Quantification of TetO-Cdt1 BrdU positive S phase MEFs at indicated time points corresponding to MEFs growing in media with (blue bars) or without (white bars) dox. Histogram shows the mean percentage values and SD of positive cells. No statistically significant differences were detected at any time point. (n=2 assays. Statistical significance was calculated using Student's t-test).

Replication dynamics after CDC6 and CDT1 overexpression

To evaluate how CDC6 and CDT1 overexpression affected DNA replication dynamics, we used the stretched DNA fiber assay to measure fork rate (FR) and inter-origin distance (IOD) at single-molecule level. FR serves as an indication of the velocity of ongoing forks. In turn, the IOD is proportional to the frequency of origin activation. A schematic of the assay and examples of commonly observed structures are depicted in Fig 19A, B.

These analyses of replication parameters revealed that TetO-Cdc6 MEFs display shorter IOD after CDC6 expression, relative to the control growing conditions in the absence of

dox (79 Kb vs 149 Kb; Fig 19C, left panel). This effect was correlative with the increase in MCM loading, as it was also observed in TetO-Cdc6+Cdt1 cells but not in TetO-Cdt1 cells (Fig 19C middle and right panels). Therefore, the extra origins licensed by CDC6 overexpression are functional and can be activated during S phase. FR was decreased in TetO-Cdc6 and TetO-Cdc6+Cdt1 cells (1.4 vs 0.74 Kb/min and 1.4 vs 1.1 Kb/min, respectively) while it did not change upon CDT1 overexpression (Fig 19D). A direct relationship between FR and IOD is expected (Zhong et al, 2013) as exacerbated origin activation affects the dNTPs pool, and/or could activate the checkpoint response, slowing down active forks (Petermann et al, 2010; Bester et al, 2011). At least in the case of TetO-Cdc6+Cdt1 MEFs, activation of the DNA damage checkpoint in response to re-replication could also contribute to the observed effects on fork progression and origin activity.

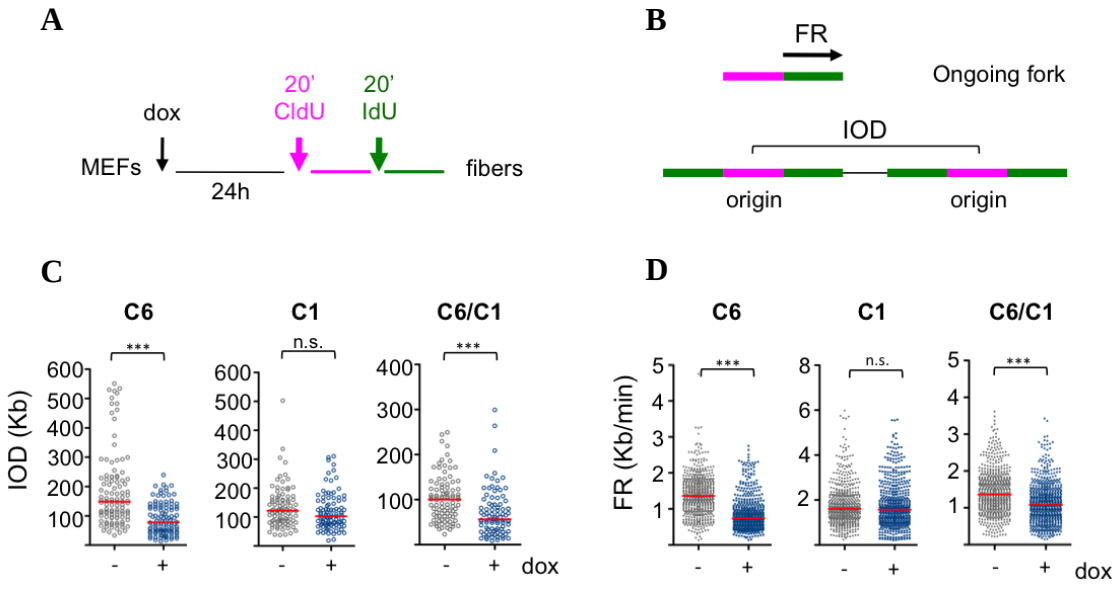

FIGURE 19. A. Schematic representation of DNA fiber experiment. **B.** Structures observed and measurements in DNA fiber assay. **C.** Inter-origin distance (IOD) in TetO-Cdc6 (C6), TetO-Cdt1 (C1) and TetO- Cdc6+Cdt1 (C6/C1) MEFs grown in media with or without dox. Data from two separate experiments are pooled (n=88-106 measurements/condition; p-values were calculated with Mann-Whitney test; ***, p<0.001; n.s., not significant). **D.** Fork rate (FR) values in the same MEFs used in (C). Data from two separate experiments are pooled (n=584-716 measurements/condition; p-values were calculated with Mann-Whitney test; ***, p<0.001; n.s., not significant).

Re-replication induces replication stress and DNA damage

As mentioned in the Introduction, re-replication induces RS and DNA damage. In addition, at least one report has suggested that CDT1 deregulation could also induce chromosomal damage in the absence of re-replication (Tatsumi et al, 2006). To evaluate

these possibilities we measured the levels of γH2AX, the phosphorylated form of H2A that serves as a marker of RS and DNA damage, using HTM detection. Only dox-treated TetO-Cdc6+Cdt1 MEFs displayed increased levels of γH2AX (Fig 20A). γH2AX signal did not change in TetO-Cdt1 MEFs, suggesting that in our experimental conditions, CDT1 overexpression is no sufficient to induce significant chromosomal damage.

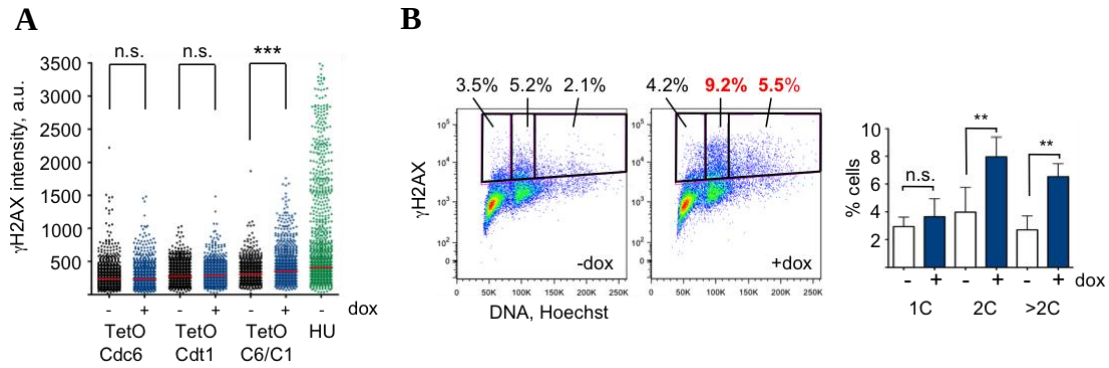

FIGURE 20. A. HTM acquisition of γH2AX fluorescence intensity in TetO-Cdc6, TetO-Cdt1 and TetO-Cdc6+Cdt1 MEFs grown in media with (blue dots) or without (black dots) dox. As a positive control, MEFs were treated with 2.5 mM HU for 3h (green dots). A representative assay is shown (n=3 assays; >1000 nuclei/condition in each assay). Statistical significance was assessed using Anova (Kruskal-Wallis test followed by Dunn's post-test; ***, p<0.001; n.s, not significant). **B.** Flow cytometry analysis of γH2AX vs DNA content (Hoechst) in TetO-Cdc6+Cdt1 MEFs. Gates indicate γH2AX-positive cells with DNA content <2C, 2C and >2C. Histogram shows mean percentage values and SD of γH2AX-positive cells in each gate (n=3 assays). Statistical significance was assessed with One way Anova and Bonferroni's's post test; **, p<0.01; n.s., not significant.

To confirm that DNA re-replication was the cause of DNA damage observed in TetO-Cdc6+Cdt1 cells, γH2AX signal and DNA content were simultaneously analyzed by flow cytometry. As expected, the vast majority of γH2AX-positive cells had 2C or >2C DNA content (Fig 20B). Importantly, a double IF staining showed that γH2AX foci colocalized with 53BP1 protein in a high percentage in dox-treated TetO-Cdc6+Cdt1 MEFs, confirming the presence of DNA DSBs (Fig 21A). We also confirmed that re-replication induced accumulation of ssDNA, as the percentage of cells positive for RPA staining was increased (Fig 21B; S. Búa, Doctoral thesis, UAM, 2013).

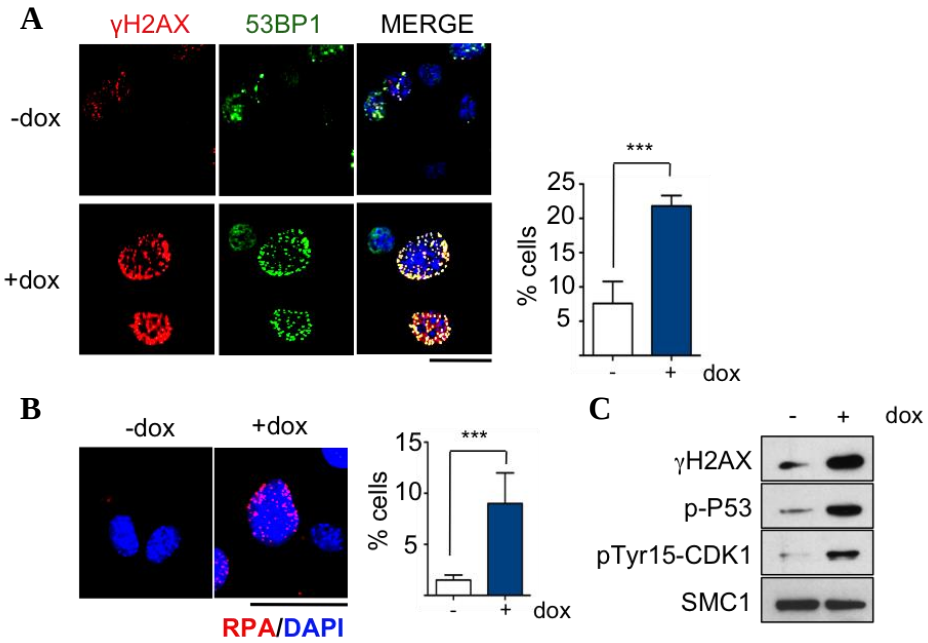

FIGURE 21. A. Representative images of control and dox-treated TetO-Cdc6+Cdt1 cells immunostained for γH2AX (red) and 53BP1 (green) proteins. DNA was counterstained with DAPI (blue). Scale bar, 25 μm. Histogram shows the mean percentage values and SD of TetO- Cdc6+Cdt1 MEFs positive for both γH2AX and 53BP1 foci. White bar, control MEFs. Blue bar, dox-treated MEFs (n=3 assays; >500 nuclei/condition in each assay; statistical analysis was performed using Fisher's exact test. ***, $p<0.001$). **B.** Representative images of control and dox-treated TetO-Cdc6+Cdt1 cells immunostained for RPA (red) protein. DNA was counterstained with DAPI (blue). Scale bar, 50 μm. Histogram shows the mean percentage values and SD of positive TetO-Cdc6+Cdt1 MEFs. White bar, control MEFs. Blue bar, dox-treated MEFs. (n=5 assays; 500 nuclei/condition in each assay; statistical analysis was performed using Fisher's exact test. ***, $p<0.001$). **C.** Immunoblot detection of the indicated proteins in TetO-Cdc6+Cdt1 MEFs cultured in the absence or presence of dox for 24h. MEK2 levels are shown as loading control. Samples correspond to the same experiment showed in Fig 13C. The experiment was conducted three times with similar results; one example is shown.

As expected, the DNA damage checkpoint was activated after Ccd6+Cdt1 overexpression. Besides γH2AX activation, dox-treated TetO-Cdc6+Cdt1 cells showed the activating phosphorylation of p53 protein and the inhibitory phosphorylation of CDK1 (Fig 21C), indicating a possible block in G2 to prevent that cells carrying re-replicated DNA progress into mitosis. This was not immediately observed by flow cytometry analyses of DNA content (Figure 15). However, when the percentage of cells in G2 and M was quantified using specific immunostaining patterns of phospho-H3 (pH3) and phospho-Aurora B (p-AurB) proteins, we found an increase in G2 and a concomitant decrease in mitotic cells (Fig. 22), which likely correspond to the cells with re-replicated DNA.

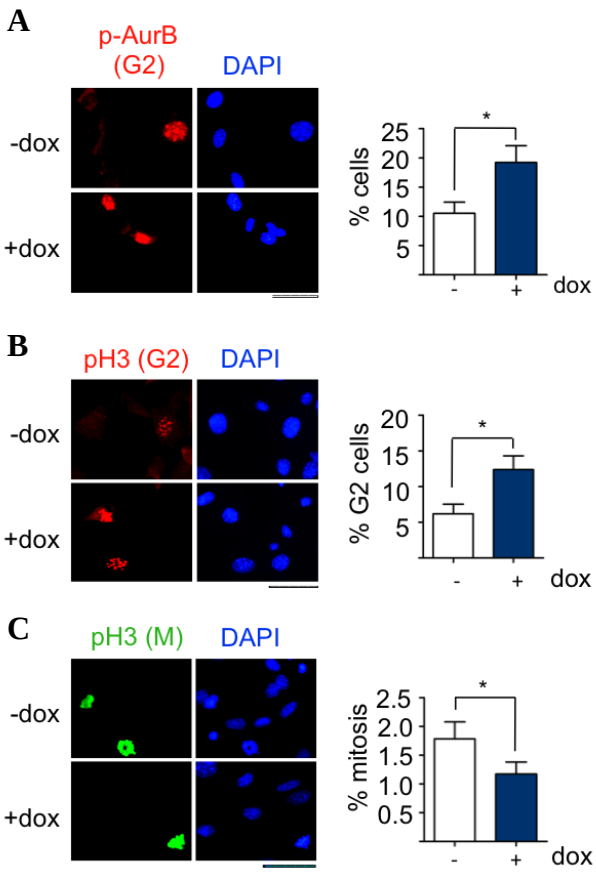

FIGURE 22. A. Representative images of control and dox-treated TetO-Cdc6+Cdt1 cells immunostained for p-AurB (red) protein. Scale bar, 50 μm. **B.** Representative images of control and dox-treated TetO-Cdc6+Cdt1 cells immunostained for G2 pH3 (red) protein. Scale bar, 50 μm. **C.** Representative images of control and dox-treated TetO-Cdc6+Cdt1 cells immunostained for mitotic pH3 (green) protein. Scale bar, 50 μm. In all cases histograms show the mean percentage values and SD of positive TetO-Cdc6+Cdt1 MEFs. White bars, control MEFs. Blue bars, dox-treated MEFs. n=3 assays. >300 cells/condition were scored for pAurB. >500 cells/condition were scored for G2 pH3. >1000 cells/condition were scored for mitotic pH3. In all cases statistical significance was calculated using Student's t-test; *, $p<0.05$.

Re-replication decreases cell proliferation and induces apoptosis

At this time, we wondered if the presence of re-replicated DNA would compromise the proliferation capacity of TetO-Cdc6+Cdt1 cells. Proliferation curves indicated that dox-treated TetO-Cdc6 and TetO-Cdt1 MEFs proliferate at the same rate than their controls (Fig 23A, B), whereas CDC6 and CDT1 combined overexpression decreased the proliferation rate (Fig 23C). This result is not surprising because TetO-Cdc6+Cdt1 MEFs displayed DNA damage and a partial G2 arrest. In addition, we asked whether cell death could contribute to the slower proliferation dynamics. Apoptotic and dead MEFs were detected by flow cytometry after a double staining with TMRE mitochondrial dye and DAPI. Dead cells lose the integrity of plasmatic membrane and are stained with DAPI, while apoptotic cells lose mitochondrial integrity and cannot be stained with TMRE (Fig 24A). Indeed, increased levels of apoptotic activation and cell death were observed only when CDC6 and CDT1 were overexpressed in combination (Fig 24B, C).

Combined, the results obtained with MEFs argue that simultaneous deregulation of Cdc6 and Cdt1 is necessary to induce re-replication in primary MEFs. Re-replication induces RS and DNA damage, leading to checkpoint activation and an increase in apoptosis-mediated cell death.

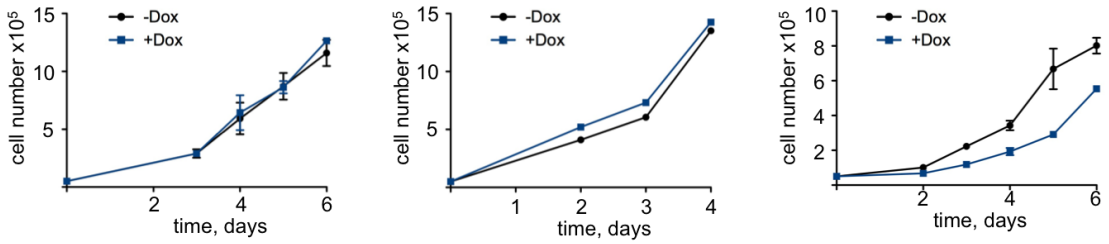

FIGURE 23. Proliferation curves of TetO-Cdc6 (n=2 assays), TetO-Cdt1 (n=1 assay) and TetO-Cdc6+Cdt1 (n=2 assays) cells cultured without or with dox. Mean and SD are represented for TetO-Cdc6 and TetO-Cdc6+Cdt1 MEFs.

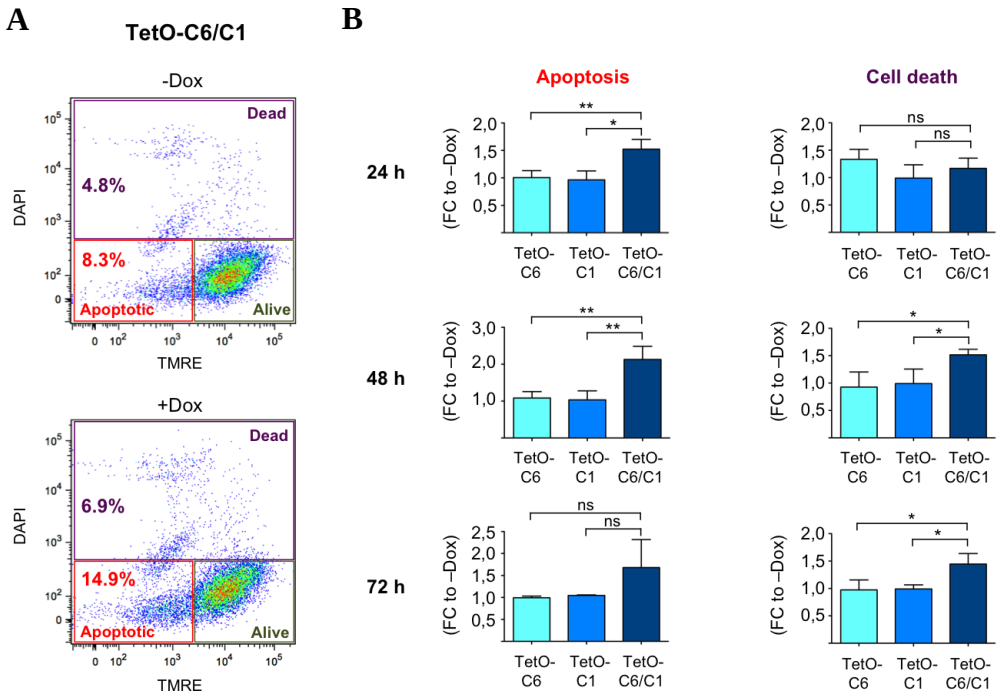

FIGURE 24. A. Representative flow cytometry graphs showing DAPI staining vs TMRE staining in TetO-Cdc6+Cdt1 MEFs grown in media with or without dox at 48 hours. Purple gates represent dead cells (permeable to DAPI); red gates represent apoptotic cells (negative for TMRE) and green gates represent alive cells (positive for TMRE). **B.** Histograms show the mean percentage values and SD of apoptotic or dead cells in each population, expressed as fold-change with respect to control situation (n=3 assays in each case. Results were analyzed with one-way Anova and Bonferroni's post test; *, $p<0.05$; **, $p<0.01$; n.s.= not significant).

DNA re-replication is lethal during embryonic development

After evaluating the impact of CDC6 and CDT1 overexpression at the cellular level, we decided to investigate whether similar effects would be observed *in vivo*. Embryonic development was tested first, as most tissues are highly proliferative at this stage. A mating strategy between TetO-Cdc6 and TetO-Cdt1 mice was designed in which all embryos carried both Cdc6 and Cdt1 alleles at Col1A1, but only 50% of them carried the rtTA transactivator at Rosa26, providing experimental and control embryos in the same litter (Fig 25A). The diet of pregnant mice was supplemented with dox during three days in mid gestation (E10.5-E13.5) and the embryos were extracted and analysed immediately afterwards. Approximately 50% of them were smaller and paler and showed signs of underdevelopment (Fig 25B, top panel). When the dox treatment was extended to six days (E7.5-E13.5), these phenotypes were exacerbated and half of the embryos were at advanced stages of regression (Fig 25B, bottom panel). Fetal liver cell suspensions were prepared from embryos (following a 3-day dox treatment to the mother) and labelled with BrdU *ex vivo* to monitor DNA replication and possible re-replication. The rest of embryonic tissue was used for genotyping and immunoblotting (Fig 25C, D). Remarkably, all embryos expressing rtTA had an increased percentage of cells with partially re-replicated DNA (Fig 25C). Overexpression of CDC6 and CDT1 in these embryos was confirmed by immunoblots in fetal cell extracts (Fig 25D). These results suggest that re-replication is incompatible with embryonic development and that highly proliferative tissues could be more sensitive to re-replication, as re-replication levels were higher in fetal liver cells than in MEFs.

The same strategy was used with the individual overexpressor models. Embryos overexpressing CDC6 did not display any abnormalities, and fetal liver cells displayed normal DNA content and BrdU incorporation profiles (Fig 26A). Interestingly, CDT1 overexpressor embryos displayed extensive re-replication in the liver (Fig 26B) after *in vivo* exposure to dox for 3 days and signs of underdevelopment after 6 days (not shown). This result is different from MEFs, in which CDT1 overexpression was not sufficient to induce re-replication. However, we also observed that the endogenous levels of CDC6 in fetal liver cells were much higher than in MEFs, even after dox treatment of the latter (Fig 27), whereas CDT1 endogenous levels in MEFs and fetal liver cells were comparable. These results imply that endogenous CDC6 levels could establish the susceptibility of any given cell type to CDT1 overexpression. We also

noticed that GMN levels were elevated in fetal liver cells (Fig 27A), probably to exert a stricter control on CDT1 in a cell type that seems to be very sensitive to fluctuations in CDT1 levels.

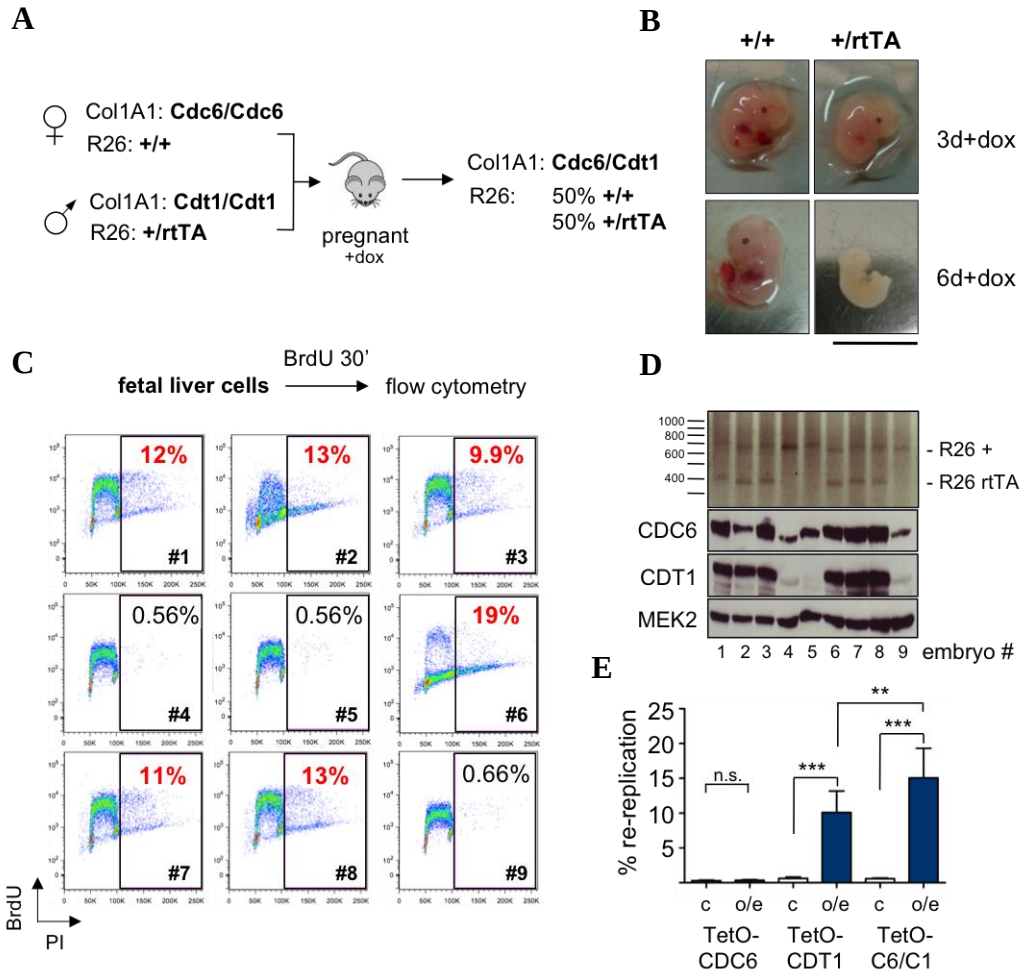

FIGURE 25. DNA re-replication causes embryonic lethality. **A.** Schematic of the genetic cross used in the experiment. **B.** Representative TetO-Cdc6+Cdt1 embryos isolated at E13.5, following dox administration to the mother for 3 days (upper images) or 6 days (lower images). Molecular genotyping at the Rosa26 locus distinguished wild- type (+/+) from Cdc6+Cdt1 overexpressor (+/rtTA) embryos; see (D). Bar, 1 cm. **C.** Flow cytometry analysis of fetal liver cells isolated from nine littermate embryos and pulse-labelled with BrdU ex vivo for 30 min. Gates show cells with re-replicated (>2C) DNA content. **D.** Top, Rosa26 locus PCR genotype indicates the presence or absence of rtTA. Bottom, immunoblots showing protein levels of CDC6, CDT1 and MEK2 (loading control) in the liver of the 9 embryos shown in (C). All embryos that carried rtTA (#1-3, 6-8) expressed higher levels of CDC6 and CDT1 and underwent DNA re- replication. **E.** Histogram shows the mean percentage and SD of fetal liver cells with >2C DNA content in TetO-Cdc6, TetO-Cdt1 and TetO-Cdc6+Cdt1 embryos. See also Fig 26. One litter was evaluated for TetON-Cdc6 mice (n=2 control and n=6 overexpressors). 2 litters were evaluated for TetON-Cdt1 mice (n= 6 controls and n=6 overexpressors). 2 litters were evaluated for TetON-Cdc6+Cdt1 mice (n= 5 controls and n=10 overexpressors). One way Anova and Bonferroni's post test were applied; **, $p<0.001$; **, $p<0.01$; n.s., not significant). C, control; o/e, overexpressor.

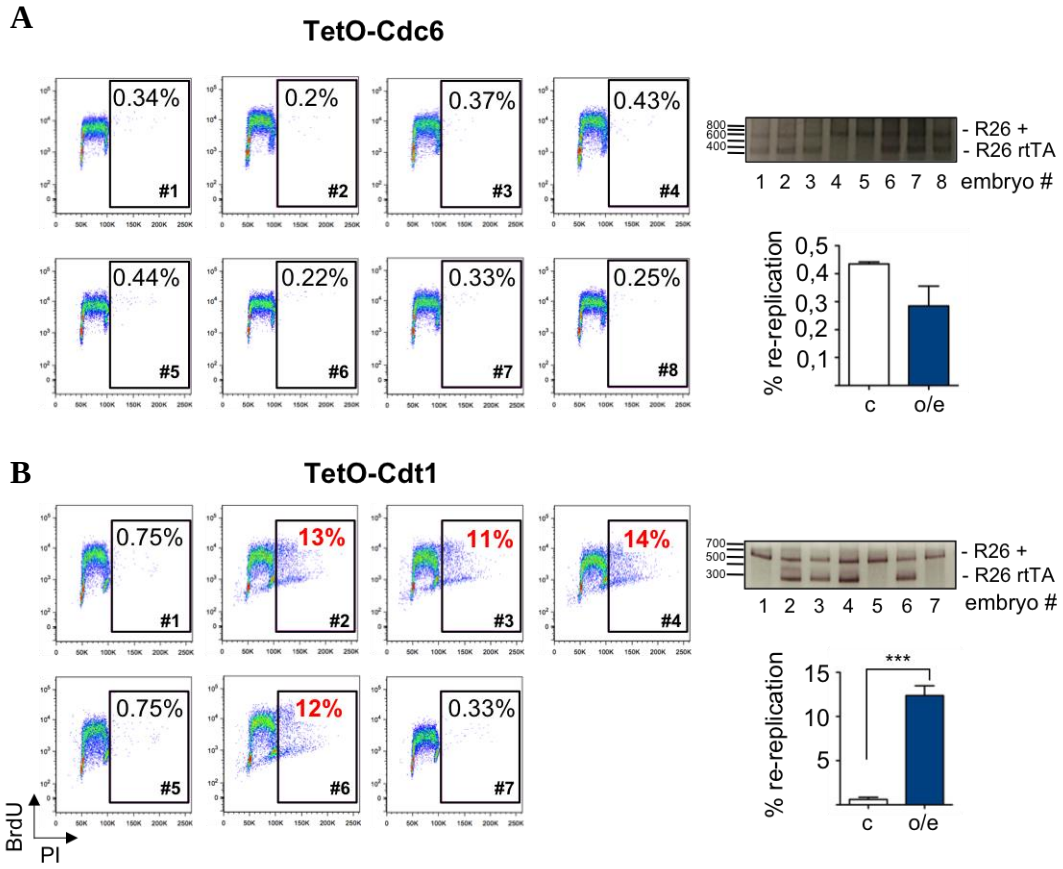

FIGURE 26. A. The experiment follows the outline described in Fig 25, using fetal liver cells isolated from 8 littermate embryos derived from a cross between TetO-Cdc6 mice, in which only the father carried rtTA at Rosa26. 50% of the embryos are expected to overexpress Cdc6. Fetal liver cells were pulse-labelled ex vivo with BrdU for 30 min. Gates show cells with >2C DNA content. Top right, Rosa26 locus PCR genotype indicates the presence or absence of rtTA. Histogram shows the percentage of cells with >2C DNA content. C, control; o/e, Cdc6 overexpression. **B.** Same as (A), using 7 embryos derived from TetO-Cdt1 mice. Statistical significance was calculated using Student's t-test; ***, $p<0.001$.

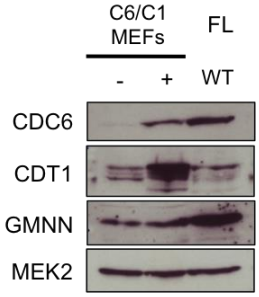

FIGURE 27. Immunoblots showing endogenous levels of CDC6, CDT1 and GMN in fetal liver (FL) cells. For comparison, the levels of the same proteins are shown in TetO-Cdc6 MEFs cultured in medium with or without dox. MEK2 levels are shown as loading control.

Cdc6 and Cdt1 overexpression cause rapid morbidity in adult mice

We next evaluated the effect of Cdc6 and Cdt1 overexpression in young adult mice. For this experiment, cohorts of 4 mice from each genotype were fed with dox-supplemented diet during 4 weeks (control groups of 4 mice were kept in regular chow diet). Mice were sacrificed at the end of the experiment and transgene expression was evaluated in

multiple organs by RT-qPCR. As expected, Cdc6 was overexpressed in most tissues in TetO-Cdc6 and TetO-Cdc6+Cdt1 mice (Fig 28A, C), while Cdt1 was overexpressed in TetO-Cdt1 and TetO-Cdc6+Cdt1 mice (Fig 28B, C). Different levels of transgenic expression were observed in different tissues, probably due to different efficiency in dox delivery. In this regard, virtually no overexpression was detected in brain and testes, a known limitation in this method of transgenesis (Beard et al, 2006). We also noticed that Cdc6 and Cdt1 mRNA accumulated to lower levels when combined in the same model (Fig 28C).

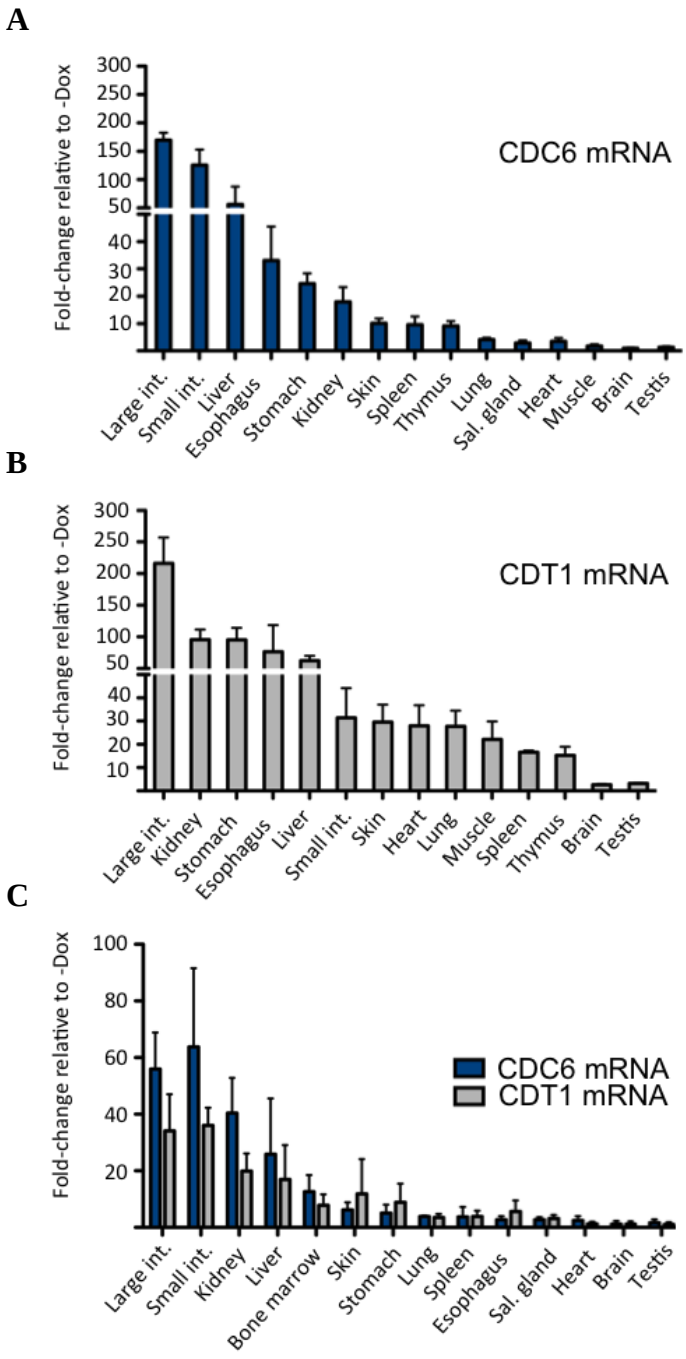

FIGURE 28. Histogram showing the fold-change in mRNA levels of Cdc6 and Cdt1 in different tissues from TetO-Cdc6 (**A**), TetO-Cdt1 (**B**), and TetO-Cdc6+Cdt1 (**C**) mice after dox administration, relative to control tissues (n= 4 control mice and n=4 dox-treated mice). No overexpression was detected in brain and testes, due to inefficient dox delivery to these organs (Beard et al, 2006).

In both TetO-Cdc6 and TetO-Cdt1 strains, control and dox-treated mice showed no phenotypic changes for the duration of the experiment. In striking contrast, TetO-Cdc6+Cdt1 mice showed morbidity signs, including weight loss, as early as 4-5 days after dox administration, and their mean survival was less than two weeks (Fig 29A). At the time of reaching the humane endpoint, dox-treated TetO-Cdc6+Cdt1 mice displayed a reduction of approximately one third of their body weight (Fig 29B).

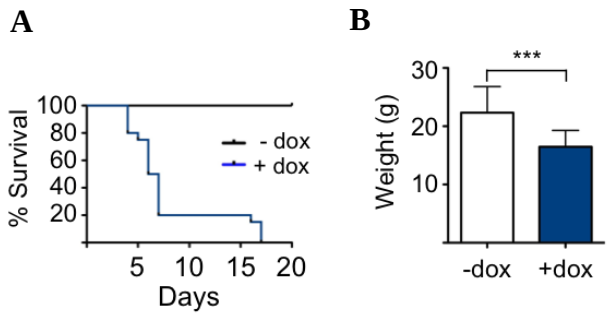

FIGURE 29. A. Kaplan-Meier survival curve of TetO-Cdc6+Cdt1 mice (n=16 control; 20 dox-treated). **B.** Histogram shows mean weight of control and dox-treated TetO-Cdc6+Cdt1 mice at the humane end point (n=15 control; n=16 dox-treated). Statistical significance was assessed with Student's t-test; ***, $p<0.001$.

Combined Cdc6 and Cdt1 overexpression cause lethal tissue dysplasias

At the histopathological level, the gastrointestinal (GI) tract of TetO-Cdc6+Cdt1 mice was severely dysplastic (Fig 30 and 31). This is the likely cause of death, as it would lead to impaired water and nutrient absorption. Besides the GI, tissue alterations were observed in the bone marrow (BM), spleen and thymus (Fig 30).

The tisular alterations observed in the intestine of TetO-Cdc6+Cdt1 mice included severe nuclear pleomorphism, increased nuclear size and crypt disorganization Extensive crypt loss, mucosal atrophy and shortened villi were found throughout the entire intestine, with the colon displaying the most severe phenotypes. Dilated crypts were filled with cell debris and inflammatory cells. Moderate inflammatory infiltrates were also found in the lamina propria (Fig 31).

The stomach of TetO-Cdc6+Cdt1 mice showed related phenotypes, including nuclear pleomorphism, increased nuclear size and apoptosis within the glands that lead to mucosal atrophy. In some cases, multifocal epithelial hyperplasia and mild hyperkeratosis of the non-glandular stomach was observed (Fig 30).

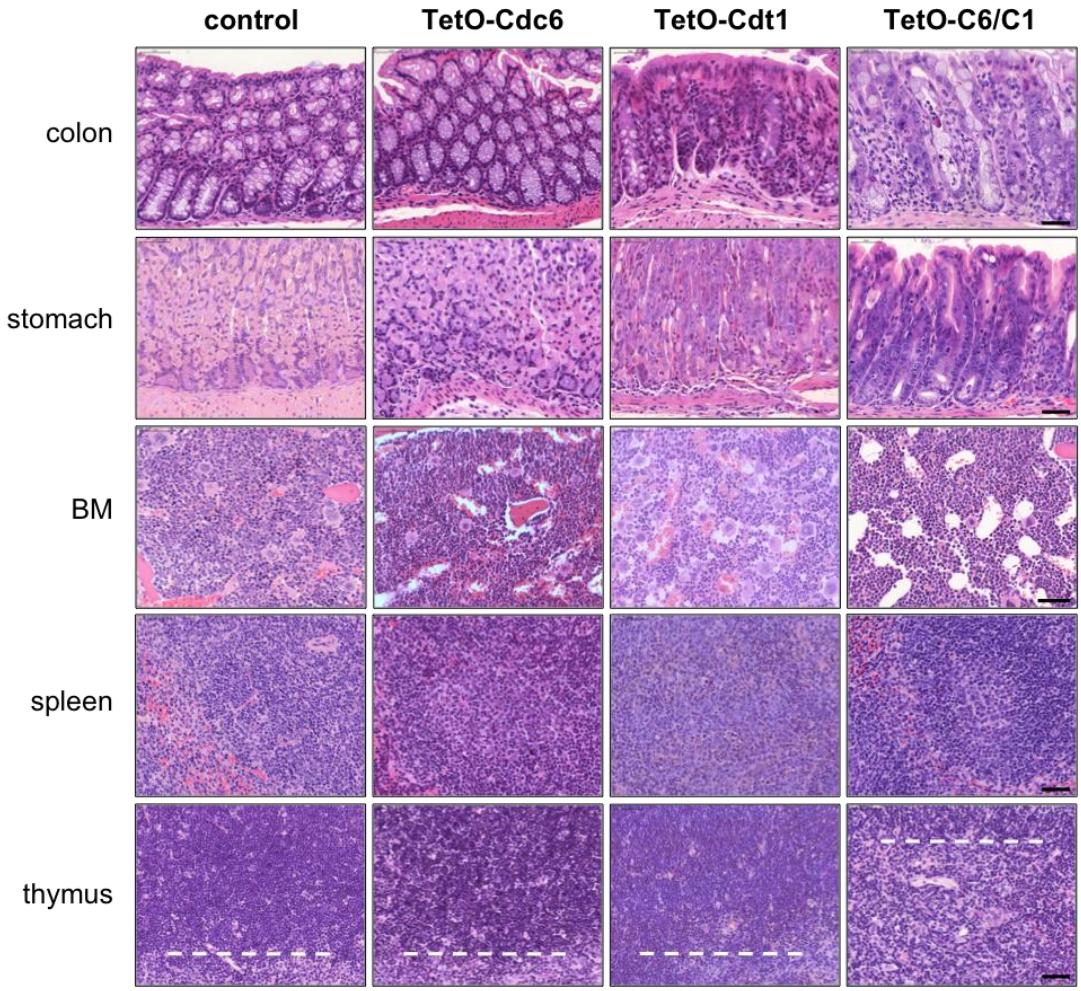

FIGURE 30. Haematoxylin-eosin stainings of indicated tissue sections. BM, bone marrow. In the thymus sections, dashed lines indicate the boundary between cortical (top) and medullar (bottom) tissue. See text for details. Bars, 50μm.

Moderate spleen atrophy was also observed in TetO-Cdc6+Cdt1 mice. Germinal centers were activated, probably to elicit the inflammatory response in the GI tract. The white pulp displayed increased apoptosis and decreased follicle size; in addition, the red pulp displayed an increment of immature cells with abnormal chromatin patterns. Some degree of extramedullary hematopoiesis was observed in dox-treated animals in the three groups, and TetO-Cdt1 and TetO-Cdc6+Cdt1 mice showed accumulation of erythroid precursors (Fig 30).

In the BM, TetO-Cdc6+Cdt1 mice displayed moderate aplasia, reduction of mature cell populations, increased apoptosis and cell nuclei with abnormal chromatin patterns. Finally, the thymus of these mice showed severe cortical atrophy, to the extent that the organ was practically ablated in some individuals (Fig 30).

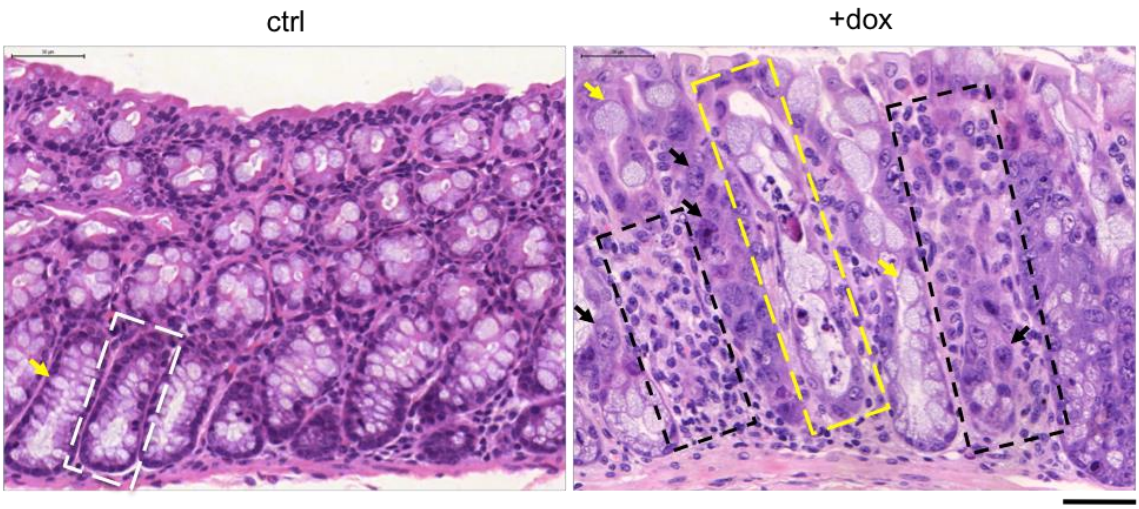

FIGURE 31. Higher magnification view of control (left) and TetO-Cdc6+Cdt1 (right) mice colon tissues shown in Figure 30. A normal intestinal crypt in control tissue is indicated (white dashed box). TetO-Cdc6+Cdt1 colon displayed inflammatory infiltrates (black dashed boxes) and global disorganization of the crypt structures. Remaining crypts contained few goblet cells, which were enlarged (yellow arrows). Some crypts were filled with cell debris (yellow dashed box). Cells with increased nuclear size and stippled chromatin were abundant (black arrows). Bar, 50μm.

TetO-Cdc6 mice did not present any of these alterations. However, phenotypes similar to those described for TetO-Cdc6+Cdt1 mice were also found in TetO-Cdt1 mice, albeit much attenuated (Fig 30). For instance, increased immature populations were found in the spleen and BM, and multifocal areas of dysplasia were observed in the GI tract. Therefore, CDT1 overexpression may be sufficient to induce mild tissue alterations in some organs, similar to the situation observed in the fetal liver. Interestingly, all affected tissues are highly proliferative, suggesting a relationship between proliferation dynamics and sensitivity to CDT1 overexpression.

Notably, organs such as kidney and liver suffered no alterations despite elevated transgene expression levels. This rules out a direct correlation between the penetrance of dox and the grade of dysplasia observed in different tissues.

DNA re-replication and DNA damage in adult mice tissues

Some of the cellular phenotypes such as nuclear pleomorphism and increased nuclear size could be directly related to DNA re-replication. To demonstrate the existence of DNA re-replication *in vivo*, cells were isolated from the epithelial lining of the intestine (Sato and Clevers, 2013) of control and dox-treated TetO-Cdc6; TetO-Cdt1 and TetO-Cdc6+Cdt1 mice, to evaluate their DNA content by flow cytometry. Only dox-treated

TetO-Cdc6+Cdt1 mice contained a percentage of cells with re-replicated DNA (Fig 32A). To further confirm this phenotype, confocal microscopy was used to measure the DNA content of colon crypt cells stained with DAPI. An analysis of >900 crypt cells per condition revealed higher DNA content in dox-treated TetO-Cdc6+Cdt1 mice (Fig 32B), a result strongly indicative of DNA re-replication *in vivo*.

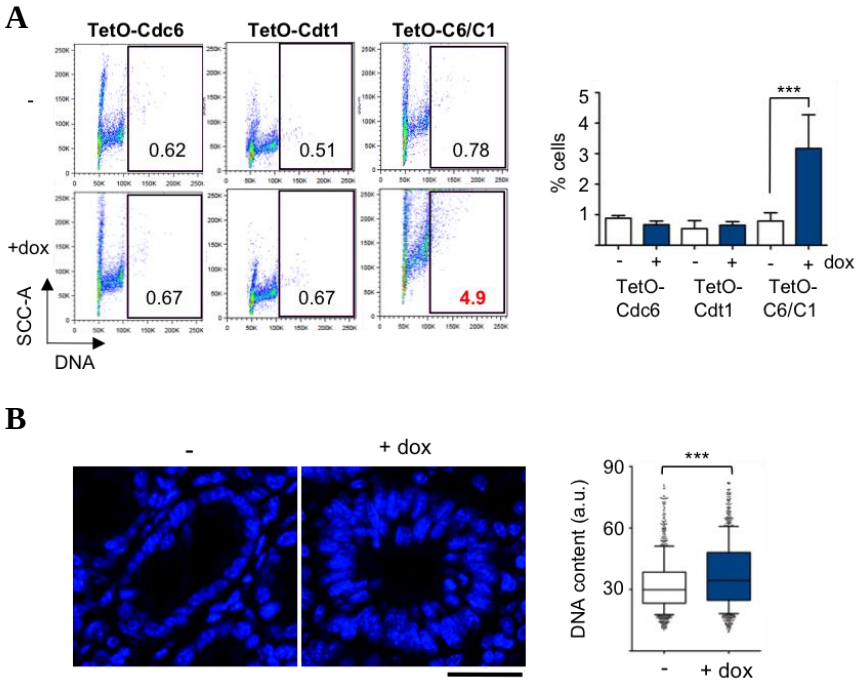

FIGURE 32. A. Detection of DNA re-replication in crypt-enriched intestinal cells, stained with PI to visualize DNA content by flow cytometry. Plot shows Side Scatter Area (SSC-A) vs DNA content (PI). Gates include cells with >2C DNA content. Histogram shows quantification of the percentage of cells with >2C DNA content (n=4 mice/ strain and condition; One way Anova and Bonferroni's post-test were applied; ***, $p<0.001$; n.s., not significant). **B.** DAPI-stained images of crypt cells from colon tissue of control and dox-treated TetO-Cdc6+Cdt1 mice. Bar, 30 µm. Box-plot shows the integral intensity of DAPI staining in crypt cells from 3 control and 3 dox-treated TetO-Cdc6+Cdt1 mice. >300 crypt cells were taken from 4 different colon areas in each mouse (>900 crypt cells per genotype; statistical significance were calculated with Mann-Whitney test; ***, $p<0.001$).

We then extended the analysis to other tissues. BM cell suspensions were pulse-labelled *ex vivo* with BrdU and stained with PI. As expected, TetO-Cdc6+Cdt1 mice presented cells with re-replicated DNA (Fig 33A). In this tissue, TetO-Cdt1 cells also displayed some degree of re-replication (Fig 33A), which was not observed in intestinal cells. As it was the case of the fetal liver, this effect could be explained by the high expression levels of endogenous Cdc6 in the BM (Fig 33B; see Bastian et al, 2008; http://bgee.org/?page=gene&gene_id=ENSMUSG00000017499; and Wu et al, 2009; http://biogps.org/#goto=genereport&id=23834).

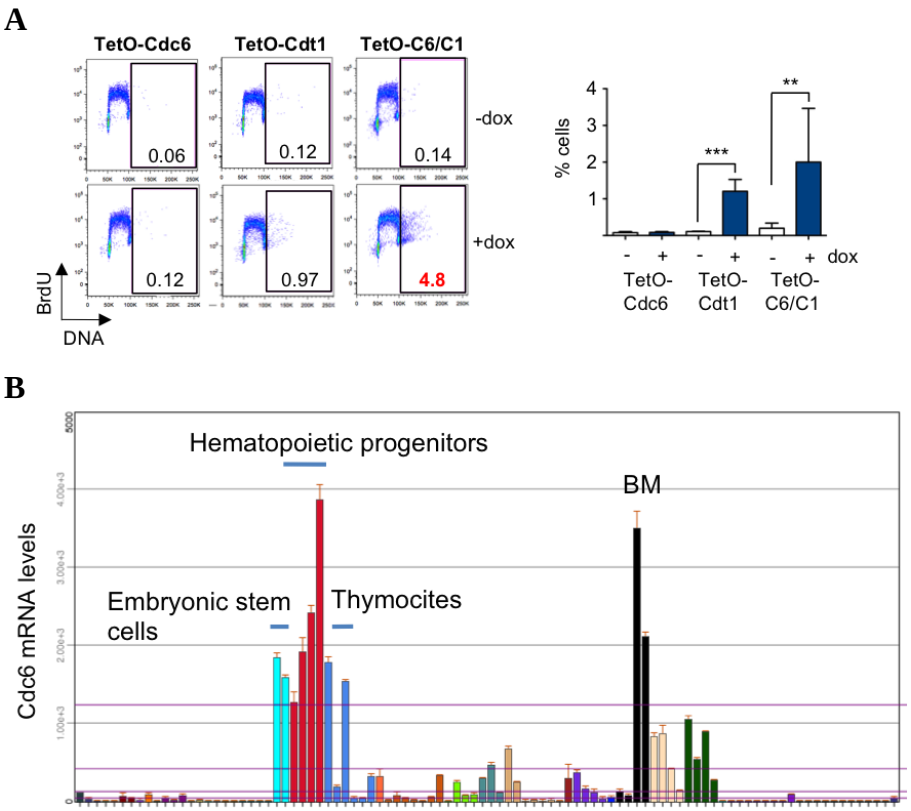

FIGURE 33. A. Detection of DNA re-replication in BM cells, pulse-labelled with BrdU ex vivo for 30 min and processed for flow cytometry. Plot shows BrdU vs DNA content (PI). Gates include cells with >2C DNA content. Histogram shows quantification of the percentage of cells with >2C DNA content (n=4 mice/strain and condition; One way Anova and Bonferroni's post-test were applied; ***, p<0.001; **, p<0.01; n.s., not significant). **B.** Cdc6 expression levels in different mice tissues as shown in Wu et al, 2009 (http://biogps.org/#goto=genereport&id=23834). Embryonic stem cells, hematopoietic progenitors, thymocites and BM cells that display the highest Cdc6 expression levels, are highlighted.

Finally, the extent of DNA damage caused by re-replication was analyzed by measuring the levels of γH2AX in different tissues. Combined CDC6 and CDT1 overexpression led to DNA damage in colon, stomach and BM (Fig 34). TetO-Cdt1 mice also accumulated γH2AX-positive cells in the stomach and BM, consistent with partial DNA re-replication and limited tissue dysplasia (Fig 34).

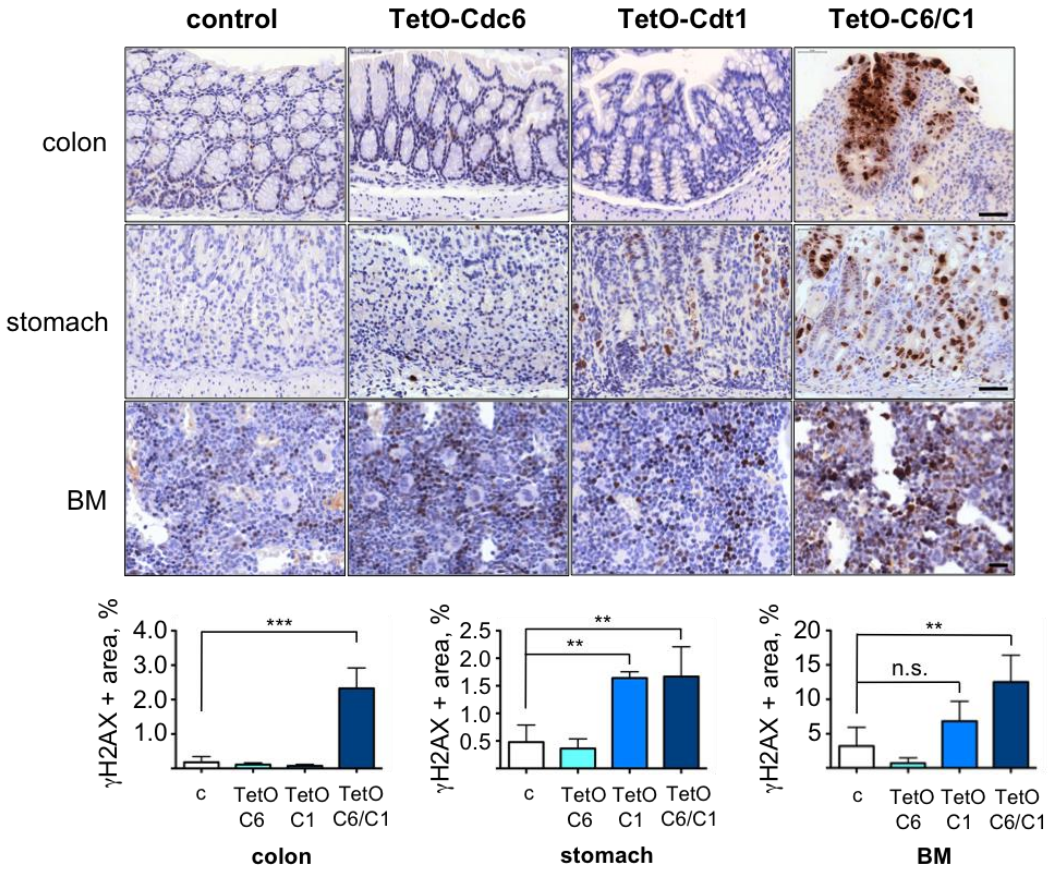

FIGURE 34. γH2AX IHC staining in the indicated tissues of control and dox-treated TetO-Cdc6, TetO-Cdt1 and TetO-Cdc6+Cdt1 mice. Scale bar, 50 μm (colon and stomach) and 20 μm (BM). Histograms show the mean percentage value and SD of γH2AX-positive area in each case (n=3 mice/condition; One way Anova and Bonferroni's post-test were applied; ***, $p<0.001$; **, $p<0.01$. n.s.= not significant).

Immunohistopathological characterization of TetO-Cdc6+Cdt1 colon

To further characterize the consequences of Cdc6 and Cdt1 overexpression in the intestine, control and dox-treated TetO-Cdc6+Cdt1 colon sections were stained with different cellular markers. Staining with proliferation marker Ki67 was similar in control and dox-treated tissues (Fig 35A). SOX9, a marker of precursor cells in the intestine (Barker, 2013; Vermeulen and Snippert, 2014), was decreased in dox-treated tissue (Fig 35B). This is consistent with the histopathological findings and indicates that re-replication interferes with precursor cell maturation. The absence of p16 staining (Fig 35C) suggests that senescence was not induced, whereas increased p21 staining (Fig 35D) is indicative of DNA damage checkpoint activation in dox-treated colon cells. Although no difference was observed in mitotic index (Fig 35E), pH3 staining revealed an increase in the percentage of G2 cells, suggesting a cell cycle arrest (Fig 35F).

Finally, an increase in apoptotic cells in the tissue was confirmed with cleaved-Caspase 3 (Fig 35G).

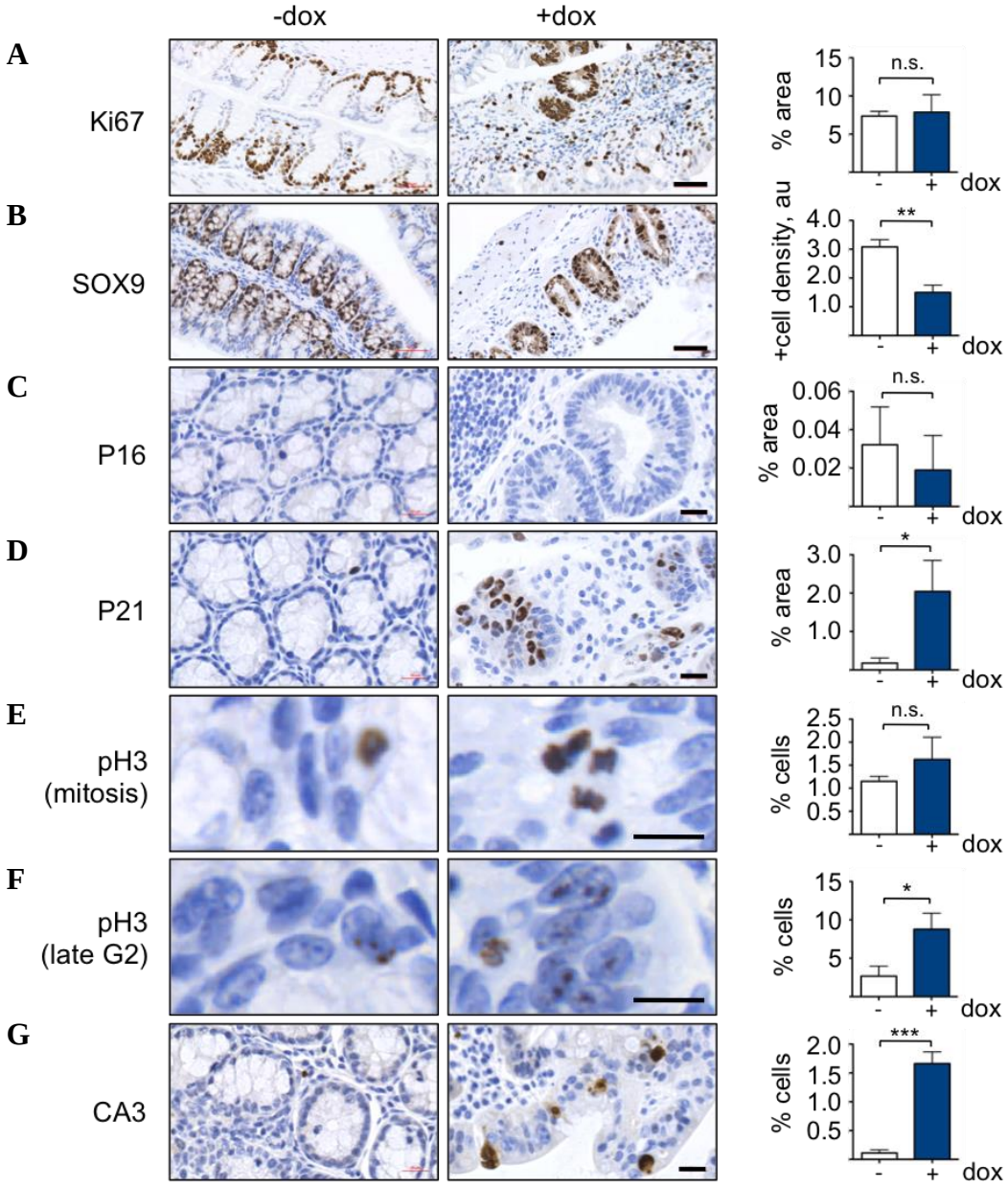

FIGURE 35. A. Ki67 IHC staining in colon sections of control and dox-treated TetO-Cdc6+Cdt1 mice. Scale bar, 50 μm. Histogram shows the mean percentage value and SD of Ki67-positive area. **B.** Same for SOX9. Scale bar, 50 μm. Histogram shows the mean percentage value and SD of SOX9-positive cell density. **C.** Same for p16. Scale bar, 20 μm. Histogram shows the mean percentage value and SD of p16-positive area. **D.** Same for p21. Scale bar, 20 μm. Histogram shows the mean percentage value and SD of p21-positive area. **E.** Same for mitotic-specific pH3. Scale bar, 10 μm. Histogram shows the mean percentage value and SD of pH3 mitotic cells. **F.** Same for G2-specific pH3. Scale bar, 10 μm. Histogram shows the mean percentage value and SD of pH3 G2 cells. **G.** Same for Cleaved Caspase 3. Scale bar, 20 μm. Histogram shows the mean percentage value and SD of CA3-positive cells. For all stainings, n=3 mice per condition. Statistical significance was calculated using Student's t-test; ***, $p<0.001$; **, $p<0.01$; *, $p<0.05$; n.s., not significant. CA3 and pH3 staining were scored manually. For CA3, >1400 cells from three different areas were counted in each animal. For pH3, >1200 from five different areas were counted in each animal.

Interestingly, around 7% of the colon area is positive for Ki67 (Fig 35A) and 2.5% is positive for γH2AX (Fig 34). This indicates that approximately one third of the proliferative cells in the colon display DNA damage, possibly corresponding to those most affected by DNA re-replication.

Taken together, these results suggest that unscheduled origin refiring and its associated DNA damage cause cell death and loss of progenitor cells in tissues that require rapid renovation (such as the intestinal epithelia), rapidly leading to lethal tissue dysplasias.

Long-term effects of single CDC6 or CDT1 overexpression

As CDT1 overexpression caused limited tissue damage, and considering that deregulation of Cdc6 and Cdt1 could promote malignancy (Liontos et al, 2007), we also evaluated the long-term effects of Cdc6 or Cdt1 deregulation using the TetO-Cdc6 and TetO-Cdt1 mouse strains. In an ageing experiment in which cohorts of TetO-Cdc6 and TetO-Cdt1 mice were kept permanently in control or dox-supplemented diet, median survival was reduced in approximately 11 weeks in both cases: 102 vs 91 weeks in TetO-Cdc6 mice and 93,5 vs 83 weeks in TetO-Cdt1 mice. Although these differences in survival did not reach statistical significance (Fig 36A, B), preliminary post-mortem analyses suggest a slightly higher frequency of splenomegaly and/or late-onset lymphomas in Cdc6 and Cdt1 overexpressor strains.

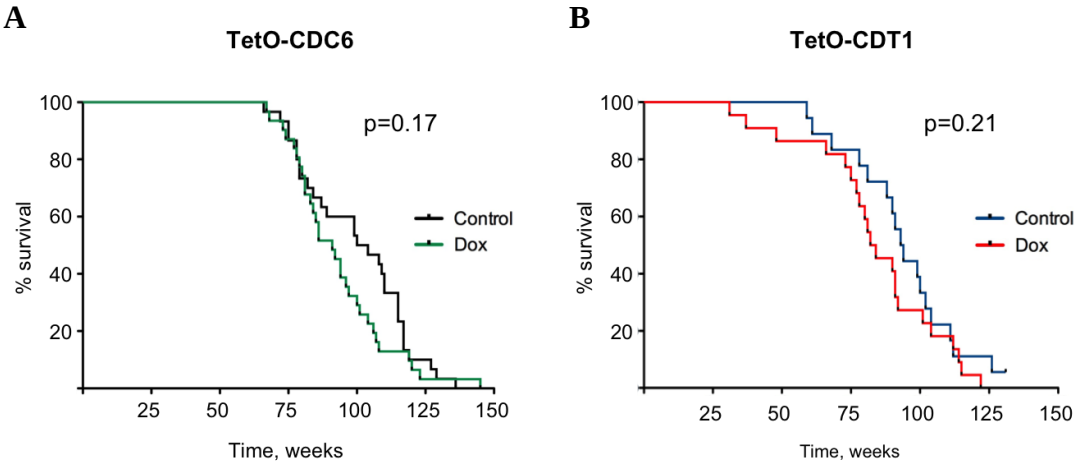

FIGURE 36. A. Kaplan-Meier survival curve of TetO-Cdc6 mice (n=30 control; 31 dox-treated). Gehan-Breslow-Wilcoxon test was performed and p-value is represented. **B.** Kaplan-Meier survival curve of TetO-Cdt1 mice (n=18 control; 22 dox-treated). Gehan-Breslow-Wilcoxon test was performed and p value is represented.

RESULTS CHAPTER 2

A screening to identify proteins involved in DNA re-replication control

In the first part of the Thesis we investigated the *in vivo* consequences of DNA re-replication. In the second part, we became interested in identifying proteins that participate in the regulation of re-replication. We wondered whether new proteins could be identified that control origin re-firing or inhibit the elongation of re-replicated forks. Moreover, whether specific molecular mechanisms are in charge of resolving the structures generated by origin reactivation remains unknown (Fig 37).

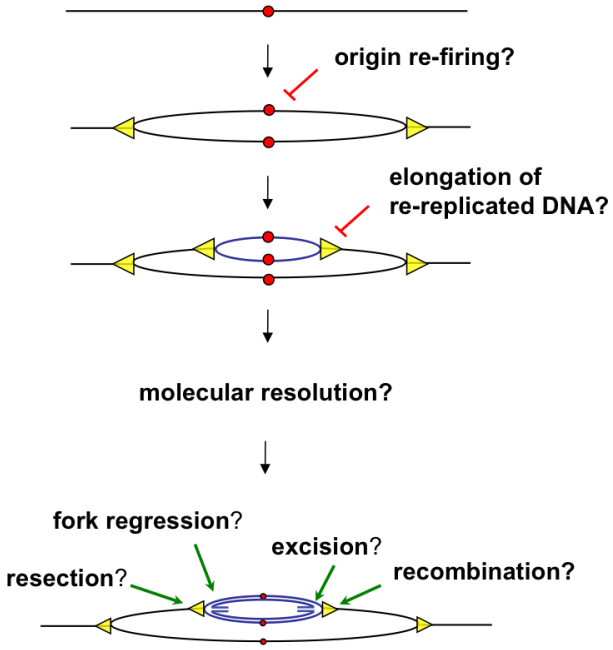

FIGURE37. Schematic representation of an origin refiring event leading to DNA Re-replication. Potential processes to limit re-replication are indicated.

To address these questions, a genetic screening was designed to identify factors involved in inhibiting or promoting DNA re-replication. A candidate-based esiRNA library was designed against genes implicated in DNA damage and/or RS response (Table 6). The library included RNAi molecules inhibiting three groups of genes. Group 1 is integrated by helicases with fork remodeling activity. Group 2 are proteins involved in DNA damage signalling or repair. These include checkpoint proteins, nucleases with the ability to process stalled forks, and HR factors. Group 3 is constituted by helicases that act as chromatin remodelers. Our goal was to explore the role of the selected proteins in modulating re-replication caused by the disruption of origin licensing. As an experimental system amenable to rapid transfection of RNAi reagents, we decided to integrate a dox-inducible shRNA molecule targeting GMN in the HCT116 colorectal

cancer cell line. In the resultant cells (HCT116-shGMN), re-replication can be readily induced by the depletion of GMN, which is the main inhibitor of origin relicensing in cancer cell lines (Zhu and DePamphilis, 2009). DNA re-replication elicits an enlargement of cell nuclei (Zhu et al, 2004), which could be used as readout of re-replication after microscopy analyses. We confirmed HCT116-shGMN cells downregulated GMN, underwent DNA re-replication and increased nuclear size upon dox addition (Fig 38A, B, C).

Gene name	Function
RECQL	Helicase
WRN	Helicase
BLM	Helicase
RECQL4	Helicase
RECQL5	Helicase
SMARCAL1	Helicase
FBH1	Helicase
PIF1	Helicase
ZRANB3	Helicase
BRIP1	Helicase
HLTF	Helicase
SHPRH	Helicase
ASCC3	Helicase
HELQ	Helicase
SETX	RNA Helicase
DDX1	RNA Helicase

Gene name	Function
CLSPN	Checkpoint
ATR	Checkpoint
ATM	Checkpoint
MRE11A	Nuclease
DNA2	Nuclease
EXO1	Nuclease
MUS81	Nuclease
GEN1	Nuclease
SLX4	Nuclease
RAD51	HR
NBS	HR
RAD54	HR
BRCA2	HR
POLD3	BIR
XRCC6	NHEJ
ERCC2	NER
ERCC3	NER

Gene name	Function
ATRX	Chromatin remodeler
CHD2	Chromatin remodeler
CHD3	Chromatin remodeler
CHD4	Chromatin remodeler
CHD5	Chromatin remodeler
CHD7	Chromatin remodeler
SMARCA1	Chromatin remodeler
SMARCA2	Chromatin remodeler
SMARCA4	Chromatin remodeler
SMARCA5	Chromatin remodeler
HELLS	Chromatin remodeler
INO80E	Chromatin remodeler
RUVBL1	Chromatin remodeler
EP400	Chromatin remodeler

Table 6. List of genes selected for the esiRNA-based library, and their known biochemical activities.

A schematic of the experimental plan for the screening is depicted in Fig 38D. HCT116-shGMN cells were treated with dox to elicit re-replication and then transfected with each component of the esiRNA library. 48 hours after transfection, nuclear size was evaluated by HTM.

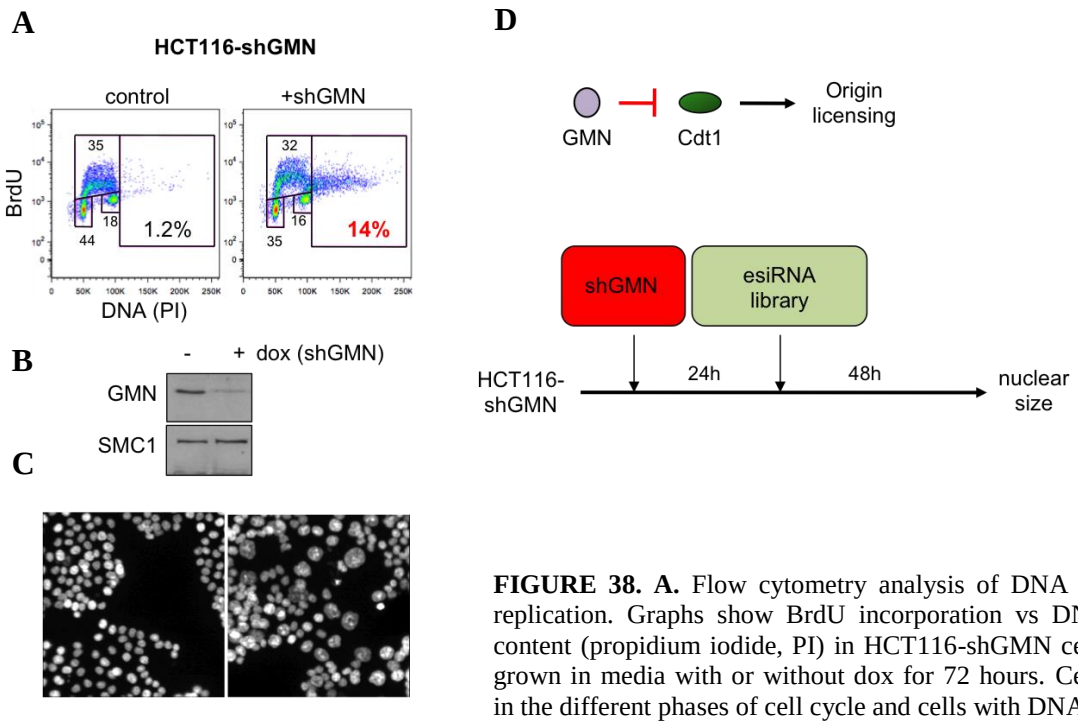

FIGURE 38. A. Flow cytometry analysis of DNA re-replication. Graphs show BrdU incorporation vs DNA content (propidium iodide, PI) in HCT116-shGMN cells grown in media with or without dox for 72 hours. Cells in the different phases of cell cycle and cells with DNA content >2C are gated. **B.** Immunoblot detection of GMN in HCT116-shGMN cells from (**A**). SMC1 levels are shown as loading control. **C.** Representative images of DAPI-stained HCT116-shGMN cells grown in media with or without dox for 72 hours. **D.** Top: Regulation of origin relicensing by GMN. Bottom: Schematic representation of the screening designed to test the effect of the library genes in DNA re-replication.

A large group of the genes tested, particularly the chromatin remodelers, did not affect the extent of re-replication, at least as monitored by nuclear size (Fig 39). In contrast, several helicases involved in fork remodeling and proteins that participate in the DNA damage response (DDR), modulated the process in different ways. In general, the loss of helicases increased the nuclear size (Fig 39), suggesting that fork remodelling limits re-replication. We focused our attention in two proteins, FBH1 and RAD51, which affected re-replication in opposite ways. FBH1 downregulation reduced nuclear size, whereas loss of RAD51 increased it (Fig 39). Interestingly, FBH1 is a negative regulator of RAD51 (Fig 40). Both RAD51 and FBH1 mediate fork reversal upon stalling (Fugger et al, 2015; Zellweger et al, 2015), but an antirecombinase activity in FBH1 prevents RAD51-dependent HR (Fugger et al, 2009; Chu et al, 2015). FBH1 can displace RAD51 filaments from DNA and monoubiquitilate RAD51 to prevent new loading (Fig 40) (Simandlova et al, 2013; Chu et al, 2015).

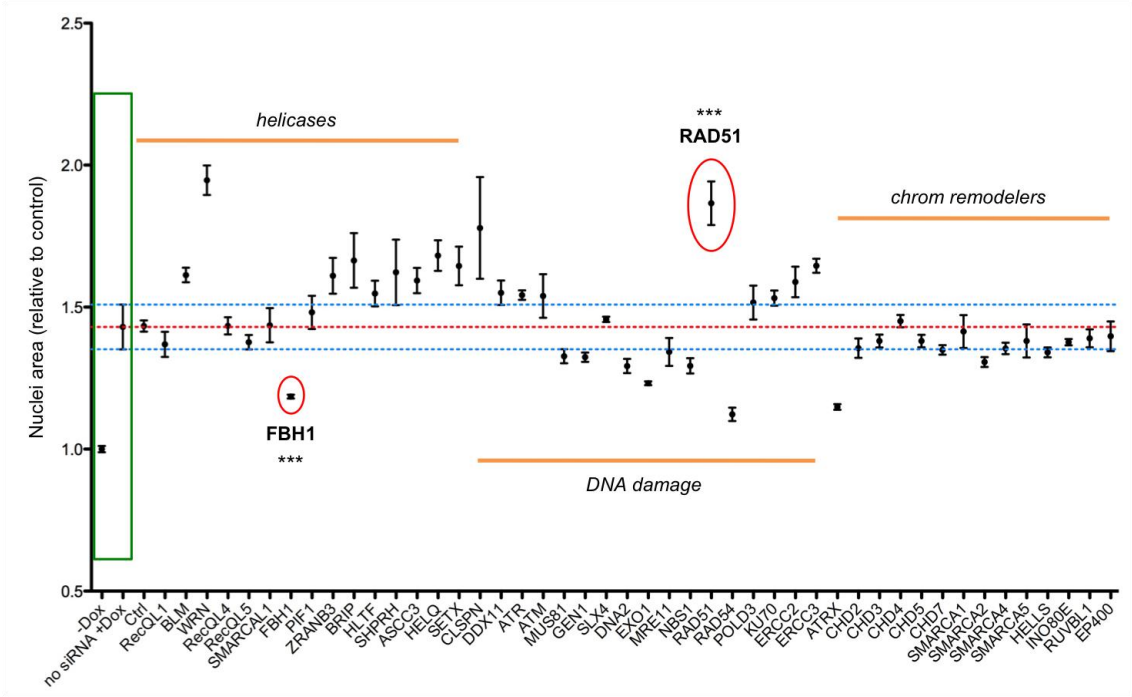

FIGURE 39. Screening results. Histogram shows mean of median nuclei area (expressed as fold-change with respect to control) and SD of each member of the library. –dox and +dox controls are shown inside a green rectangle. Red dotted line represents the mean value for +dox (+shGMN) condition. Blue dotted lines indicate the SD for this condition. FBH1 and RAD51 results are marked in red circles. Different gene groups from the library are indicated with orange lines. (3 replicas of each gene were assessed; >900 cells of each replica were scored; results were analyzed with one-way Anova and Bonferroni's post test; ***, $p<0.001$).

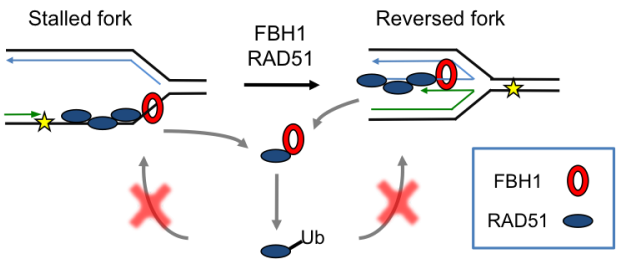

FIGURE 40. Schematic representation of FBH1 and RAD51 functions in response to DNA damage or RS. Upon fork stalling, both proteins are necessary to mediate fork reversal. In addition, FBH1 negatively regulates RAD51 by displacing it from chromatin and by preventing its re-association with DNA. See text for details.

The effects of FBH1 and RAD51 downregulation on cell size upon loss of GMN were confirmed with two specific siRNAs (Fig 41), reinforcing the notion that these two proteins are involved in re-replication control.

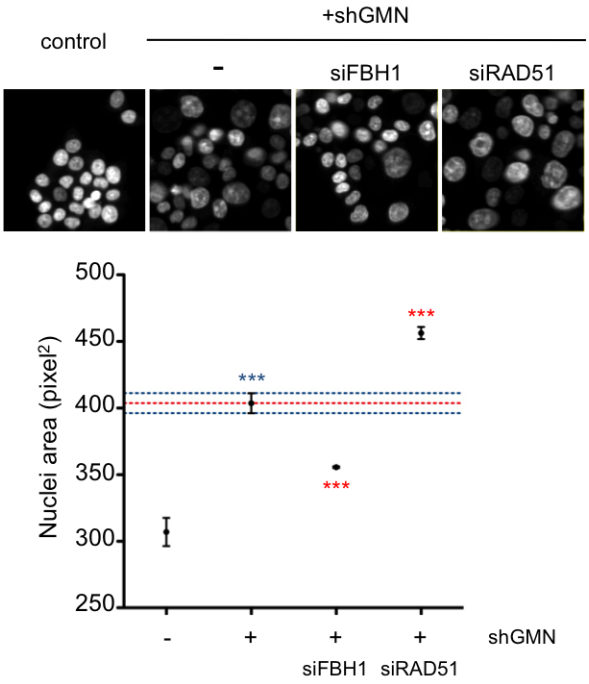

FIGURE 41. Top: Representative images of DAPI-stained HCT116-shGMN cells grown in media with or without dox for 72 h and treated with the indicated siRNAs. Bottom: Histogram shows mean and SD of nuclei area. (3 replicas of each condition were assessed; >900 cells of each replica were scored; results were analyzed with one-way Anova and Bonferroni's post test; ***, $p<0.001$).

FBH1 downregulation attenuates re-replication

To confirm that FBH1 modulates re-replication induced by GMN depletion, BrdU incorporation and DNA content were measured by flow cytometry. FBH1 downregulation was ensured with a combination of two siRNA molecules (Fig 42A). In the absence of GMN, FBH1 silencing decreased the percentage of cells with re-replicated DNA (Fig 42B). Efficient downregulation of GMN and FBH1 was assessed by immunoblot and RT-qPCR, respectively (Fig 42C, D). As a control of specificity, we confirmed that both siRNAs reduced Fbh1 mRNA and re-replication levels when used independently (Fig 43A, B). In subsequent experiments, we used the combination of both siRNAs to downregulate Fbh1.

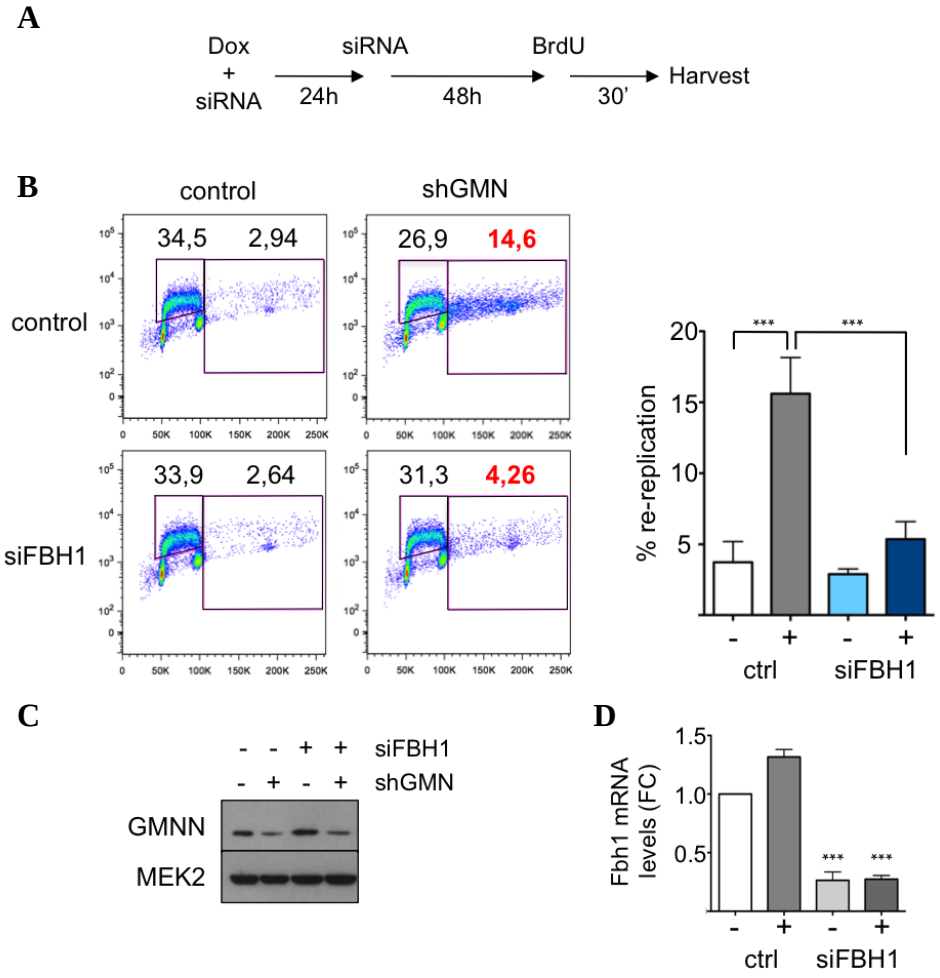

FIGURE 42. A. Schematic of DNA re-replication detection after gene siRNA downregulation. **B.** Flow cytometry analysis of re-replication in HCT116-shGMN cells grown in media with or without dox for 72 h and treated with the indicated siRNAs. Right gate represents cells with over-replicated DNA. Histogram shows the percentage of cells within this gate (mean value and SD; n=3 assays; results were analyzed with one-way Anova and Bonferroni's post test; ***, $p<0.001$; n.s.= not significant). **C.** Immunoblot detection of GMN in HCT116-shGMN cells from (**B**). MEK2 levels are shown as loading control. **D.** Histogram showing fold-change in Fbh1 mRNA levels relative to control in HCT116-shGMN cells from (**B**). Mean value and SD are shown; n= 3 assays; results were analyzed with one-way Anova and Bonferroni's post test; ***, $p<0.001$; n.s.= not significant.

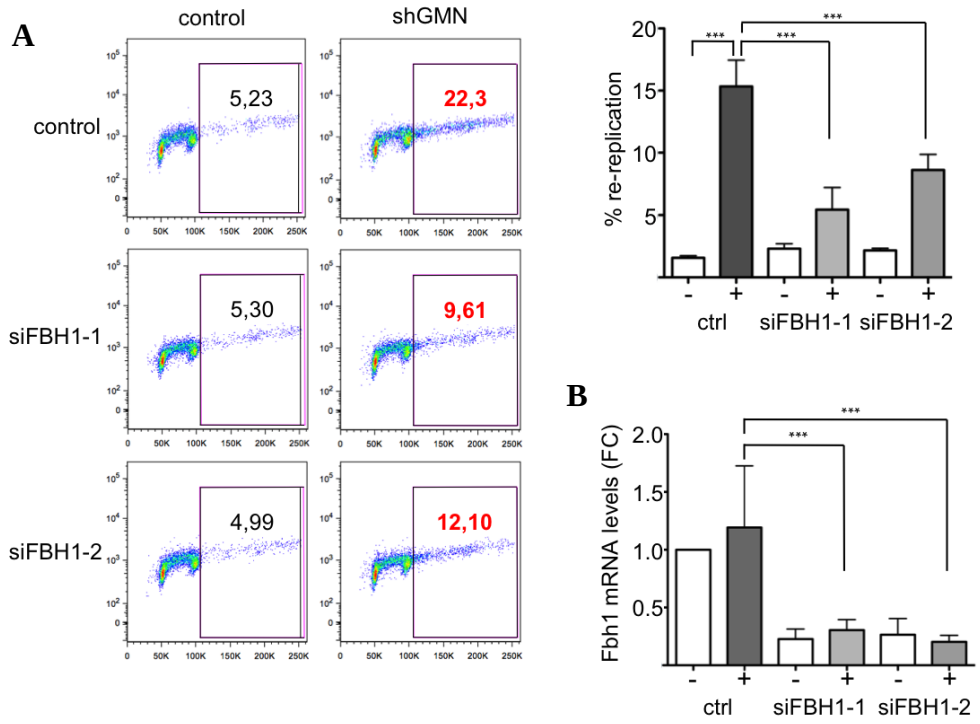

FIGURE 43. A. Flow cytometry analysis of re-replication in HCT116-shGMN cells grown in media with or without dox for 72 h and treated with the indicated siRNAs. Gate includes cells with over-replicated DNA. Histogram shows the percentage of cells within this gate (mean value and SD; n=3 assays; results were analyzed with one-way Anova and Bonferroni's post test; ***, p<0.001; n.s.= not significant). **B.** Histogram showing fold-change in Fbh1 mRNA levels relative to control in HCT116-shGMN cells from (**A**). Mean value and SD are shown; n= 3 assays; results were analyzed with one-way Anova and Bonferroni's post test; ***, p<0.001; n.s.= not significant.

RAD51 downregulation enhances re-replication

To confirm the effect of RAD51 downregulation on re-replication, two specific siRNAs against RAD51 were used. In the absence of RAD51, the extent of re-replication in GMN-depleted cells was increased (Fig 44A), arguing that RAD51 is necessary to limit re-replication. When FBH1 and RAD51 proteins were downregulated simultaneously the effect of individual RAD51 downregulation was attenuated (Fig 44).

The two RAD51 siRNAs were tested independently to confirm specificity. Both siRNAs reduced RAD51 protein levels to a similar extent and led to increased re-replication (Fig 45). In subsequent experiments, the combination of two siRNAs was used to downregulate Rad51.

Taken together, these results suggest that FBH1 and RAD51 may be part of a pathway that limits DNA re-replication in response to a failure in origin licensing control.

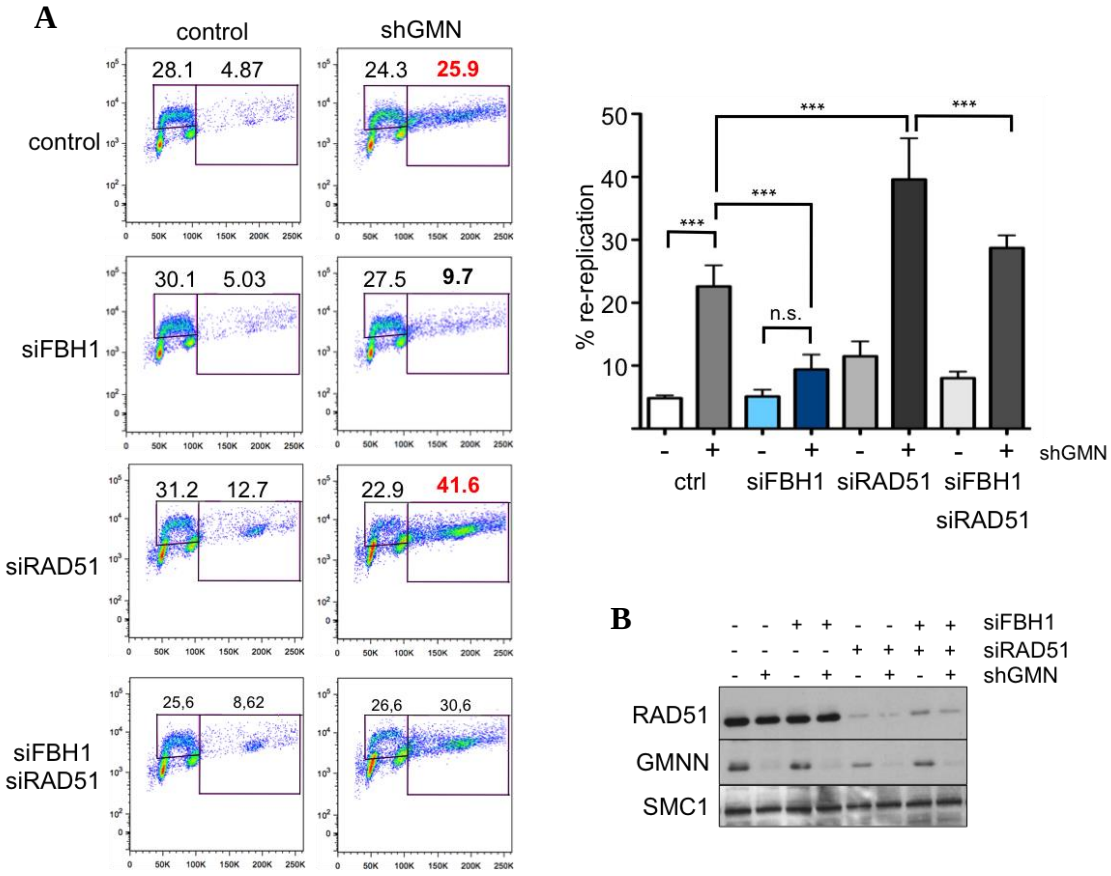

FIGURE 44. A. Flow cytometry analysis of re-replication in HCT116-shGMN cells grown in media with or without dox for 72 h and treated with the indicated siRNAs. Right gate includes cells with over-replicated DNA. Histogram shows the percentage of cells within this gate (mean value and SD; n=3 assays; results were analyzed with one-way Anova and Bonferroni's post test; ***, $p<0.001$; n.s.= not significant). **B.** Immunoblot detection of GMN and RAD51 in HCT116-shGMN cells from (**A**). SMC1 levels are shown as loading control.

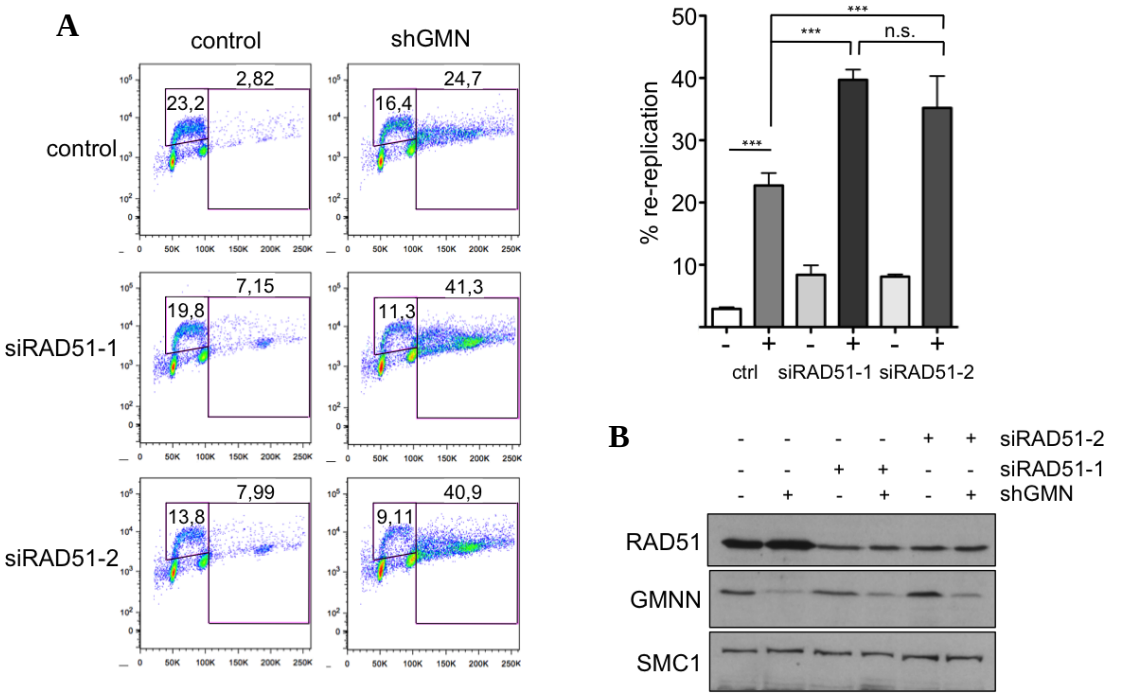

FIGURE 45. A. Flow cytometry analysis of re-replication in HCT116-shGMN cells grown in media with or without dox for 72 h and treated with indicated the siRNAs. Right gate includes cells with over-replicated DNA. Histogram shows the percentage of cells within this gate (mean value and SD; n=3 assays; results were analyzed with one-way Anova and Bonferroni's post test; ***, $p<0.001$; n.s.= not significant). **B.** Immunoblot detection of GMN and RAD51 in HCT116-shGMN cells from (**A**). SMC1 levels are shown as loading control.

Fbh1 downregulation reduces RS in GMN-depleted cells

As described above, FBH1 downregulation counteracted re-replication caused by loss of GMN. Accordingly, it also reduced the signs of RS and DNA damage in GMN-depleted cells, including phosphorylation of RPA32, histone H2AX, CHK1 and p53 (Fig 46A, compare lanes 2 and 4). GMN-depleted cells are partially arrested in G2 and this was also alleviated by FBH1 downregulation (Fig 46A, compare pH3 signal in lanes 2 and 4). Reduced RS stress in FBH1-depleted cells was confirmed by flow cytometry analysis of γH2AX levels (Fig 46B). In contrast, checkpoint activation was not affected by RAD51 downregulation, as similar levels of RPA32, CHK1, p53 and histone H3 phosphorylation were detected (Fig 46A, compare lines 2 and 6).

Because re-replication arises from re-fired origins, we wondered if it would increase the number of replication foci. GMN-depleted cells showed more BrdU foci than control cells (Fig 47). Notably, FBH1 downregulation restored foci number to control situation

(Fig 47). In contrast, RAD51 downregulation did not exacerbate the effect of GMN loss on replication foci (Fig 47).

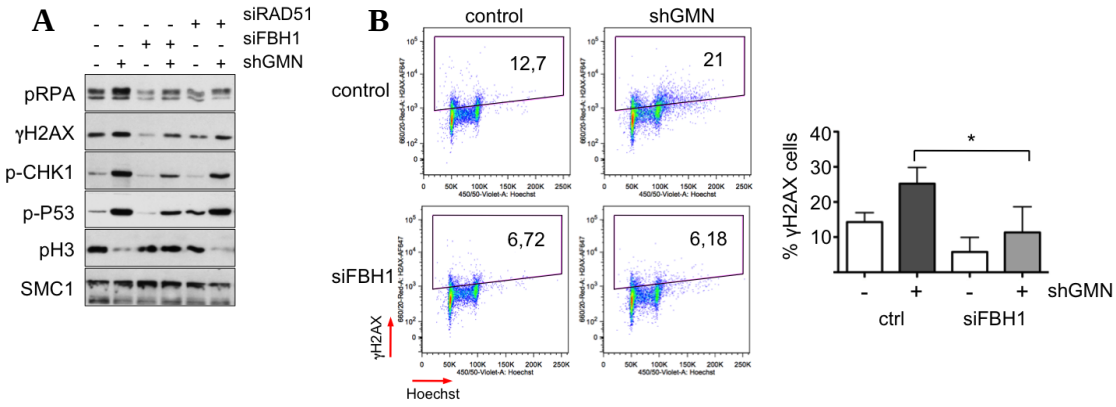

FIGURE 46. A. Immunoblot detection of the indicated proteins in HCT116-shGMN cells grown in media with or without dox for 72 h and treated with the indicated siRNAs. SMC1 levels are shown as loading control. The experiment was conducted twice with similar results; one example is shown. **B.** Flow cytometry analysis of γH2AX vs DNA content (Hoechst) in HCT116-shGMN cells. Gate includes γH2AX-positive cells. Histogram shows the percentage of γH2AX-positive cells (mean value and SD; n=2 assays; statistical significance was assessed with One way Anova and Bonferroni's's post test; *, $p<0.05$).

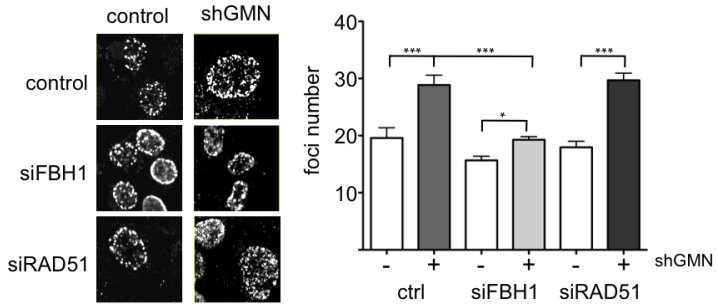

FIGURE 47. Representative images of BrdU foci in HCT116-shGMN cells grown in media with or without dox for 72 h and treated with the indicated siRNAs. Histogram shows the number of foci per cell (mean value and SD; n=3 biological replicas; >1000 cells scored in each condition and each replica; results were analyzed with one-way Anova and Bonferroni's post test; ***, $p<0.001$; *, $p<0.05$; n.s.= not significant).

Fbh1 downregulation attenuates re-replication independently of Mus81

FBH1 and MUS81 act together to induce DSBs during the response to RS (Fugger et al, 2013). To rule out a role of MUS81 in re-replication prevention, we tested how its downregulation affects DNA content after GMN loss. Indeed, MUS81 depletion did not affect the percentage of cells with re-replicated DNA in the absence of GMN. In addition, FBH1 and MUS81 co-depletion did dot further reduce re-replication levels (Fig 48) confirming that MUS81 is not implicated in re-replication modulation.

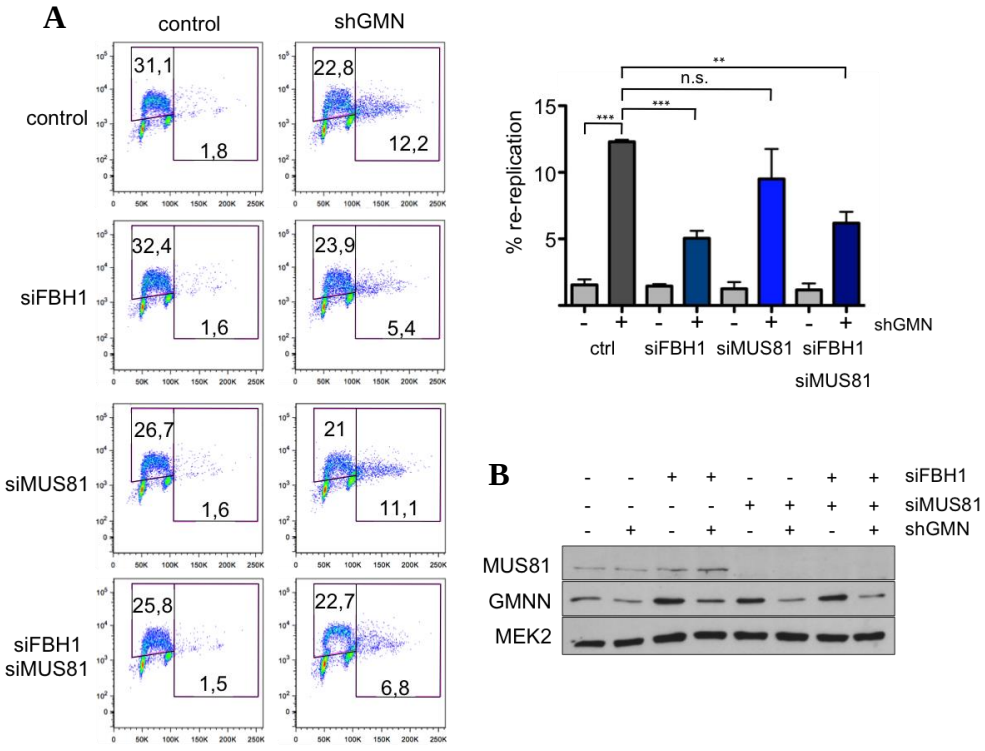

FIGURE 48. A. Flow cytometry analysis of re-replication in HCT116-shGMN cells grown in media with or without dox for 72 h and treated with the indicated siRNAs. Right gate includes cells with over-replicated DNA. Histogram shows the percentage of cells within this gate (mean value and SD; n=2 assays; results were analyzed with one-way Anova and Bonferroni's post test; ***, $p<0.001$; **, $p<0.01$; n.s.= not significant). **B.** Immunoblot detection of GMN and MUS81 in HCT116-shGMN cells from (**A**). MEK2 levels are shown as loading control.

GMN-induced re-replication does not promote fork reversal

In our screening, downregulation of helicases with fork remodelling activities affected nuclear size upon GMN loss. This is interesting as both FBH1 and RAD51 are involved in fork reversal (Fugger et al, 2015; Zellweger et al, 2015). To clarify whether fork reversal is involved in re-replication prevention, we investigated whether this process takes place after origin re-firing. We used an indirect assay based on the detection of ssDNA that is exposed when newly synthesized strands of different lengths anneal to form the characteristic three-way junction (Fig 48A; Couch et al, 2013). In this assay, cells are pulse-labelled for 10 min with BrdU after GMN depletion and harvested 1-3 h later (Fig 48B). BrdU immunostaining is performed without HCl denaturation, to restrict antibody accessibility to ssDNA (Fig 48A). As positive control, cells were treated with 2.5 mM HU in combination with ATR inhibition, as described in Couch et al (2013). No changes in "native" BrdU intensity were found after GMN downregulation, indicating similar levels of fork reversal in control and re-replication

conditions (Fig 48C, D). Actually, in GMN-downregulated cells, the intensity of native BrdU staining was similar to the negative control. We cannot absolutely conclude that fork regression does not occur in response to re-replication, as it may take place below the detection limit of the technique. However, we postulate that the frequency of these structures in response to re-replication is very limited.

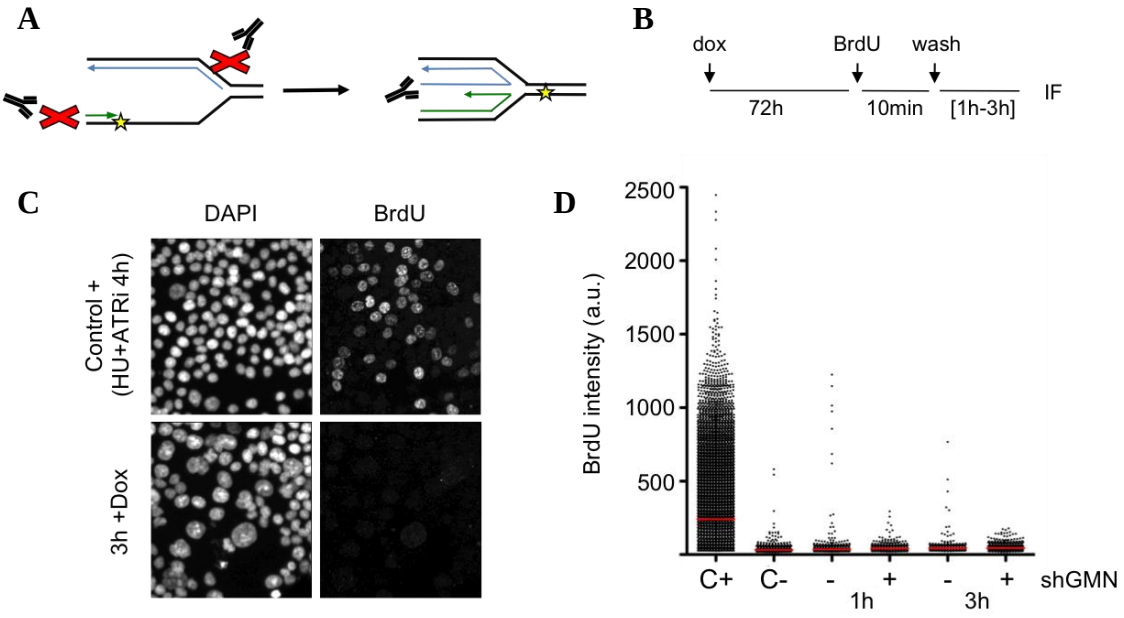

FIGURE 49. A. Schematic of the anti-BrdU recognition assay in nascent ssDNA at reversed forks. **B.** Timeline of the experiment. **C.** Representative images of BrdU staining in native conditions of HCT116-shGMN cells treated with dox for 3h after the BrdU pulse. Positive control, HCT116-shGMN cells treated with 2.5 mM HU in combination with 5 μM ATR inhibitor for 4 h **D.** HTM acquisition of BrdU fluorescence intensity in native conditions in HCT116-shGMN cells grown as indicated in (**B**). Median and distribution of BrdU intensities are plotted. Positive control (C+) as in (**C**). As negative control (C-), cells were stained without BrdU labelling. One assay is shown (n=2 assays; >1300 nuclei/condition in each assay).

To further investigate if the extent of re-replication could be limited by fork reversal, we tested the effect of SMARCAL1 downregulation. SMARCAL1 mediates fork reversal in response to HU-induced RS (Couch et al, 2013). As shown in Fig 50, SMARCAL1 loss did not significantly change the percentage of re-replicated cells (Fig 50A, B). This result reinforces the notion that fork regression is not a major mechanism to prevent DNA re-replication.

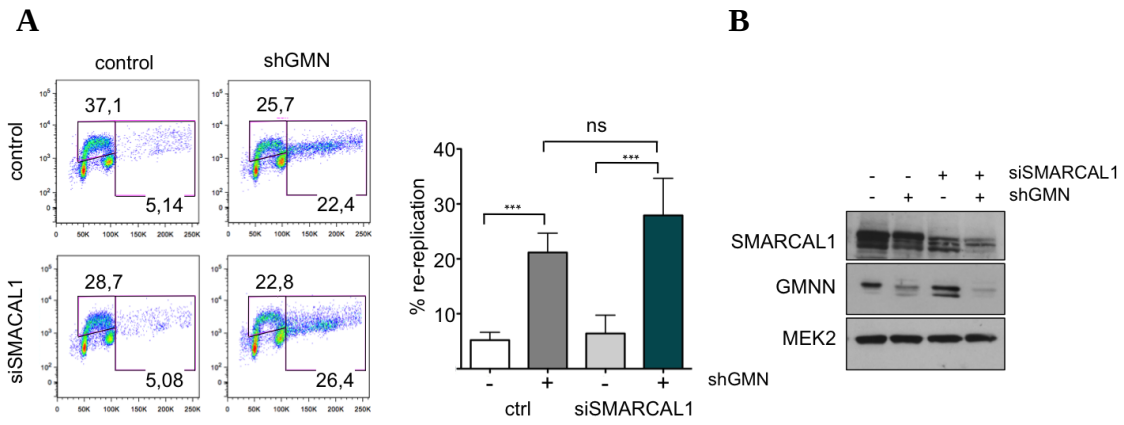

FIGURE 50. A. Flow cytometry analysis of re-replication in HCT116-shGMN cells grown in media with or without dox for 72 h and treated with the indicated siRNAs. Right gate includes cells with over-replicated DNA. Histogram shows the percentage of cells within this gate (mean value and SD; n=3 assays; results were analyzed with one-way Anova and Bonferroni's post test; ***, $p<0.001$; n.s.= not significant). **B.** Immunoblot detection of GMN and SMARCAL1 in HCT116-shGMN cells from (**A**). MEK2 levels are shown as loading control.

The role of RAD51 in re-replication control is independent of HR

The results presented above showed how an anti-recombinogenic protein (FBH1) favoured re-replication while a pro-recombinogenic one (e.g. RAD51) limited it. Therefore, we next asked whether the functions of FBH1 and RAD51 in modulating re-replication required HR. If this was the case, we reasoned that depletion of other HR proteins that operate downstream of RAD51 should render similar effects in terms of re-replication. RAD51AP1 was chosen to explore this possibility, as it co-operates with RAD51 during strand invasion and stabilization of the D-loop (Wiese et al, 2007; Daley et al, 2013; Fig 51A). We found that, upon GNN downregulation depletion of RAD51AP1 did not affect the percentage of cells with re-replicated DNA (Fig 51B, C), suggesting that strand invasion reaction and HR are not necessary to restrict re-replication.

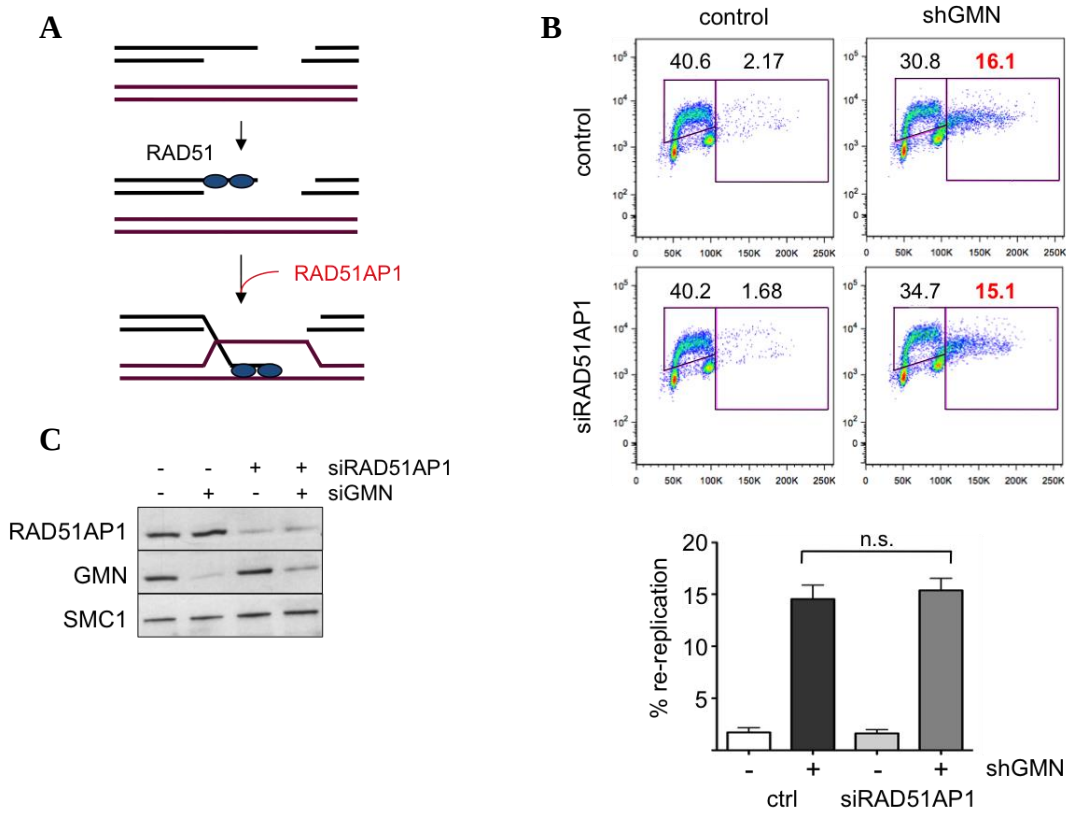

FIGURE 51. A. Schematic of the role of RAD51AP1 in the strand invasion step of HR. **B.** Flow cytometry analysis of re-replication in HCT116-shGMN cells grown in media with or without dox for 72 h and treated with the indicated siRNAs. Right gate includes cells with over-replicated DNA. Histogram shows the percentage of cells within this gate (mean value and SD; n=3 assays; results were analyzed with one-way Anova and Bonferroni's post test; n.s.= not significant). **C.** Immunoblot detection of GMN and RAD51AP1 in HCT116-shGMN cells from experiment showed in (**B**). MEK2 levels are shown as loading control.

RAD51 binds to chromatin during the S-phase

None of the canonical FBH1 and RAD51 functions seemed to be involved in prevention of re-replication, so we entertained another possibility. FBH1 might be a general regulator of the stability of RAD51 on chromatin, not only at stalled forks, as described to date. In turn, chromatin-bound RAD51 might be responsible of limiting the extent of re-replication following aberrant origin licensing and re-firing.

This model predicts that RAD51 binds to chromatin even in an unperturbed S phase. This hypothesis was tested by IF stainings of chromatin-bound RAD51 in the presence or absence of GMN. PCNA staining allowed differentiating the cells undergoing S phase. With this approach, we first confirmed that re-replication increased nuclear RAD51 intensity and induced the formation of RAD51 foci due to the generation of DSBs (Fig 52A, B; Melixetian et al, 2004; Zhu and Dutta 2006). In control conditions,

PCNA-positive cells displayed higher intensity of RAD51 than PCNA-negative cells (Fig 52C). Most of the RAD51 signal was not concentrated in foci but rather distributed through chromatin (Fig 52A, upper panel). This result suggests that a fraction of RAD51 binds to DNA during unchallenged S phase and possibly has functions outside recombination foci.

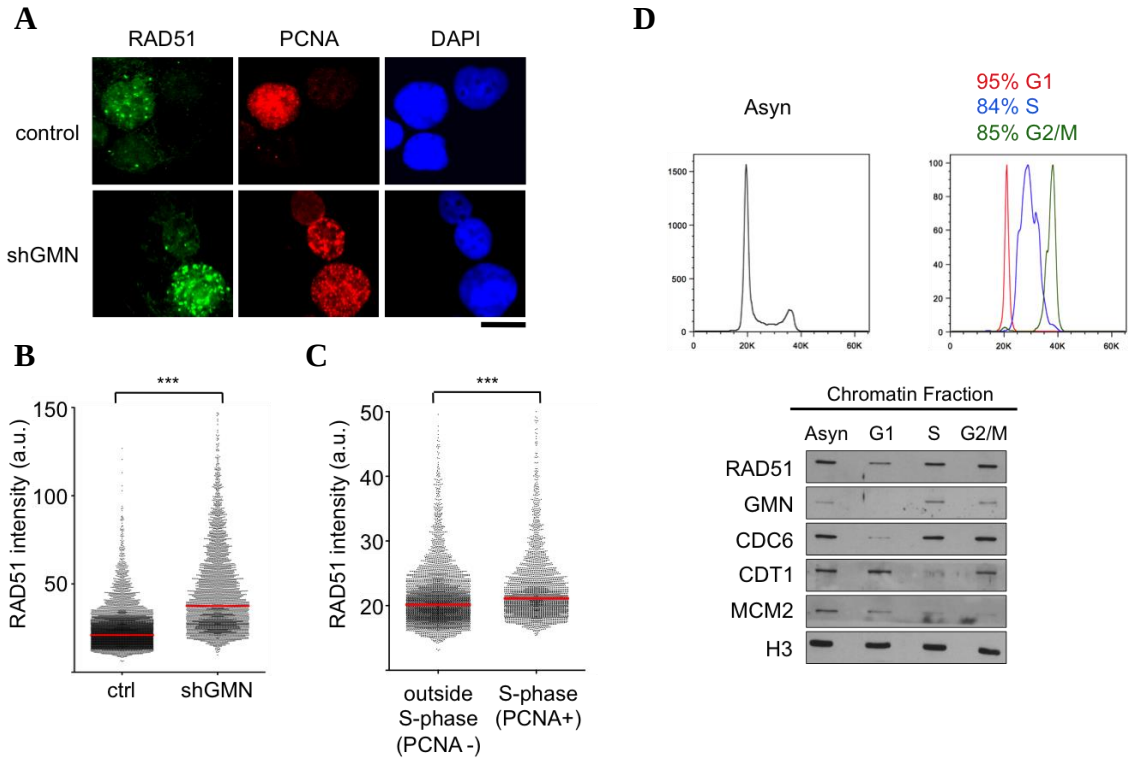

FIGURE 52. A. Representative images of control and dox-treated (72 h) HCT116-shGMN cells, immunostained for chromatin-bound RAD51 (green) and PCNA (red) proteins. DNA was counterstained with DAPI (blue). Scale bar, 15µm. **B.** Plot shows the median and the distribution of RAD51 intensity in the cells used in (**A**). 8013 and 4034 nuclei in each condition respectively; statistical analysis was performed using Mann-Whitney test; ***, p<0.001). **C.** Plot shows the median and the distribution of RAD51 intensity in PCNA-negative and PCNA-positive HCT116-shGMN control cells 4960 and 3053 nuclei in each condition respectively; statistical analysis was performed using Mann-Whitney test; ***, p<0.001). **D.** Upper panel, DNA content profiles of asynchronous HCT116-shGMN control cells and the different fractions obtained after cell sorting. Lower panel, immunoblot detection of the indicated proteins after biochemical fractionation of sorted cells. Chromatin-bound fraction is shown. GMN, CDC6, CDT1 and MCM2 proteins serve as control of cell cycle position. Chromatin-bound H3 levels serve as loading control.

The kinetics of RAD51 chromatin binding in unperturbed cells was evaluated by biochemical fractionation in cells sorted in the G1, S and G2/M phases of the cell cycle (Fig 52D). GMN, CDC6, CDT1 and MCM2 proteins are shown as controls since they behave as expected (reviewed by Arias and Walter, 2007). Higher levels of RAD51 on chromatin were found in S and G2/M than in G1 (Fig 52D) suggesting that RAD51 is recruited to chromatin during the S phase. Considering that the RAD51 staining pattern

is pan-nuclear during S phase (Fig 52A) and that HR did not influence re-replication, we hypothesize that the fraction of RAD51 that is associated to chromatin but not enriched in foci might be responsible for limiting re-replication.

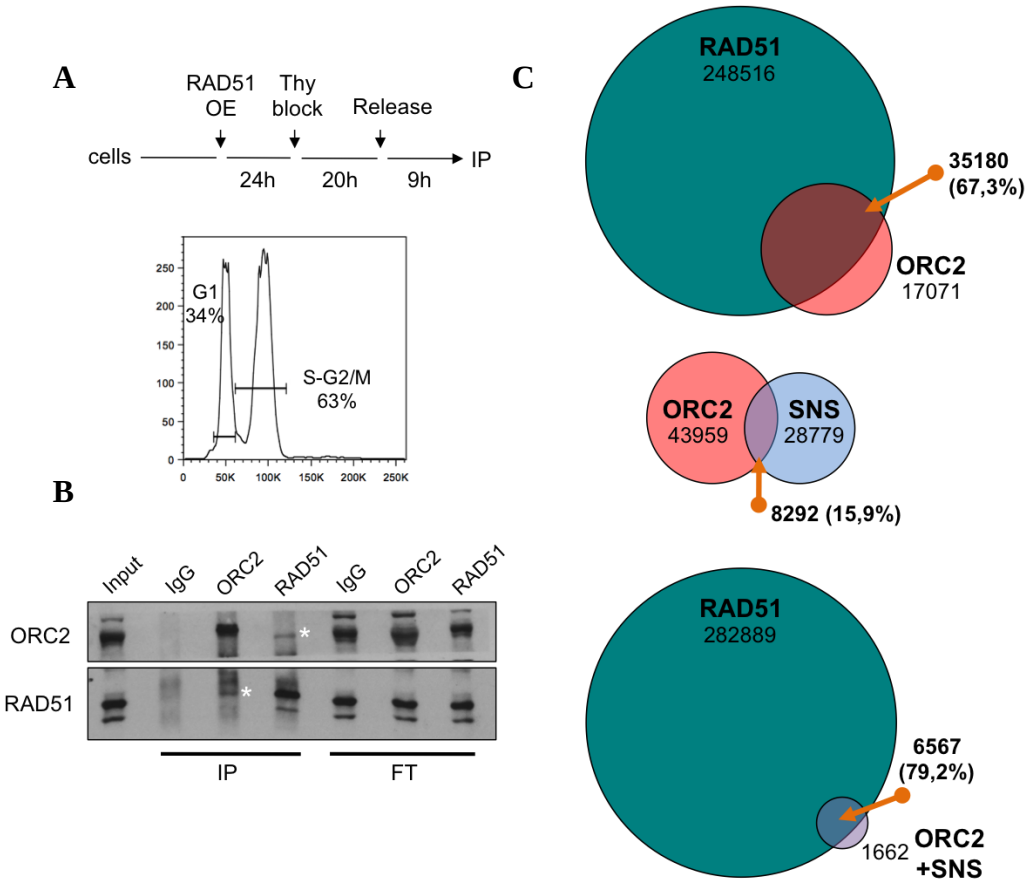

FIGURE 53. A. Upper panel, schematic of the experiment. Lower panel, DNA content profile of HCT116-shGMN cells after thymidine (Thy) block and release. Gates include G1 cells (left) and S/G2/M cells (right). **B.** Immunoprecipitation (IP) assays using IgG, hORC2 and hRAD51 antibodies, in HCT116-shGMNN cells transfected with pDEST47-RAD51 plasmid and enriched in S/G2/M phases. IP samples, input (2% of the amount used in the IP) and flow-through (FT) samples were analyzed by immunoblot with the indicated antibodies. Asterisks mark RAD51 and ORC2 interaction. **C.** Venn diagrams showing overlap between hRAD51, hORC2 and SNS genomic positions as indicated. Percentages are relative to ORC2 positions (top and middle panels) and ORC2+SNSs positions (down panel). See text for details.

Interestingly, RAD51 has been detected at ongoing replication forks by iPOND (Zellweger et al, 2015) and it interacts with several MCM subunits (Shukla et al, 2005) Based on these antecedents, it is possible that RAD51 also binds to replication origins. To test this hypothesis, RAD51 was overexpressed in a cell population enriched in S and G2 by thymidine 'block and release' (Fig 53A). Reciprocal immunoprecipitation

(IP) reactions revealed an interaction between RAD51 and endogenous ORC2 (Fig 53B).

Available data about RAD51 occupancy on chromatin (RAD51 ChIP-seq from ENCODE project, GEO accession nr GSE91838) further support the notion that RAD51 binds to replication origins. A comparison of RAD51 ChIP positions and ORC2 binding sites (Miotto et al, 2016) in K562 cells indicated that >67% (35180) of ORC2 positions contained RAD51 (Fig 53C). Intriguingly, only 16% (8292) of the defined ORC2 positions overlapped with short-nascent DNA strands (SNS) mapped in a separate study (Picard et al, 2014). However, almost 80% (6567 peaks) of these *bona fide* replication origins (positive for both Orc2 and SNS) contained RAD51 (Fig 53C).

Taken together, these experiments suggest that a population of RAD51 binds to chromatin during the S phase that is not organized in recombination or repair foci. We propose that this population plays a role in the control of DNA re-replication.

Stabilization of RAD51 on chromatin reduces re-replication

In our model, the lack of FBH1 would stabilize RAD51 on chromatin, resulting in lower re-replication levels. In fact, this effect has been documented in different systems (Fugger et al, 2009; Simandlova et al, 2013). In our cellular system, FBH1 downregulation increased the IF signal of chromatin-bound RAD51 in S phase cells (Fig 54).

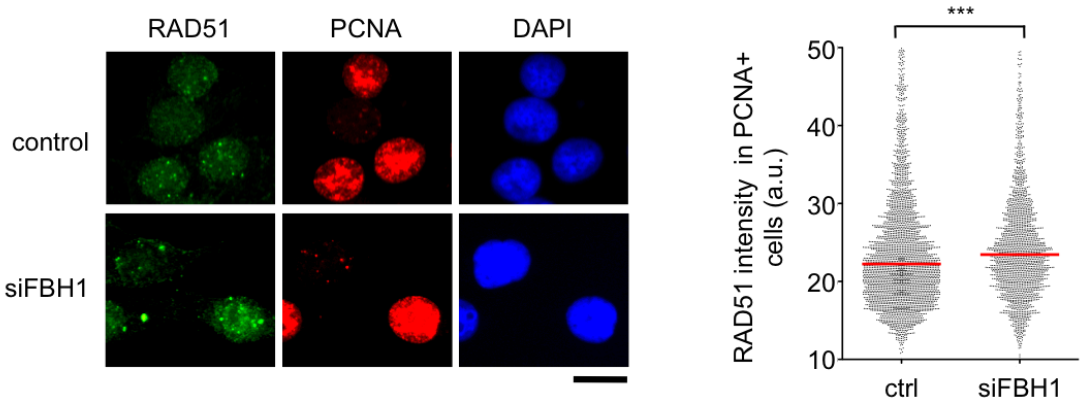

FIGURE 54. Representative images of HCT116-shGMN cells treated with FBH1 siRNA for 48 h, immunostained for chromatin-bound RAD51 (green) and PCNA (red) proteins. DNA was counterstained with DAPI (blue). Scale bar, 15 μm. Histogram shows the median and the distribution of RAD51 intensity from PCNA-positive cells. 3053 and 1939 nuclei in each condition respectively; statistical analysis was performed using Mann-Whitney test; ***, $p<0.001$).

We reasoned that other treatments that modulate the stability of RAD51 on chromatin should have an influence in re-replication levels. Different strategies were used to test this hypothesis. First, we tested RAD51 mutant versions in the ATPase domain (Fig 55A) that affect its ability to form functional filaments (Stark et al, 2004; Chi et al, 2006; Kim et al 2012). RAD51 K133A mutant is defective for ATP binding and K133R mutant is unable to hydrolyse ATP. Both mutants in Lys133 are dominant-negative when co-expressed with endogenous RAD51 (Kim et al 2012), preventing the efficient formation of RAD51 filaments (Stark et al, 2002; Stark et al, 2004; Laulier et al, 2011; Kim et al 2012). When these mutants were transfected in HCT116-shGMN cells and tested in the DNA re-replication assay, both of them increased the extent of re-replication caused by GMN loss (Fig 55B, C, D). This result suggests that RAD51 ATPase activity and formation of functional filaments are necessary to limit re-replication.

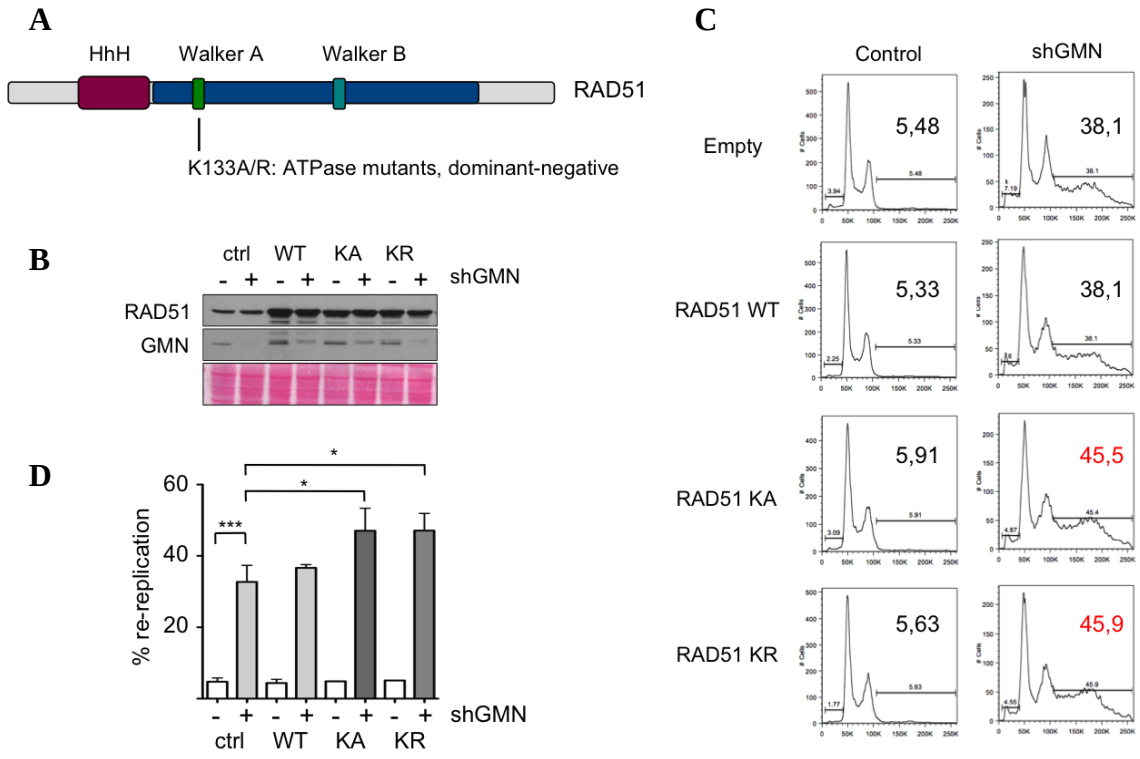

FIGURE 55. A. Schematic of RAD51 primary structure. HhH (Helix-hairpin-Helix) DNA binding domain, Walker A and B motifs are indicated. Lysine 133 is located in the Walker A motif. The conserved domain between RecA and Rad51 is represented in blue. **B.** Immunoblot detection of GMN and RAD51 mutants in HCT116-shGMN cells 48 h after a single transfection with pDEST47-RAD51 expressing either WT, K133A (KA) or K133R (KR) mutant forms of RAD51. Ponceaus staining is shown as loading control. **C.** DNA profiles measured by Hoechst signal of HCT116-shGMN cells grown in media with or without dox for 72 h and transfected with the indicated plasmids. Right gate includes cells with >2C DNA content. **D.** Histogram shows the percentage of cells with >2C DNA content (mean value and SD; n=2 assays; results were analyzed with one-way Anova and Bonferroni's post test; ***, $p<0.001$; *, $p<0.05$).

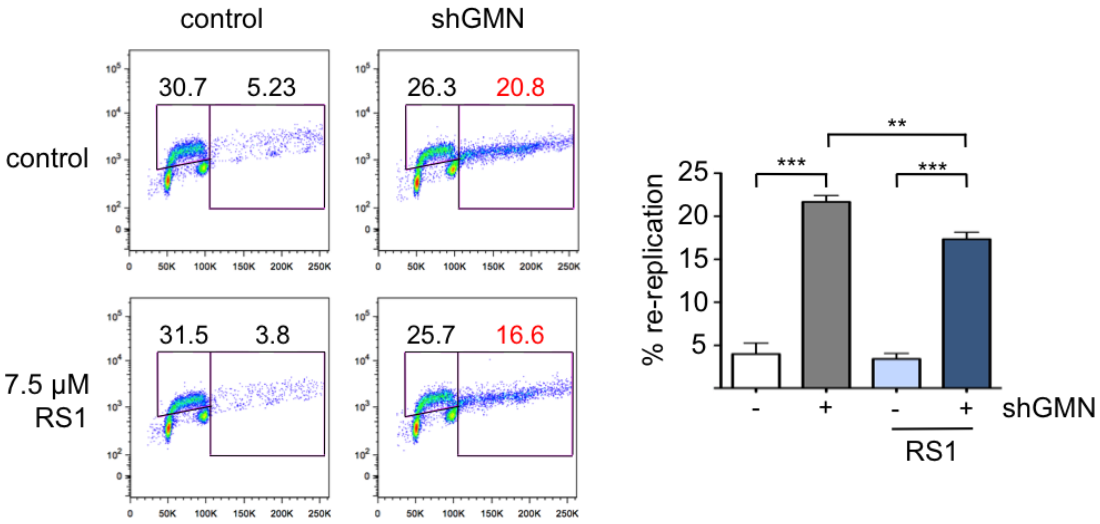

FIGURE 56. Flow cytometry analysis of re-replication in HCT116-shGMN cells grown in media with or without dox for 72 h and treated with 7.5µM RS1 for the last 24 h. Right gate includes cells with over-replicated DNA. Histogram shows the percentage of cells within this gate (mean value and SD; n=3 assays; results were analyzed with one-way Anova and Bonferroni's post test; ***, p<0.001; **, p<0.01).

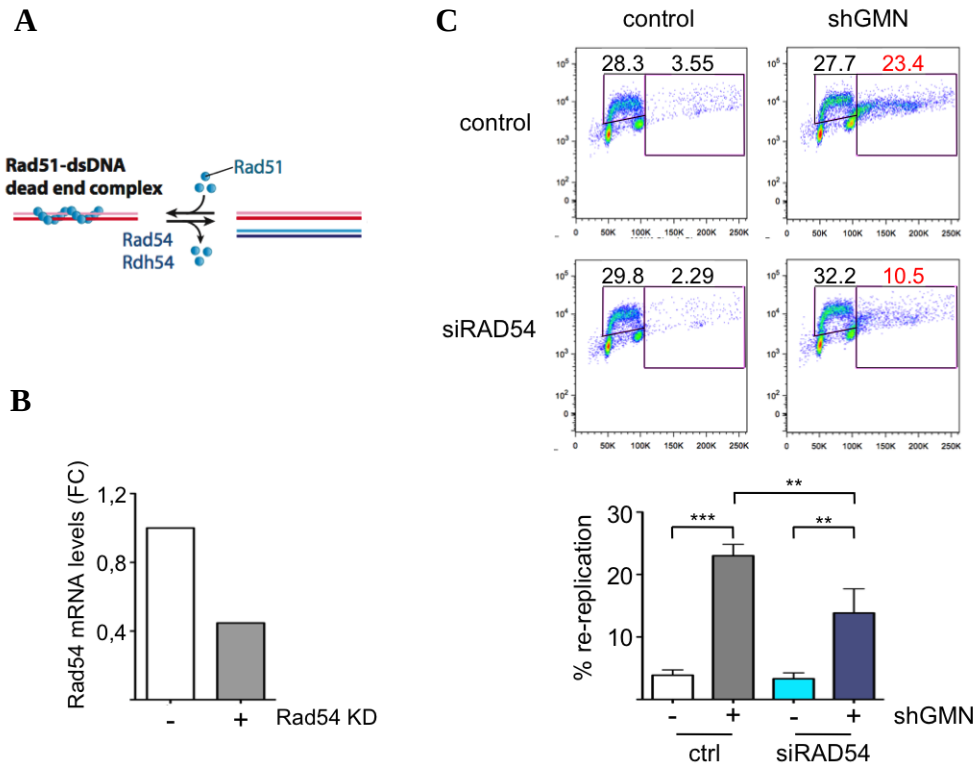

FIGURE 57. A. Schematic of RAD54 role in destabilizing RAD51 nucleofilaments on DNA. Taken from Heyer et al. (2010). **B.** Histogram shows RAD54 mRNA levels (fold-change relative to control) in HCT116-shGMN cells. **C.** Flow cytometry analysis of re-replication in HCT116-shGMN cells grown in media with or without dox for 72 h and treated with the indicated siRNAs. Right gate includes cells with over-replicated DNA. Histogram shows the percentage of cells within this gate (mean value and SD; n=3 assays; results were analyzed with one-way Anova and Bonferroni's post test; ***, p<0.001; **, p<0.01).

As a second approach, cells were treated with RS-1, a drug that stabilizes RAD51 binding to ssDNA (Jayathilaka et al, 2008). RS-1 slightly reduced re-replication levels caused by GMN loss (Fig 56). Finally, we tested the effect of RAD54, a translocase responsible for destabilizing RAD51 filaments on dsDNA (Solinger et al, 2002; Shah et al, 2010; Ceballos and Heyer, 2011; Fig 57A). In the absence of a good antibody for RAD54, the efficiency of siRNA was tested by mRNA levels (Fig 57B). Interestingly, we found that in the absence of GMN, a 50% downregulation of RAD54 mRNA was sufficient to reduce the percentage of re-replicated cells (Fig 57C). Taken together, these results suggest that stabilization of RAD51 protein on chromatin contributes to limit DNA re-replication.

MCM binding to chromatin does not influence re-replication levels

Because RAD51 interacts with ORC and MCM, we wondered whether FBH1 or RAD51 downregulation might affect the binding of pre-RC proteins or the CMG helicase complex to the DNA. Biochemical fractionation assays showed that upon GMN depletion, the amount of pre-RC components on chromatin was reduced (Fig 58, compare lanes 1 and 2). This effect can be explained because GMN protects a fraction of CDT1 protein from degradation during G2 and M, facilitating licensing in the next G1 phase (Ballabeni et al, 2004). As expected, not only CDT1 but also MCM components were slightly less abundant in the chromatin fraction of GMN-depleted cells (Fig 58). Although CDC6 binding to DNA is independent of CDT1, at least in yeast (Yeeles et al, 2015), we found that CDC6 chromatin association was also affected by GMN depletion.

FBH1 or RAD51 downregulation did not affect CDC6 or CDT1 binding to chromatin (Fig 58, compare lanes 1 and 3; 1 and 5). Unexpectedly, downregulation of RAD51 slightly increased the amount of chromatin-bound MCM proteins, but not CDC45, another component of the CMG helicase. Therefore, the number of active helicases might not increase. As CDC6, CDT1 or CDC45 DNA binding are virtually not affected by RAD51 downregulation, the effect of RAD51 on re-replication is not likely to be mediated by changes in origin licensing. The increase in MCM loading could be caused by fork stalling associated to re-replication or alterations in cell cycle progression.

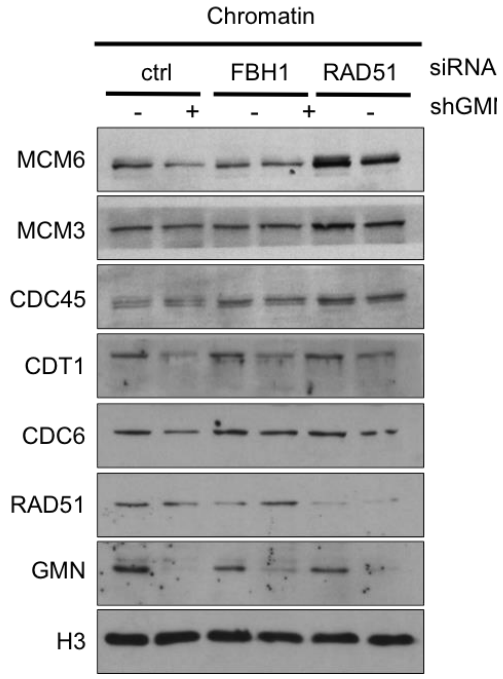

FIGURE 58. Immunoblot detection of the indicated proteins after biochemical fractionation of HCT116-shGMN cells grown in media with or without dox for 72 h and treated with the indicated siRNAs. Chromatin-bound fraction is shown. H3 is shown as loading control.

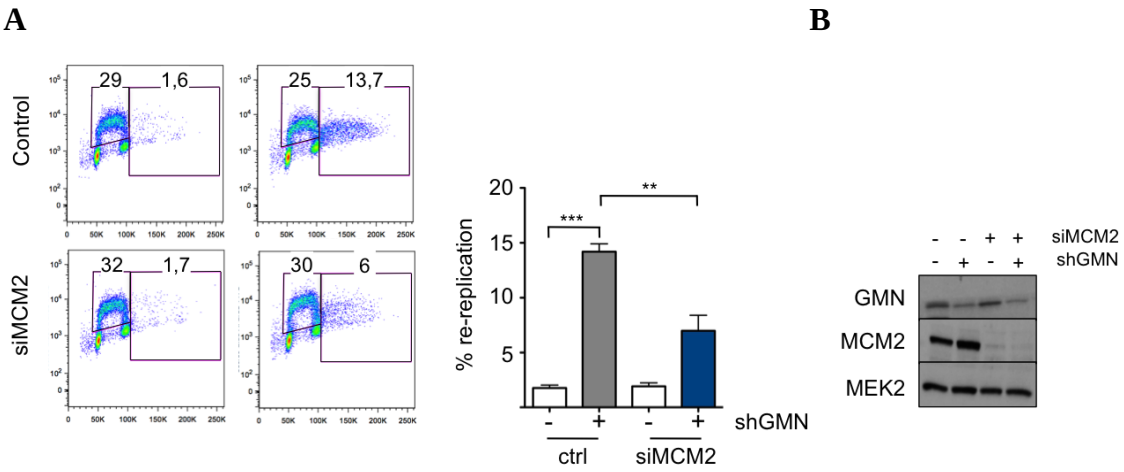

FIGURE 59. A. Flow cytometry analysis of re-replication in HCT116-shGMN cells grown in media with or without dox for 72 h and treated with the indicated siRNAs. Right gate includes cells with over-replicated DNA. Histogram shows the percentage of cells within this gate (mean value and SD; n=3 assays; results were analyzed with one-way Anova and Bonferroni's post test; ***, $p<0.001$; **, $p<0.01$). **B.** Immunoblot detection of GMN and MCM2 in HCT116-shGMN cells from (**A**). MEK2 levels are shown as loading control.

The fact that MCM levels do not correlate with re-replication seems counterintuitive. We considered the possibility that re-replication depends on the unscheduled association of MCM complexes with the DNA (e.g. during S or G2) rather than their absolute amount. To test this idea, we evaluated whether GMN depletion could still induce re-replication after siRNA-mediated MCM downregulation. Indeed, GMN depletion induced substantial re-replication even after a significant reduction (>90%) in

MCM2 protein (Fig 59). This result suggests that some replication origins might have particularly high affinity for MCMs and could be relicensed despite of the reduction in MCM concentration. Accordingly, yeast cells contain origins that are prone to re-replication and are characterized by specific sequences called re-initiation promoters (Richardson and Li; 2014).

RAD51 blocks the progression of re-replicated forks

At this point we considered the possibility that RAD51 might block the progression of forks originated form re-fired origins. Origin activity and fork progression rate (FR) were monitored using stretched DNA fiber assays (Fig 60A) to explore this possibility.

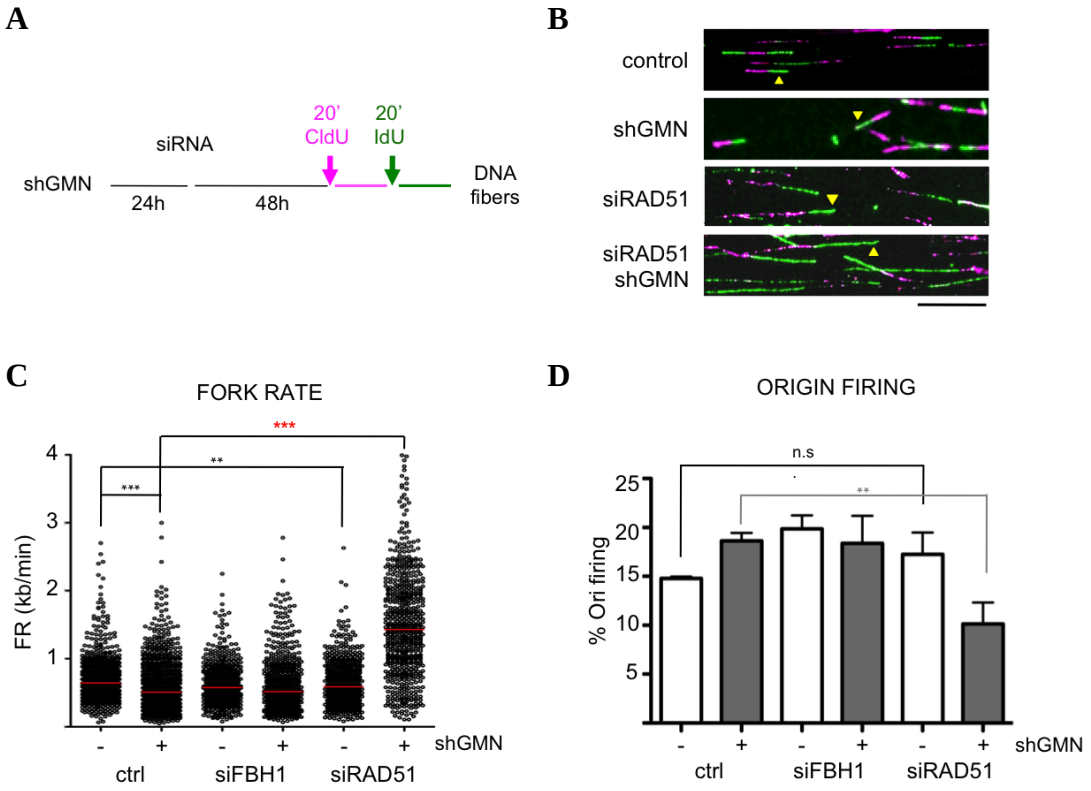

FIGURE 60. A. Representation of the DNA fiber experiment **B.** Examples of DNA fiber images from the indicated cells. Bar, 20 μM **C.** Histogram shows the median and the distribution of FR values in HCT116-shGMN cells grown in media with or without dox for 72 h and treated with the indicated siRNAs. Data from three separate experiments are pooled (n>900 measurements/condition; p-values were calculated with Mann-Whitney test; ***, p<0.001; **, p<0.01). **D.** Histogram shows the percentage of origin firing in the same cells used in (**C**). Mean value and SD; n=2 assays. 500 1st label structures/condition were measured in each assay; p-values were calculated with one-way Anova and Bonferroni's post test; **, p<0.01;n.s., not significant.

GMN depletion reduced fork speed (Fig 60B, C). This result was expected considering that re-replication induces DNA damage (Neelsen et al, 2013) that slows replication forks (Seiler et al, 2007). In control cells, FBH1 and RAD51 downregulation slightly

diminished FR, suggesting that both factors may facilitate fork progression during S phase (Fig 60C). Interestingly, in re-replication conditions, RAD51 downregulation markedly increased fork speed (Fig 60B, C). Considering that RAD51 downregulation only had a limited effect on FR in control cells, we reasoned that the effect observed upon GMN loss might be due mainly to re-replicated forks. Moreover, RAD51 depletion in control cells did not change origin activity, while in the absence of GMN it reduced origin activation, which is consistent with the increased FR (Zhong et al, 2013). These results point out to a function of RAD51 in impeding fork progression.

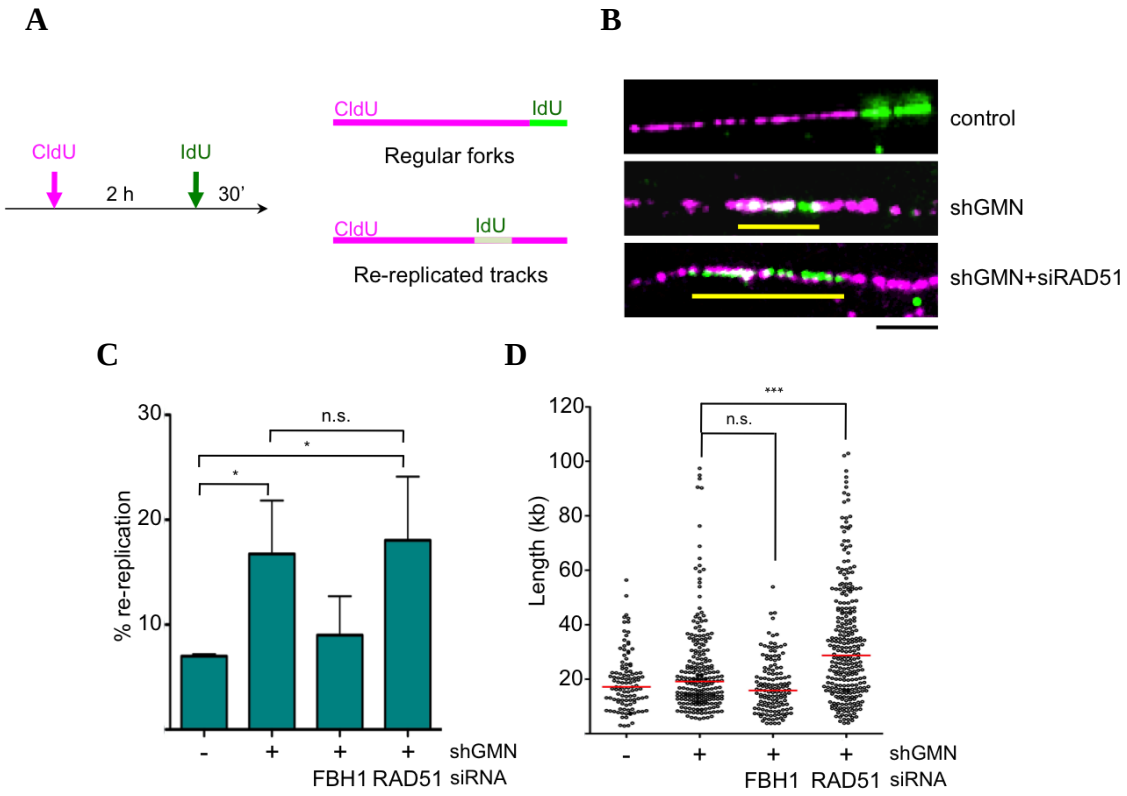

FIGURE 61. A. Detection of re-replication using stretched DNA fibers. Schematic of the experiment and representation of observed structures **B.** Examples of HCT116-shGMN cells grown in media with or without dox for 72 h and treated with RAD51 siRNA. Bar, 5 μM **C.** Histogram shows the percentage of re-firing events (re-replicated tracks relative to the total number of green tracks) in HCT116-shGMN cells (mean value and SD; n= 3 assays; 394-551 green track measurements/condition in each assay; n>1400 total green tracks scored in each condition; one-way Anova followed by Bonferroni's post test was applied; *, $p<0.05$; n.s., not significant). **D.** Plot shows the length of re-replicated tracks in the same cells used in (**C**). The median and the distribution of lengths are plotted. Data from three different experiments are pooled (mean value and SD; 111, 234, 139 and 280 re-replicated tracks were measured respectively in each condition; Mann-Whitney test was applied; ***, $p<0.001$; n.s., not significant).

To confirm that RAD51 specifically blocks the progression of forks originated from refired origins we evaluated the length of re-replicated tracks in single molecules, using the variation of the DNA fiber assay described in the first chapter of Results (Fig 61A,

B). As expected, the percentage of re-replicated tracks was similar when GMN was depleted alone or in combination with RAD51 (Fig 61C), arguing against a regulation of origin re-firing. In contrast, re-replicated tracks were much longer when RAD51 was absent (Fig 61B, D). This result provides direct evidence that chromatin-bound RAD51 during S phase limits re-replication by hindering the progression of re-replicated forks.

MRE11 is involved in the degradation of re-replicated DNA

A HR-independent role for RAD51 during DNA replication was proposed in *X. laevis*, consisting in the protection of nascent strands from MRE11 nuclease degradation (Hashimoto et al, 2010). We wondered if MRE11 might participate in re-replication control, possibly by degrading the re-replicated strands. The role of MRE11 was evaluated in GMN-depleted cells using mirin, a chemical inhibitor of MRE11 (Dupré et al, 2008). Indeed, MRE11 inhibition resulted in a higher percentage of cells with partially re-replicated DNA (Fig 62A). When MRE11 and RAD51 were simultaneously downregulated, the percentage of cells with over-replicated DNA was further increased (Fig 62B).

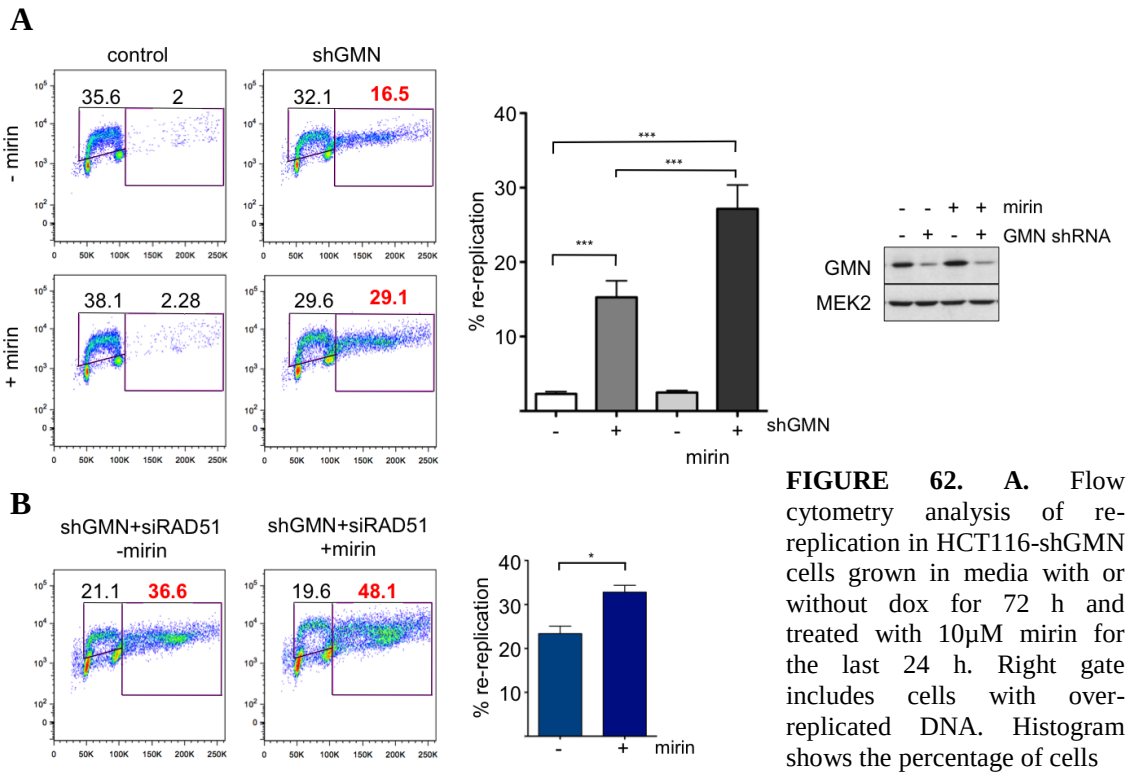

FIGURE 62. A. Flow cytometry analysis of re-replication in HCT116-shGMN cells grown in media with or without dox for 72 h and treated with 10µM mirin for the last 24 h. Right gate includes cells with over-replicated DNA. Histogram shows the percentage of cells within this gate (mean value and SD; n=3 assays; results were analyzed with one-way Anova and Bonferroni's post test; ***, p<0.001; **, p<0.01). Immunoblot shows GMN downregulation. **B.** Flow cytometry analysis of re-replication in HCT116-shGMN cells treated with the indicated siRNAs, grown in media with or without dox for 72 h and treated with 10µM mirin for the last 24 h. Right gate includes cells with over-replicated DNA. Histogram shows the percentage of cells within this gate (mean value and SD; n=2 assays; results were analyzed with Student's t-test; *, p<0.05).

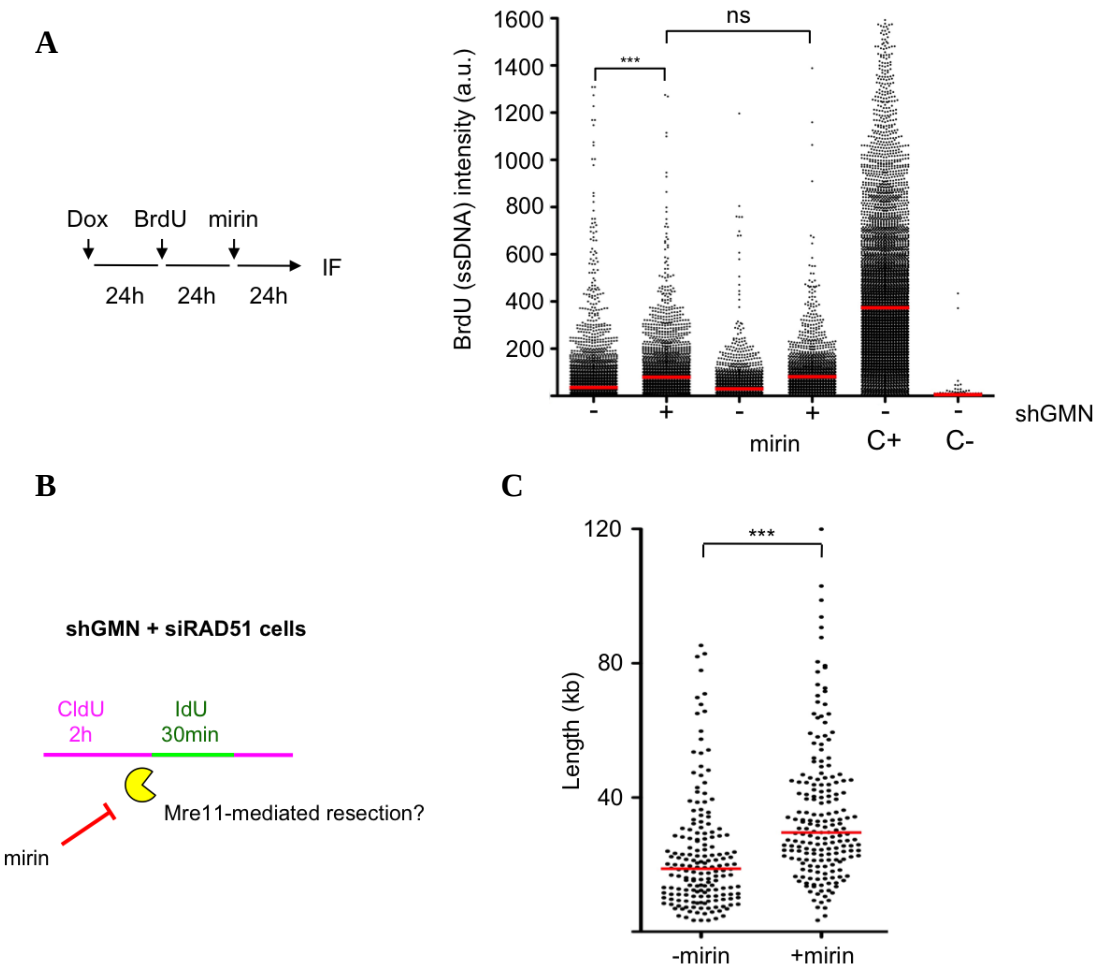

FIGURE 63. A. Left panel, schematic of the experiment. Right panel, HTM acquisition of BrdU fluorescence intensity in native conditions in HCT116-shGMN cells grown in media with or without dox and treated with 10µM mirin for 24 h. Median and distribution of BrdU intensities are plotted. As positive control, cells were treated with 2.5 mM HU for 24 h (C+). As negative control, the BrdU labelling step was omitted (C-). A representative assay is shown (n=3 assays; >1900 nuclei/condition in each assay). Statistical significance was assessed using Kruskal-Wallis test followed by Dunn's post-test; ***, $p<0.001$; n.s, not significant. **B.** Detection of re-replication using stretched DNA fibers. Schematic of the experiment: Dox-treated and RAD51-depleted HCT116-shGMN cells are treated or not with 10µM mirin for 24 h and pulse labelling with CldU (2h; pink) and IdU (30 min; green). **C.** Plot shows the length of re-replicated tracks in the indicated cells. The median and the distribution of lengths are plotted. Data from two different experiments are pooled (178 and 190 total re-replicated tracks were measured respectively in each condition; Mann-Whitney test was applied; ***, $p<0.001$).

Origin re-firing promotes the accumulation of ssDNA gaps by unknown mechanisms (Neelsen et al, 2013). If MRE11 degrades re-replicated DNA, we reasoned that end resection might be a source of ssDNA. In this case, inhibition of MRE11 should increase the levels of re-replicated DNA without increasing the amount of ssDNA. This possibility was investigated by measuring ssDNA levels by BrdU native detection in cells treated with mirin (Fig 63A). We confirmed that GMN depletion leads to ssDNA accumulation (Fig 63A, lanes 1 and 2). As anticipated, MRE11 inhibition did not further increase the amount of ssDNA (Fig 63A, lanes 2 and 4).

Finally, to confirm that MRE11 degrades over-replicated DNA, we evaluated the length of re-replicated tracks in GMN and RAD51 co-depleted cells treated with the MRE11 inhibitor (Fig 62B). After 24 h of mirin treatment, re-replicated tracks were significantly longer (Fig 62C), confirming that MRE11 participates in the clearance of re-replicated DNA.

Taken together, our results indicate that disruption of licensing control by ablation of GMN causes the reactivation of some replication origins during S or G2. In these circumstances, RAD51 and MRE11 participate in backup mechanisms to limit the progression of re-replicated forks and degrade the over-replicated DNA.

DISCUSSION

DISCUSSION

Mouse models to study the effects of deregulated origin activity

The consequences of origin licensing disruption have been extensively addressed in cell lines (reviewed by Hills and Diffley, 2014). Several MCM-deficient mouse models that address the effects of insufficient origin activity have also been generated. These mice display RS, DNA damage, stem cell deficiency, hematopoietic defects and cancer susceptibility (Shima et al, 2007; Pruitt et al, 2007; Chuang et al., 2010; Kunnev et al, 2010; Alvarez et al, 2015). In contrast, mouse strains that allow the study of origin over-activity were missing. A mouse model in which Cdc6 was over-expressed in the skin under the control of the keratin 5 (K5) promoter has recently been described in our lab (Búa et al, 2015). K5-CDC6 mice showed increased MCM loading in keratinocytes, but origin hyper-activation was not reported. It was also noted that Cdc6 overexpression sensitized the skin to carcinogen agents, facilitating papilloma formation (Búa et al, 2015).

The TetO-Cdc6 and TetO-Cdt1 mice that we have used in this work are the first tools to investigate the impact of pre-RC proteins overexpression in the whole organism. Interestingly, our models may lead to two different types of origin deregulation: while Cdc6 overexpression increased the frequency of origin activation in a controlled manner (Fig 19C), combined overexpression of Cdc6 and Cdt1 led to origin re-firing (Figures 14, 16). The consequences for mice survival were drastically different (Figures 29, 36).

Origin re-licensing and DNA re-replication *in vivo*

We have shown that Cdc6 overexpression, but not Cdt1, increased MCM loading on chromatin (Fig 13A). Moreover, DNA fiber assays showed that these extra origins are functional and can be activated in S phase (Fig 19C). These observations suggest a hierarchy in the origin licensing process in which Cdc6 would be a limiting factor. We propose a model in which CDC6 limits the number of licensed origins during G1, while CDT1 protein would be in excess. At this stage, the concentration of CDC6 is tuned to ensure a proper amount of replication origin licensing (Fig 64A). It should be noted that in G1, CDT1 protein is not strongly regulated while CDC6 levels are limited by the action of APC/Cdh1 (Figures 5, 17D and 18B) (Petersen et al, 2000; Sugimoto et al,

2008). In this scenario, additional (overexpressed) CDC6 is capable of licensing more origins during G1 (Fig 64B). Importantly, elevated levels of CDC6 induced more MCM loading only in G1, and did not facilitate origin refiring because CDT1 is inhibited and degraded in S phase (Fig 64A, B).

When CDT1 is overexpressed, neither increased origin licensing nor origin refiring were observed, because CDC6 levels would be still limiting both in G1 and S phases (Fig 64C). Therefore, ectopic CDT1 expression in S phase is not sufficient to induce re-replication in primary cells.

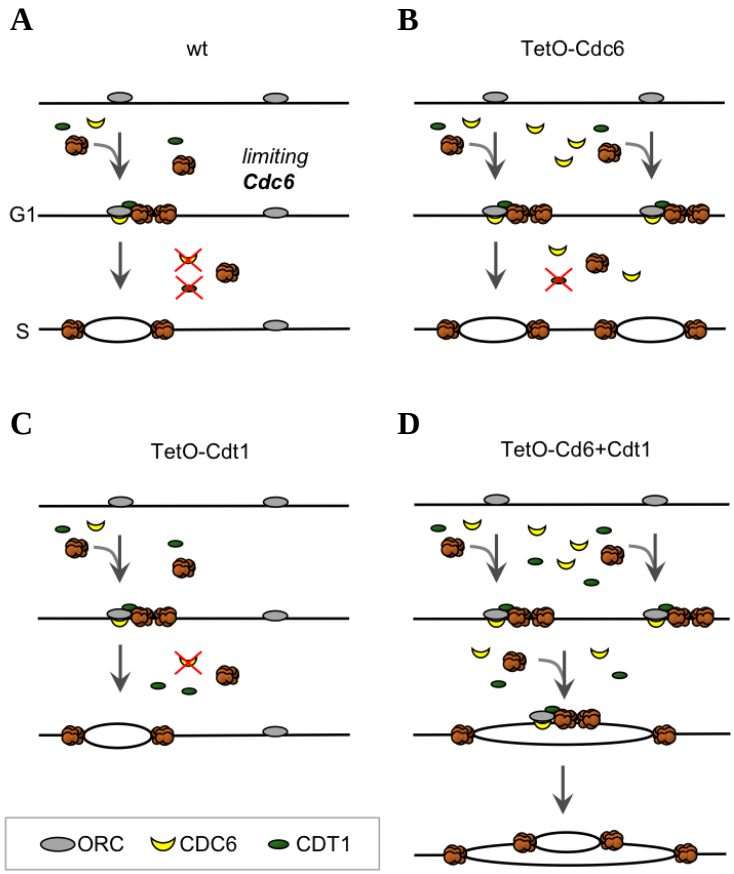

FIGURE 64. A. Model of the origin licensing process in G1. A hypothetical region is drawn with two potential origins marked by ORC complexes. The levels of CDC6 protein are limiting for pre-RC formation in G1, and only one origin is licensed and activated in S phase. After G1/S, both CDC6 and CDT1 proteins become limiting. **B.** After deregulated Cdc6 expression, more origins are licensed in G1 and fired in S phase. However, no re-replication occurs because CDT1 protein is still limiting after G1/S. **C.** After deregulated Cdt1 expression, the situation is similar to the WT cells because CDC6 is limiting. **D.** After the combined deregulation of Cdc6 and Cdt1, both proteins are available to facilitate origin re-licensing and re-replication in S phase.

Finally, when both CDC6 and CDT1 are overexpressed, more origin licensing and origin re-firing events were observed (Fig 64D). We propose that primary cells have a "double-check" mechanism to prevent DNA re-replication. In agreement with this model, GMN depletion is not sufficient to induce DNA re-replication in primary cells (Zhu and DePamphilis, 2009). In contrast, silencing of APC/Cdh1 inhibitor Emi1, efficiently induce re-replication in non-tumoral cells (Machida and Dutta, 2006; Lee et

al, 2012). Emi1 downregulation decreased both GMN and Cyclin A levels (Fig 65), disrupting both CDC6 and CDT1 levels (Machida and Dutta, 2006).

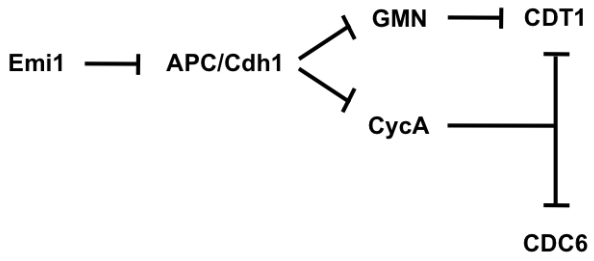

FIGURE 65. Schematic of CDC6 and CDT1 regulation by EMI1 through the APC/C complex. EMI1 restrains APC/C activity during S and G2 phases. When EMI1 is downregulated, APC/C is activated and GMN and CycA are targeted to degradation. In the absence of these proteins, CDC6 and CDT1 activity in S and G2 phases can lead to origin re-licensing.

Implications for CDC6 as origin licensing limiting factor

The fact that more MCM loading is observed when CDC6 is overexpressed opens two interesting questions: First, how and where are these new origins licensed? Second, how do cells respond to these extra origins?

Regarding the first question, it seems that Cdc6 overexpression is able to create new functional origins. During licensing, MCM, CDC6 and ORC ATPase activities load the MCM hexamer and releases CDT1 from the origin (Fernández-Cid et al, 2013; Coster et al, 2014; Kang et al, 2014). MCMs may travel passively on DNA once loaded (Powell et al, 2015). It is conceivable that additional CDC6 levels result in the loading of more than one MCM double hexamer in each origin. The extra MCM double hexamers would move away of the loading site and relocate to other regions where they could be later activated during the S phase.

Another possibility is that not all chromatin-bound ORC sites are able to recruit CDC6. This implies that some potential origins cannot be licensed during G1 (Fig 64A). However, in the presence of additional CDC6, these potential origins would be licensed (Fig 64B). Additional experiments, ideally the elucidation of high-definition maps of ORC, CDC6 and MCM binding sites, will be needed to better understand this issue.

Since excessive origin activity has been linked to RS (Bester et al, 2011; Jones et al, 2013; Hills and Diffley, 2014), the anticipated answer to the second question would be that dox-treated TetO-Cdc6 MEFs should display RS. However, these cells exhibit

γH2AX levels comparable to control cells (Fig 20A), arguing that, within certain limits, primary cells are able to cope with different levels of origin activation. Supporting this notion, progenitor cells have different requirements for origin activity during the process of hematopoietic differentiation (Alvarez et al, 2015). Therefore, the prevailing view that excessive origin activation induces RS needs to be reconsidered. The ability of CDC6 to change the amount of licensed origins at G1 provides a tool to control these fluctuations. By modulating CDC6 levels, cells could change origin activity to adapt replication to differentiation programmes and/or proliferation requirements (Fig 66).

Re-replication sensitive cells

In this study, we have reported apparent exceptions to our model, e.g. fetal liver cells and adult BM cells displayed re-replication in response to Cdt1 overexpression alone (Figures 26B and 33A). Interestingly, we found that endogenous CDC6 levels in fetal liver WT cells were higher than in dox-treated MEFs (Fig 27). Moreover, Cdc6 mRNA levels are high in hematopoietic progenitors and BM cells (Fig 33B; Wu et al, 2009; http://biogps.org/#goto=genereport&id=23834).

In general, cells with fast proliferation cycles display higher CDC6 levels (Fig 66) to facilitate the licensing of more replication origins that would be needed to support rapid proliferation. At the same time, these cells would be more sensitive to re-replication, as prevention of origin re-licensing would depend only on CDT1 regulation. We propose that beyond a threshold level of CDC6 protein levels, deregulation of CDT1 is sufficient to induce DNA over-replication (Fig 66).

This view is supported by several published studies. First, embryonic stem cells show rapid proliferation and have adapted their cell cycle by increasing the levels of CDC6, CDT1 and GMN (Fuji-Yamamoto et al, 2005; Ballabeni et al, 2011). Interestingly, ESCs and embryonal carcinoma cells are strongly dependent on GMN to prevent DNA re-replication, and this control is no longer essential when ESCs differentiate *in vitro* (Yang et al, 2011; Huang et al, 2015). Second, leukocyte precursors undergo re-replication in the absence of GMN (Shinnick et al, 2010) and genetic ablation of GMN reduces mature hematopoietic cells (Karamitros et al, 2015). While this study suggests a transcriptional role for GMN that is responsible for the phenotype, additional effects on re-replication cannot be excluded. Finally, many tumoral cells have high levels of

CDC6 (Tatsumi et al, 2006; Petrakis et al, 2016), and this fact could explain their sensitivity to Cdt1 overexpression or GMN downregulation (Vaziri et al, 2003; Melixetian et al, 2004).

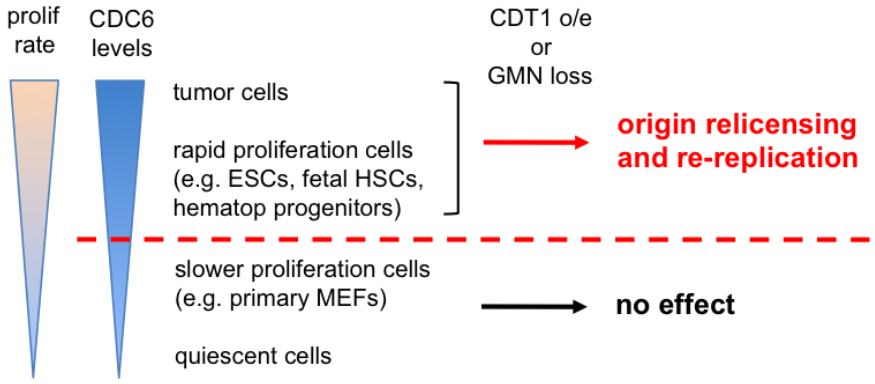

FIGURE 66. Re-replication sensitive cells. Cells may adjust pre-RC protein levels (especially CDC6) to their proliferation requirements and/or developmental programme. In cells with lower proliferation rate, deregulation of Cdc6 and Cdt1 is necessary to override licensing control and induce re-replication. On the other hand, cells with higher proliferation rate (e.g. fetal liver progenitor cells, tumoral cells) and higher levels of endogenous CDC6 are susceptible to individual Cdt1 deregulation. In the latter, the control mechanisms that restrict CDT1 activity become essential.

Re-replication induces severe dysplasia in proliferative tissues

We have found that combined Cdc6 and Cdt1 overexpression induces severe dysplasias in several proliferative tissues and reduces the lifespan of adult mice (Figures 29A and 30). We demonstrated that TetO-Cdc6+Cdt1 MEFs experience DNA re-replication (Figures 14 and 16) and exhibit features of cells with over-replicated DNA: RS, DNA damage, G2 arrest and apoptosis (Figures 20 to 24). We have also shown that DNA re-replication is extensive in fetal liver of developing embryos (Fig 25) and we found evidence of limited but consistent re-replication in adult tissues such as the intestine and the BM (Figures 32 and 33). In agreement with cellular data, IHC stainings showed that re-replication induced extensive DNA damage, activation of DNA damage response, a partial G2/M arrest and cellular apoptosis in intestinal tissue (Figures 34, 35).

It seems intriguing that a relatively low percentage of the intestinal cells underwent DNA re-replication (less than 5% of the population, as measured by flow cytometry) elicits these severe defects. In this regard, it should be noted that there are detection limits to the level of re-replication that can be measured. When DNA content is

measured by flow cytometry, only cells with a fair amount of over-replicated DNA will be considered positive, whereas cells that undergo single events of origin refiring may escape detection. A similar detection problem has been reported when using comparative genomic hybridization (Green et al, 2006). In fact, the DNA fiber assay allows detection of DNA re-replication at levels that would be undetectable by flow cytometry (Dorn et al, 2008). This technique showed that >15% of total replicating forks were originated from refired origins in dox-treated TetO-Cdc6+Cdt1 MEFs (Fig 16A). Interestingly, approximately one third of proliferating cells in the colon were positive for γH2AX (Figures 34 and 35). In BM, γH2AX staining is positive in 15% of the total tissue area in some individuals, even if < 4% of the cells displayed re-replication levels that could be measured by flow cytometry (Figures 33A and 34). Considering these evidences, it could be argued that a significant number of cells were affected by re-replication in mice tissues.

Different mechanisms have evolved to prevent or minimize the extension of aberrant DNA re-replication (reviewed by Arias and Walter, 2007). Surprisingly, the GI tract tissues showed a strong sensitivity to DNA re-replication, with dramatic consequences for survival. In humans, the whole intestinal epithelium is replaced within approximately 5 days (Barker, 2013; Vermeulen and Snippert, 2014). Differentiation of progenitor cells to mature cells normally involves several rounds of cell division (Zhu and Skoultchi, 2001; Barker, 2013). Hematopoietic and intestinal stem and progenitor cells are sensitive to DNA re-replication (Figures 30, 35 and 66; Shinnick et al, 2010; Huang et al, 2015; Karamitros et al, 2015). Therefore, tissue cell renewal will be rapidly compromised by re-replication, and a blockage of cell supply is likely to cause extensive tissue damage in just a few days, as observed in our mouse model.

DNA over-replication and cancer

CDC6 and CDT1 have been proposed to have oncogenic properties, based on multiple lines of evidence: both proteins are overexpressed in several types of tumours and precancerous lesions (Ohta et al, 2001; Bonds et al, 2002; Karakaidos et al 2004; Xouri et al, 2004; Bravou et al, 2005; Murphy et al, 2005; Pinyol et al, 2006; Liontos et al, 2007; Petrakis et al, 2016) likely due to gene amplification (Liontos et al, 2007). It has been proposed that aberrant CDC6 expression could inhibit the transcription of p16INK4 and CDH1 (Gonzalez et al, 2006; Sideridou et al 2011) and overexpression of

CDC6 in the skin of mice favours papilloma formation upon DMBA-TPA treatment (Búa et al, 2015). CDT1 overexpression in thymocytes promotes lymphoma development in the absence of p53 (Seo et al, 2005), and nude mice injected with 3T3 fibroblasts overexpressing CDT1 develop tumours (Arentson et al, 2002). Moreover, re-replication induced by CDT1 may favour carcinogenesis after papillomavirus infection (Fan et al, 2013). CDC6 and CDT1 overexpression promotes genome instability and malignant behaviour in papilloma premalignant cells (Liontos et al, 2007). Finally, in a subset of p53-null atypical carcinoma cells, chronic p21 expression results in CDC6 and CDT1 deregulation and cells display aggressive behaviour (Galanos et al, 2016).

Here, we have addressed the carcinogenic potential of CDC6 and CDT1 overexpression by performing ageing experiments in TetO-Cdc6 and TetO-Cdt1 mice. Individual overexpression of these proteins did have a modest impact on spleen size and tumour formation and overall survival was only marginally affected (Fig 36A, B). These results strongly suggest that the presumed oncogenic activity of CDC6 and CDT1 overexpression observed in cellular systems probably requires additional genetic alterations. Consistent with this notion, previous studies only reported tumour formation in immunocompromised mice, mice with mutant backgrounds or in the presence of other carcinogens (Arentson et al, 2002; Seo et al 2005; Búa et al, 2016).

In yeast, DNA re-replication induces gene amplification and chromosomal instability (Green et al, 2010; Hanlon and Lee, 2015), two frequent features of cancer cells (Hanahan and Weinberg, 2011). Whether re-replication is sufficient to promote cell transformation or contributes to tumour development has not been formally addressed in mammalian systems. Despite the fact that CDC6 or CDT1 overexpression are tumorogenic when combined with other oncogenic features, re-replication has not been reported within tumours (Arentson et al, 2002; Seo et al 2005; Liontos et al, 2007; Búa et al, 2016).

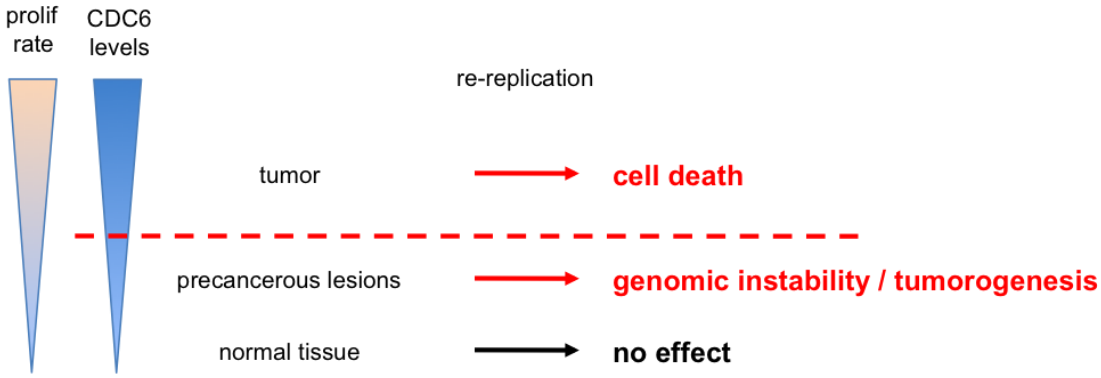

FIGURE 67. Differential outcomes of re-replication. In normal cells, re-replication is largely limited by multiple mechanisms. Precancerous lesions are closer to the "CDC6 threshold" that facilitates re-replication. In those cells, re-replication may contribute to accumulate genomic instability. Finally, cancer cells display high levels of preRC proteins and are strongly dependent on GMN activity. CDT1 overexpression, GMN depletion or disruption of other regulatory mechanisms rapidly induce extensive DNA damage and lead to cell death.

According to our data, the notion that re-replication might lead to cell transformation must be taken with caution. We found that combined deregulation of CDC6 and CDT1 in the mice induced levels of DNA re-replication that were lethal during embryonic development and also in adult mice, not allowing the study of tumour formation (Figures 25 and 29A). Interestingly, dox-treated TetON-Cdt1 mice had an essentially normal lifespan, even if re-replication and DNA damage were detected in several tissues after the first month of treatment (Figures 33 and 34). This suggests that mice tissues may tolerate limited amounts of re-replication, at least in the absence of additional genetic alterations. We consider two non-exclusive possibilities: (a) re-replication is more prevalent than previously acknowledged, and can be tolerated to some extent; (b) those cells that re-replicate DNA undergo apoptosis and are removed from the tissue. In support of the first possibility, short DNA fragments seem to accumulate at origins during initiation of DNA replication (Gómez and Antequera, 2008). In support of the second scenario, the final outcome of cancer cells when re-replication is induced is cell death, rather than survival with increased genomic instability (Vaziri et al, 2003; Melixetian et al, 2004; Zhu and DePamphilis, 2009). These ideas are summarized in our working model (Fig 67). Normal tissues tolerate some degree of origin relicensing and re-replication. In precancerous cells that have accumulated mutations, origin relicensing may induce a higher degree of re-replication that may contribute to genome instability and transformation. In turn, tumoral cells with high levels of pre-RC proteins such as CDC6 become very sensitive to origin reinitiation, probably because excessive DNA re-replication causes cell death.

Genetic screenings for modulators of DNA re-replication

In recent years, high-throughput screenings have been designed that uses as readout the nuclear DNA content of individual cells using laser scanning cytometer technology (Lee et al, 2012). This method has been applied to identify cell cycle or mitotic regulators (e.g. Mukherji et al, 2006; Kittler et al, 2007) and more recently, small molecules and genes that induce DNA re-replication (Zhu et al, 2011; Vassilev et al, 2016). Vassilev et al (2016) have recently identified 42 genes that prevent excessive DNA replication that could be caused by re-replication or endoreplication. Re-replication is promoted by origin refiring and leads to cells with incomplete DNA ploidy (between 2C and 4C). In contrast, endoreplication is produced by two or more rounds of complete genome duplication without intervening cytokinesis, leading to cells whose DNA content is a multiple of 2C (Zielke et al, 2013). From the 42 reported genes, only 7 were involved in the control of re-replication, through previously described mechanisms that inhibit origin relicensing. The remaining 35 genes were involved in mitotic processes and their absence promoted endoreplication instead of re-replication (Vassilev et al, 2016).

The screening presented in Chapter 2 of this Thesis was carried out in HCT116 colon cancer cells, the same cell line used in the study by Vassilev et al (2016). HCT116 cells display little or no chromosomal instability, are competent for the DNA damage checkpoint and sensitive to GMN depletion. A fundamental difference between our approach and that of Vassilev et al (2016) is that we aimed at the identification of proteins that play a role in controlling the extent of re-replication *after it has been triggered by GMN depletion*. In this type of screening, targeting GMN provided several advantages. First, as opposed to other genes whose ablation causes re-replication (e.g. CDT2, SKP2 or EMI1), GMN downregulation does not interfere with protein ubiquitilation, reducing the risk of indirect effects. Second, GMN may have extra-replicative roles during embryonic development but not in adult differentiated cells (Gonzalez et al, 2006; Yang et al 2011; Yellajoshyula et al, 2011; de Renty et al 2014).

Our candidate-based library was designed to evaluate the participation of the selected proteins in promoting or limiting re-replication, but also in the potential processing of over-replicated DNA. Interestingly, neither FBH1 nor RAD51 had been identified in

previous screenings (Vassilev et al, 2016), probably because their downregulation has virtually no effect in DNA content in the presence of GMN (Figures 42 and 44).

Amongst other proteins that prevent DNA re-replication we found three helicases with fork remodelling activity, two proteins involved in ICL repair, one RNA helicase, and two components from the nucleotide excision repair (NER) pathway. Fewer proteins were found that enhanced DNA re-replication, including one chromatin remodeler (ATRX), and one RAD51-interacting protein (RAD54).

Chromatin remodelers had a minimal impact on GMN-dependent re-replication with the exception of ATRX, which increased the extent of re-replication. ATRX is responsible for H3.3 deposition in heterochromatin and telomeres (Watson et al, 2015). In contrast, several fork-remodelling proteins might contribute to limit re-replication especially BLM, WRN, ZRANB3 and to a lesser extent BRIP, ASCC3, HELQ and SETX. BRIP1 (FANCJ) belongs to FA pathway and interacts with BRCA1 during ICL repair (Hiom, 2010), ASCC3 is needed for DNA alkylation repair (Dango et al, 2011), HELQ together with RAD51 paralogues promotes ICL repair (Adelman et al, 2013; Takata et al, 2013) and SETX is involved in R-loop unwinding (Alzu et al, 2012). The links between these processes and re-replication prevention will require validation and additional study.

The three main structure-specific endonucleases MUS81, SLX4 and GEM1 are not likely involved, while exonucleases may have a limited effect in re-replication promotion. The role of Rad54, a protein related to RAD51 function, is discussed later. Finally, a possible role of nucleotide excision repair (NER) proteins should also be considered, as two members of this pathway (ERCC2 and ERCC3) restrained re-replication in our screening.

As it occurs in every genetic screening, possible hits are to be confirmed and validated to rule out false positives, e.g. those caused by RNAi inespecificity or in this specific case, by any gene involved in the control of nuclear size independently or DNA replication. In this work, we focused in the validation and further investigation of the roles of FBH1 and RAD51 proteins.

DNA re-replication and fork reversal

RAD51 is required for fork reversal in response to different genotoxic agents (Zellweger et al, 2015). In addition, three helicases with fork remodelling activities (BLM, WRN and ZRANB3) are likely to prevent re-replication (Fig 39) and all of them participate in the restart of stalled forks (reviewed by Muñoz and Mendez, 2016). So, it could be argued that generation of reversed forks restricts DNA re-replication. However, downregulation of other proteins involved in this process, e.g. RECQ1, RECQ5 or SMARCAL1, did not affect nuclear size upon GMN loss (Fig 39). Actually, a possible role of SMARCAL1 in the control of DNA re-replication was ruled out by evaluation of DNA content (Fig 50). In addition, FBH1 favours re-replication despite its role in promoting fork reversal.

We found no evidence of reversed forks after GMN downregulation using a published method based on BrdU detection in native conditions (Couch et al, 2013; Fig 49). However, we cannot exclude the possibility that fork reversal occurs below the detection limit of this technique. Further investigation on this issue would require electron microscopy (EM) detection of these structures. Intriguingly, two studies that have used EM to detect fork reversal in cells undergoing re-replication have yielded different results. In the first study, re-replication caused by EMI1 depletion led to an accumulation of these structures (Neelsen et al, 2013). In the second study, using a cell line that displayed re-replication associated to Cdc6 and Cdt1 overexpression (Galanos et al, 2016) the percentage of reversed forks was lower than in control cells. While our results do not support a role of fork reversal in the control of re-replication, further experiments will be required to clarify this aspect.

A model for RAD51 prevention of DNA re-replication

Direct evaluation of re-replication by DNA content confirmed that RAD51 prevents re-replication while FBH1 promotes it (Figures 42 to 45). FBH1 downregulation not only decreased re-replication but also attenuated its consequences (Figures 46 and 47). Other proteins necessary for strand invasion such as RAD51AP1 were not involved in re-replication prevention, suggesting a recombination-independent mechanism (Fig 51). We have also shown that a fraction of RAD51 is bound to chromatin during S phase and could be located to replication origins (Figures 52, 53). Furthermore, changes that affect the stability of RAD51 on chromatin were immediately reflected in changes in the

extent of re-replication in the absence of GMN (Figures 54 to 57). Importantly, RAD51 downregulation increased fork rate and the length of re-replicated tracks only when GMN is not present (Figures 60 and 61). In agreement with this result, it has been recently described that physiological re-replicated fork progression in *D. melanogaster* follicle cells is enhanced in the absence of RAD51 homologs (Alexander et al, 2016). Finally, we have observed that MRE11 inhibition also increases the percentage of cells with over-replicated DNA and the length of re-replicated tracks (Figures 62, 63). Taken together, these results have led us to propose the following model (Fig 68): after regular origin firing, RAD51 would be recruited to the newly synthesized DNA, possibly through its interaction with ORC2. RAD51 filaments could probably stretch from the origins to nearby regions. In the event of aberrant origin refiring, the presence of RAD51 on chromatin would serve as a brake to limit the progression of re-replicated forks (Fig 68). In this scenario, the action of antirecombinases and translocases that displace RAD51 nucleofilaments would promote the elongation of re-replicated forks. Finally, MRE11 and other nucleases may contribute to restrain re-replication by resecting re-duplicated strands after RAD51 is displaced from DNA.

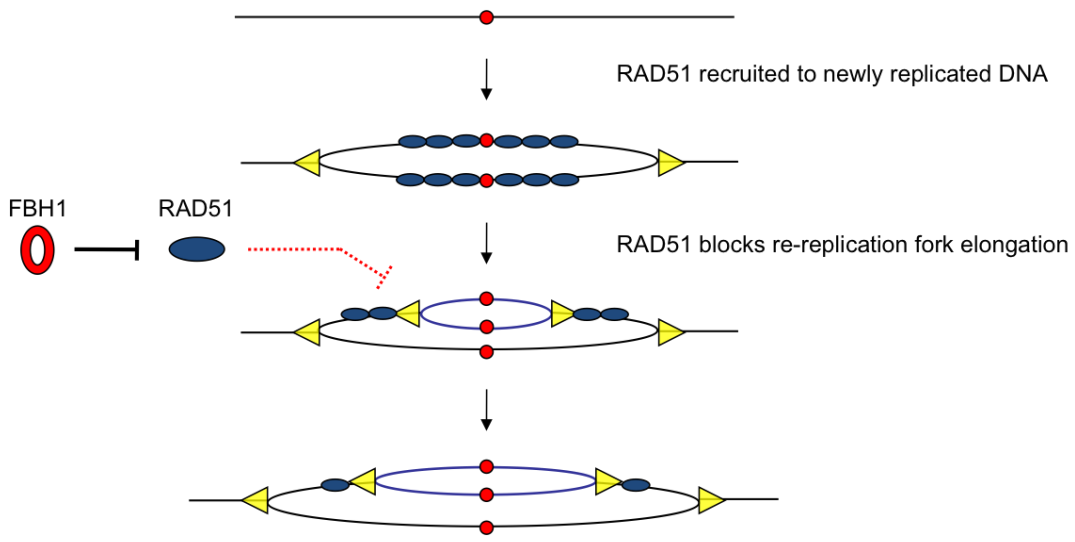

Figure 68. Schematic of RAD51 acting as a molecular brake for re-replicated forks. ORC may facilitate RAD51 binding to replication origins and chromatin in S phase, to protect newly synthesized DNA from nucleolytic degradation. FBH1 and possibly other helicases might counteract RAD51 binding to chromatin. In the event of origin refiring, RAD51 blocks the progression of re-replicated forks.

This model represents a novel mechanism that limits DNA re-replication when licensing control fails. This mechanism might be important to restrict genomic instability in precancerous cells with high levels of licensing proteins (Petrakis et al, 2016).

In the next section, some aspects about RAD51 recombination-independent roles and their connections with our model are discussed.

Recombination-independent RAD51 functions

RAD51 is the main recombinase involved in strand invasion during HR (reviewed in Heyer et al, 2010) and participates in DSB repair, ICL repair, fork restart and template switching reactions (Branzei and Foiani, 2010; Petermann and Helleday, 2010; Gaillard et al, 2015). In recent years, recombination-independent roles for RAD51 have been described; such as promoting fork reversal (Zellweger et al, 2015) and protecting stalled and reversed forks from nucleolitic degradation (Schlacher et al, 2011, 2012). In addition, experiments in *X. laevis* suggested that RAD51 protects nascent strands and promotes continuous synthesis in the unperturbed S phase (Hashimoto et al, 2010).

We have identified a novel recombination-independent role of RAD51 in blocking the elongation of re-replicated forks (Fig 68). To perform this role, RAD51 should bind to newly duplicated chromatin during S phase (Fig 52). In agreement with this notion, *X. laevis* RAD51 binds to undamaged chromatin during S phase, and its binding is prevented by inhibition of origin assembly or firing (Hashimoto et al, 2010). Furthermore, RAD51 signal can be detected in unchallenged EdU-positive cells (Fugger et al, 2009; Zellweger et al, 2015), and it binds to chromatin in S phase in synchronized U2OS cells (Somyajit et al, 2015). Moreover, in human and mouse cells, RAD51 immunoprecipitated with nascent DNA in iPOND experiments (Kim et al, 2012; Somyajit et al, 2015; Zellweger et al, 2015). RAD51 also precipitated with mature DNA suggesting that it remains temporarily bound to duplicated DNA (Zellweger et al, 2015). Finally, loss of FBH1 increases RAD51 signal in the absence of RS (Fugger et al, 2009; Simandlova et al, 2013).

The presence of RAD51 on chromatin in regular S phase imposes the necessity to strictly regulate its recombinogenic function, since unscheduled HR is detrimental for the cells (reviewed by Carr and Lambert, 2013). Several antirecombinases are

responsible for this control, and whether they affect re-replication remains unknown. For instance, we have observed that RAD51 eviction by FBH1 and RAD54 favours DNA re-replication (Fig 42, 54 and 57). Nonetheless, our screening results suggested that some helicases with antirecombinase functions as BLM or BRIP might prevent DNA re-replication (Fig 39). Therefore, the impact of each individual antirecombinase on the extent of DNA re-replication extent should be further investigated.

Another aspect of this HR-independent RAD51 function is the nature of the protein(s) responsible for RAD51 DNA loading. RAD51 paralogs, RAD52 and BRCA2 facilitate RAD51 loading on DSBs (reviewed by Heyer et al, 2010). In turn, BRCA1, BRCA2 and FA proteins are needed for RAD51-mediated protection of stalled forks, suggesting a role in RAD51 loading (Schlacher et al, 2011, 2012). Similar results were obtained for RAD51 paralogs (Somyajit et al, 2015) and for WRN and WRNIP1 (Su et al, 2014; Leuzzi et al, 2016). It remains unknown whether any these proteins mediate the binding of RAD51 to origins and nascent strands in S phase. Interestingly, in our screening WRN downregulation affected re-replication in a similar way as RAD51 (Fig 39) suggesting that it could participate in the loading or stabilization of RAD51 on DNA. Finally, RAD51 could interact with ORC2 to facilitate its binding to origins (Fig 53B). So far, there is only indirect evidence for this, but it is worth noting that most of *bona fide* replication origins identified by combination of ORC2 binding sites and SNS contained RAD51 (Fig 53C).

Role of exonucleases and DNA re-replication

We have also identified an unanticipated role for MRE11 nuclease in the resection of re-replicated DNA (Fig 62, 63). MRE11 possesses 3'-5' exonuclease (Paul and Gellert; 1998) and endonuclease activities (Cannavo and Cejka; 2014). At DSBs, MRE11 performs an endonucleolytic cleavage 100 to 300 nt away from the DSB and then starts short-range 3'-5' resection, while other exonucleases perform 5'-3' long range resection (Cejka, 2015). We propose that MRE11 might operate at re-replicated DNA in a similar way. Consistently with a role in resection of re-replicated DNA, we found that MRE11 inhibition by mirin duplicated the levels of re-replication, without changing the amount of ssDNA (Figures 62 and 63A). This result suggests that one of the causes of ssDNA accumulation during DNA re-replication is MRE11-dependent resection of re-duplicated DNA.

In any case, the changes observed in re-replicated track length upon MRE11 inhibition (Fig 63C) would require the participation of long-range resection nucleases or possibly multiple MRE11 nucleases performing endonucleolytic cleavage at different points in the same over-replicated DNA. In our screenings downregulation of most exonucleases, including MRE11, did not affect nuclear size (Fig 39). Whether MRE11 or other nucleases have effects on nuclear size that are independent or DNA re-replication remains to be elucidated.

Re-replication: An "Achilles heel" of cancer cells?

Some of the work presented in this Thesis and other recent studies invite to consider the possibility that re-replication might be used to kill cancer cells. It was described several years ago that GMN-induced re-replication preferentially kills cancer over primary cells (Zhu and DePamphilis, 2009). Another example is MLN4924, a drug that inhibits neddylation and activation of culling-RING ubiquitin ligases including CRL4 (Soucy et al, 2009; Milhollen et al, 2011). MLN4924 promotes the accumulation of CDT1, SET8 and p21, favouring re-replication and efficiently killing cancer cells (Lin et al, 2010; Milhollen et al, 2011; Benamar et al, 2016). Interestingly, FBH1 is also targeted for degradation by CRL4 complex (Bacquin et al, 2013) so its accumulation may contribute to DNA re-replication. MLN4924 has been shown to be effective against different tumoral cells (Pan et al, 2013; Benamar et al, 2016; Zhang et al, 2016; Guo et al, 2017) and is currently used in clinical trials in patients with metastatic melanoma (Bhatia et al, 2016).

Our study with mouse models supports this strategy. The susceptibility of any given cell type to DNA re-replication seems to correlate with its rate of proliferation (Fig 66). We have shown that CDT1 activity could be unleashed in mice without severe phenotypes (Fig 30, 36B). For this reason, deregulation of CDT1 might induce lethal re-replication in tumour cells with a limited impact in the surrounding healthy tissues. RAD51 is overexpressed in several cancer cell lines (Raderschall et al, 2002), and its role in limiting re-replication could be particularly important for these cells. Therefore, interventions on RAD51 chromatin binding might enhance DNA re-replication in tumoral cells. It could be interesting to use this strategy to treat tumours characterized by elevated expression of pre-RC components (Karakaidos et al, 2004; Galanos et al,

2016) or by mutations in BRCA1/2 that could affect RAD51 loading onto DNA (Fackenthal and Olopade 2007).

We believe that the mice strains characterized in this work, TetON-Cdt1 and TetON-Cdc6+Cdt1, could be useful to test this strategy in pre-clinical studies with chemical carcinogens or after crossbreeding with cancer-prone mouse models. Future *in vivo* experiments will determine whether re-replication caused by deregulated origin activity can be considered a cancer "Achilles heel".

CONCLUSIONS

CONCLUSIONES

CONCLUSIONS

1. In primary cells, CDC6 protein is limiting for origin licensing and frequency of origin activation.
2. In primary cells, DNA re-replication is only observed after the combined deregulation of CDC6 and CDT1.
3. Overexpression of CDT1 (alone or in combination with CDC6) causes DNA re-replication in fetal liver cells and is lethal during embryonic development.
4. CDC6 and CDT1 can be efficiently overexpressed in many tissues of adult mice: individual CDC6 or CDT1 overexpression does not cause major phenotypes and mice lifespan is only marginally reduced.
5. Combined CDC6 and CDT1 overexpression induces re-replication and lethal dysplasia in several tissues, mainly stomach, intestine, spleen and bone marrow. Dysplasia of the intestinal epithelium proves fatal in less than two weeks.
6. CDC6 endogenous levels determine cell susceptibility to re-replication induced by deregulation of CDT1
7. A genetic screening has identified RAD51 and FBH1 as proteins involved in the control of DNA re-replication upon loss of geminin.
8. The role of RAD51 in preventing DNA re-replication does not involve HR but it depends on its stable association with DNA: FBH1 and other factors that inhibit RAD51 chromatin association promote re-replication.
9. RAD51 associates with DNA during the S phase and acts as a molecular brake to limit the progression of re-replicated forks.
10. MRE11 and possibly other nucleases are involved in the resection of re-replicated DNA.

CONCLUSIONES

1. En células primarias, CDC6 es un factor limitante para el licenciamiento y activación de los orígenes de replicación.
2. En células primarias, la sobre-expresión simultánea de CDC6 y CDT1 conduce a la re-replicación parcial del genoma.
3. La sobre-expresión de CDT1, individual o combinada con CDC6, produce re-replicación de DNA en células del hígado fetal y resulta letal durante el desarrollo embrionario.
4. Los animales adultos son resistentes a la sobre-expresión individual de CDC6 y CDT1 en la mayoría de los tejidos, y su esperanza de vida sólo se reduce de manera marginal.
5. La sobre-expresión combinada de CDC6 y CDT1 induce re-replicación de DNA y displasia en varios tejidos, principalmente estómago, intestino, bazo y médula ósea. La displasia del epitelio intestinal resulta letal en menos de dos semanas.
6. Los niveles endógenos de proteína CDC6 determinan la susceptibilidad celular a la re-replicación inducida por desregulación de CDT1.
7. Mediante un *screening* genético se ha identificado que las proteínas RAD51 y FBH1 participan en el control de la re-replicación del DNA.
8. La función de RAD51 en el control de la re-replicación no requiere recombinación homóloga pero depende de su asociación estable al DNA: FBH1 y otros factores que inhiben su unión a cromatina promueven la re-replicación.
9. RAD51 se une al DNA durante la fase S y parece actuar como un freno molecular de la progresión de las horquillas re-replicadas.
10. MRE11 y probablemente otras nucleasas participan en la resección del ADN re-replicado.

REFERENCES

REFERENCES

Alabert C, Groth A. 2012. Chromatin replication and epigenome maintenance. Nat Rev Mol Cell Biol. 13:153-67

Alexander JL, Barrasa MI, Orr-Weaver TL. 2015. Replication fork progression during re-replication requires the DNA damage checkpoint and double-strand break repair. Curr Biol. 25:1654-60.

Alexander JL, Beagan K, Orr-Weaver TL, McVey M. 2016. Multiple mechanisms contribute to double-strand break repair at rereplication forks in Drosophila follicle cells. Proc Natl Acad Sci U S A. 113:13809-13814.

Alexandrow MG, Hamlin JL. 2004. Cdc6 chromatin affinity is unaffected by serine-54 phosphorylation, S-phase progression, and overexpression of cyclin A. Mol Cell Biol. 24:1614-27.

Alvarez S, Díaz M, Flach J, Rodriguez-Acebes S, López-Contreras AJ, Martínez D, Cañamero M, Fernández-Capetillo O, Isern J, Passegué E, Méndez J. 2015. Replication stress caused by low MCM expression limits fetal erythropoiesis and hematopoietic stem cell functionality. Nat Commun 6:8548

Alver RC, Chadha GS, Blow JJ. 2014. The contribution of dormant origins to genome stability: from cell biology to human genetics. DNA Repair (Amst). 19:182-9.

Alzu A, Bermejo R, Begnis M, Lucca C, Piccini D et al. 2012. Senataxin associates with replication forks to protect fork integrity across RNA-polymerase-II-transcribed genes. Cell 151:835–46.

Aparicio T, Guillou E, Coloma J, Montoya G, Méndez J. 2009. The human GINS complex associates with Cdc45 and MCM and is essential for DNA replication. Nucleic Acids Res. 37: 2087-95.

Archambault V, Ikui AE, Drapkin BJ, Cross FR. 2005. Disruption of mechanisms that prevent rereplication triggers a DNA damage response. Mol. Cell. Biol. 25:6707–6721.

Arentson E, Faloon P, Seo J, Moon E, Studts JM, Fremont DH, Choi K. 2002. Oncogenic potential of the DNA replication licensing protein CDT1. Oncogene. 21:1150-8.

Arias EE, Walter JC. 2006. PCNA functions as a molecular platform to trigger Cdt1 destruction and prevent re-replication. Nat Cell Biol. 8:84-90.

Arias EE, Walter JC. 2007. Strength in numbers: preventing rereplication via multiple mechanisms in eukaryotic cells. Genes Dev. 21: 497-518.

Bacquin A, Pouvelle C, Siaud N, Perderiset M, Salomé-Desnoulez S, Tellier-Lebegue C, Lopez B, Charbonnier JB, Kannouche PL. 2013. The helicase FBH1 is tightly regulated by PCNA via CRL4(Cdt2)-mediated proteolysis in human cells. Nucleic Acids Res. 41: 6501-13.

Bagley BN, Keane TM, Maklakova VI, Marshall JG, Lester RA et al. 2012. A dominantly acting murine allele of Mcm4 causes chromosomal abnormalities and promotes tumorigenesis. PLoS Genet 8, e1003034

Ballabeni A, Melixetian M, Zamponi R, Masiero L, Marinoni F, Helin K. 2004. Human geminin promotes pre-RC formation and DNA replication by stabilizing CDT1 in mitosis. EMBO J. 23:3122-32.
Ballabeni A, Park IH, Zhao R, Wang W, Lerou PH, Daley GQ, Kirschner MW. 2011. Cell cycle adaptations of embryonic stem cells. Proc Natl Acad Sci U S A 108: 19252-19527.

Barker N. 2014. Adult intestinal stem cells: critical drivers of epithelial homeostasis and regeneration. Nat Rev Mol Cell Biol. 15:19-33.

Bastian F, Parmentier G, Roux J, Moretti S, Laudet V, Robinson-Rechavi M. 2008. Bgee: Integrating and Comparing Heterogeneous Transcriptome Data Among Species. in DILS: Data Integration in Life Sciences. Lecture Notes in Computer Science 5109: 124-131.

Bhatia S, Pavlick AC, Boasberg P, Thompson JA, Mulligan G, Pickard MD, Faessel H, Dezube BJ, Hamid O. 2016. A phase I study of the investigational NEDD8-activating enzyme inhibitor pevonedistat (TAK-924/MLN4924) in patients with metastatic melanoma. Invest New Drugs. 34:439-49.

Beard C, Hochedlinger K, Plath K, Wutz A & Jaenisch R. 2006. Efficient method to generate single-copy transgenic mice by site-specific integration in embryonic stem cells. Genesis 44: 23-28.

Bell SP, Stillman B. 1992. ATP-dependent recognition of eukaryotic origins of DNA replication by a multiprotein complex. Nature. 357):128-34.

Benamar M, Guessous F, Du K, Corbett P, Obeid J, Gioeli D, Slingluff CL Jr, Abbas T. 2016. Inactivation of the CRL4-CDT2-SET8/p21 ubiquitylation and degradation axis underlies the therapeutic efficacy of pevonedistat in melanoma. EBioMedicine. 10:85-100.

Berezney R, Dubey DD, Huberman JA. 2000. Heterogeneity of eukaryotic replicons, replicon clusters, and replication foci. Chromosoma. 108:471-84.

Berti M, Ray Chaudhuri A, Thangavel S, Gomathinayagam S, Kenig S et al. 2013. Human RECQ1 promotes restart of replication forks re- versed by DNA topoisomerase I inhibition. Nat Struct Mol Biol 20: 347–354

Besnard E, Babled A, Lapasset L, Milhavet O, Parrinello H, Dantec C, Marin JM, Lemaitre JM. 2012. Unraveling cell type-specific and reprogrammable human replication origin signatures associated with G-quadruplex consensus motifs. Nat Struct Mol Biol. 19:837-44.

Bester AC, Roniger M, Oren YS, Im MM, Sarni D, Chaoat M, Bensimon A, Zamir G, Shewach DS, Kerem B. 2011. Nucleotide deficiency promotes genomic instability in early stages of cancer development. Cell 145:435–446.

Blow JJ, Gillespie PJ. 2008. Replication licensing and cancer--a fatal entanglement? Nat Rev Cancer. 8: 799-806.

Bonds L, Baker P, Gup C, Shroyer KR. 2002. Immunohistochemical localization of cdc6 in squamous and glandular neoplasia of the uterine cervix. Arch Pathol Lab Med. 126:1164-8.

Boos D, Sanchez-Pulido L, Rappas M, Pearl LH, Oliver AW, Ponting CP, Diffley JF. 2011. Regulation of DNA replication through Sld3-Dpb11 interaction is conserved from yeast to humans. Curr Biol 21:1152-7.

Boskovic J, Bragado-Nilsson E, Saligram Prabhakar B, Yefimenko I, Martínez-Gago J, Muñoz S, Méndez J, Montoya G. 2016. Molecular architecture of the recombinant human MCM2-7 helicase in complex with nucleotides and DNA. Cell Cycle.15: 2431-40.

Bowers JL, Randell JC, Chen S, Bell SP. 2004. ATP hydrolysis by ORC catalyzes reiterative Mcm2-7 assembly at a defined origin of replication. Mol Cell. 16:967-78.

van Brabant AJ, Buchanan CD, Charboneau E, Fangman WL, Brewer BJ. 2001. An origin-deficient yeast artificial chromosome triggers a cell cycle checkpoint. Mol Cell. 7:705-13.

Branzei D. 2011. Ubiquitin family modifications and template switching. FEBS Lett. 585:2810-7.

Branzei D, Foiani M. 2010. Maintaining genome stability at the replication fork. Nat Rev Mol Cell Biol. 11:208-19.

Bravou V, Nishitani H, Song SY, Taraviras S, Varakis J. 2005. Expression of the licensing factors, Cdt1 and Geminin, in human colon cancer. Int J Oncol. 27:1511-8.

Búa S. 2013. Control of DNA replication *in vivo*: study of mouse models for Cdc6 and Cdt1 overexpression. Doctoral Thesis. UAM. Madrid.

Búa S, Sotiropoulou P, Sgarlata C, Borlado LR, Eguren M, Domínguez O, Ortega S, Malumbres M, Blanpain C, Méndez J. 2015. Deregulated expression of Cdc6 in the skin facilitates papilloma formation and affects the hair growth cycle. Cell Cycle. 14:3897-907.

Bugreev DV, Yu X, Egelman EH, Mazin AV. 2007. Novel pro- and anti-recombination activities of the Bloom's syndrome helicase. Genes Dev. 21:3085-94.

Bugreev DV, Brosh RM Jr, Mazin AV. 2008. RECQ1 possesses DNA branch migration activity. J Biol Chem. 283:20231–42.

Cadoret JC, Meisch F, Hassan-Zadeh V, Luyten I, Guillet C, Duret L, Quesneville H, Prioleau MN. 2008. Genome-wide studies highlight indirect links between human replication origins and gene regulation. Proc Natl Acad Sci U S A. 105:15837-42.

Cannavo E, Cejka P. Sae2 promotes dsDNA endonuclease activity within Mre11-Rad50-Xrs2 to resect DNA breaks. Nature. 514:122-5.

Carr AM, Lambert S. 2013. Replication stress-induced genome instability: the dark side of replication maintenance by homologous recombination. J Mol Biol 425:4733-44.

Castillo Bosch P, Segura-Bayona S, Koole W, van Heteren JT, Dewar JM, Tijsterman M, Knipscheer P. 2014. FANCJ promotes DNA synthesis through G-quadruplex structures. EMBO J. 33: 2521-33.

Cayrou C, Coulombe P, Vigneron A, Stanojcic S, Ganier O, Peiffer I, Rivals E, Puy A, Laurent-Chabalier S, Desprat R, Méchali M. 2011. Genome-scale analysis of metazoan replication origins reveals their organization in specific but flexible sites defined by conserved features. Genome Res. 21: 1438-49.

Cayrou C, Coulombe P, Puy A, Rialle S, Kaplan N, Segal E, Méchali M. 2012. New insights into replication origin characteristics in metazoans. Cell Cycle. 11: 658-67.

Cayrou C, Ballester B, Peiffer I, Fenouil R, Coulombe P, Andrau JC, van Helden J, Méchali M. 2015. The chromatin environment shapes DNA replication origin organization and defines origin classes. Genome Res. 25:1873-85.

Ceballos SJ, Heyer WD. 2011. Functions of the Snf2/Swi2 family Rad54 motor protein in homologous recombination. Biochim Biophys Acta. 1809:509-23.

Cejka P. 2015. DNA End Resection: Nucleases Team Up with the Right Partners to Initiate Homologous Recombination. J Biol Chem. 290:22931-8.

Chen YH, Jones MJ, Yin Y, Crist SB, Colnaghi L, Sims RJ 3rd, Rothenberg E, Jallepalli PV, Huang TT. 2015. ATR-mediated phos- phorylation of FANCI regulates dormant origin firing in response to replication stress. Mol Cell 58:323–338.

Chi P, Van Komen S, Sehorn MG, Sigurdsson S, Sung P. 2006. Roles of ATP binding and ATP hydrolysis in human Rad51 recombinase function. DNA Repair (Amst). 5:381-91.

Chu WK, Payne MJ, Beli P, Hanada K, Choudhary C, Hickson ID. 2015. FBH1 influences DNA replication fork stability and homologous recombination through ubiquitylation of RAD51. Nat Commun 6, doi: 10.1038/ncomms6931.

Chuang CH, Wallace MD, Abratte C, Southard T, Schimenti JC. 2010. Incremental genetic perturbations to MCM2-7 expression and subcellular distribution reveal exquisite sensitivity of mice to DNA replication stress. PLoS Genet 6: e1001110, doi:10.1371/journal.pgen.1001110.

Ciccia A, Nimonkar AV, Hu Y, Hajdu I, Achar YJ, Izhar L, Petit SA, Adamson B, Yoon JC, Kowalczykowski SC, Livingston DM, Haracska L, Elledge SJ. 2012. Polyubiquitinated PCNA recruits the ZRANB3 translocase to maintain genomic integrity after replication stress. Mol Cell 47:396-409.

Cimprich KA, Cortez D. 2008. ATR: an essential regulator of genome integrity. Nat Rev Mol Cell Biol 9:616–627.

Clijsters L, Wolthuis R. 2014. PIP-box-mediated degradation prohibits re-accumulation of Cdc6 during S phase. J Cell Sci. 127:1336-45.

Cobb JA, Bjergbaek L, Shimada K, Frei C, Gasser SM. 2003. DNA polymerase stabilization at stalled replication forks requires Mec1 and the RecQ helicase Sgs1. EMBO J 22:4325–4336

Costa A, Hood IV, Berger JM. 2013. Mechanisms for initiating cellular DNA replication. Annu Rev Biochem. 82:25-54.

Costantino L, Sotiriou SK, Rantala JK, Magin S, Mladenov E, Helleday T, Haber JE, Iliakis G, Kallioniemi OP, Halazonetis TD. 2014. Break-induced replication repair of damaged forks induces genomic duplications in human cells. Science 343:88-91.

Costanzo V, Shechter D, Lupardus PJ, Cimprich KA, Gottesman M, Gautier J. 2003. An ATR- and Cdc7-dependent DNA damage checkpoint that inhibits initiation of DNA replication. Mol Cell 11:203-13.

Coster G, Frigola J, Beuron F, Morris EP, Diffley JF. 2014. Origin licensing requires ATP binding and hydrolysis by the MCM replicative helicase. Mol Cell. 55:666-77.

Cotta-Ramusino C, Fachinetti D, Lucca C, Doksani Y, Lopes M, Sogo J, Foiani . 2005. Exo1 processes stalled replication forks and counter- acts fork reversal in checkpoint-defective cells. Mol Cell 17:153–159

Couch FB, Bansbach CE, Driscoll R, Luzwick JW, Glick GG et al. 2013. ATR phosphorylates SMARCAL1 to prevent replication fork col- lapse. Genes Dev 27:1610–1623

Daley JM, Kwon Y, Niu H, Sung P. 2013. Investigations of homologous recombination pathways and their regulation. Yale J Biol Med. 86:453-61.

Dango S, Mosammaparast N, Sowa ME, Xiong LJ, Wu F, Park K, Rubin M, Gygi S, Harper JW, Shi Y. 2011. DNA unwinding by ASCC3 helicase is coupled to ALKBH3-dependent DNA alkylation repair and cancer cell proliferation. Mol Cell. 44: 373-84.

Davis AP, Symington LS. 2004. RAD51-dependent break-induced replication in yeast. Mol Cell Biol 24:2344-51.

Davidson IF, Li A, Blow JJ. 2006. Deregulated replication licensing causes DNA fragmentation consistent with head-to-tail fork collision. Mol Cell. 24:433-43.

Davies SL, North PS, Hickson ID. 2007. Role for BLM in replication-fork restart and suppression of origin firing after replicative stress. Nat Struct Mol Biol 14:677-9.

De Piccoli G, Katou Y, Itoh T, Nakato R, Shirahige K, Labib K. 2012. Replisome stability at defective DNA replication forks is indepen- dent of S phase checkpoint kinases. Mol Cell 45:696–704

Deegan TD, Diffley JF. 2016. MCM: one ring to rule them all. Curr Opin Struct Biol. 37:145-51.

Deem A, Keszthelyi A, Blackgrove T, Vayl A, Coffey B, Mathur R, Chabes A, Malkova A. 2011. Break-induced replication is highly inaccurate. PLoS Biol 9:e1000594.

Dershowitz A, Newlon CS. 1993. The effect on chromosome stability of deleting replication origins. Mol Cell Biol. 13:391-8.

Dorn ES, Chastain PD, Hall JR, Cook JG. 2009. Analysis of re-replication from deregulated origin licensing by DNA fiber spreading. Nucleic Acid Res 37: 60-69.

Dupré A, Boyer-Chatenet L, Sattler RM, Modi AP, Lee JH, Nicolette ML, Kopelovich L, Jasin M, Baer R, Paull TT, Gautier J. 2008. A forward chemical genetic screen reveals an inhibitor of the Mre11-Rad50-Nbs1 complex. Nat Chem Biol. 4:119-25.

Duursma A, Agami R. 2005. p53-Dependent regulation of Cdc6 protein stability controls cellular proliferation. Mol Cell Biol. 25:6937-47.

Edwards MC, Tutter AV, Cvetic C, Gilbert CH, Prokhorova TA, Walter JC. 2002. MCM2-7 complexes bind chromatin in a distributed pattern surrounding the origin recognition complex in Xenopus egg extracts. J Biol Chem. 277:33049-57.

Ekholm-Reed S, Méndez J, Tedesco D, Zetterberg A, Stillman B, Reed SI. 2004. Deregulation of cyclin E in human cells interferes with prereplication complex assembly. J Cell Biol. 165:789-800.

El-Shemerly M, Hess D, Pyakurel AK, Moselhy S, Ferrari S. 2008. ATR-dependent pathways control hEXO1 stability in response to stalled forks. Nucleic Acids Res 36:511-9.

Errico A, Cosentino C, Rivera T, Losada A, Schwob E, Hunt T, Costanzo V. 2009. Tipin/Tim1/And1 protein complex promotes Pol alpha chromatin binding and sister chromatid cohesion. EMBO J 28: 3681–3692

Evrin C, Clarke P, Zech J, Lurz R, Sun J, Uhle S, Li H, Stillman B, Speck C. 2009. A double-hexameric MCM2-7 complex is loaded onto origin DNA during licensing of eukaryotic DNA replication. Proc Natl Acad Sci U S A 106:20240-5.

Fackenthal JD, Olopade OI. 2007. Breast cancer risk associated with BRCA1 and BRCA2 in diverse populations. Nat Rev Cancer. 7:937-48.

Fan X, Liu Y, Heilman SA, Chen JJ. 2013. Human papillomavirus E7 induces rereplication in response to DNA damage. J Virol. 87:1200-10.

Fernández-Cid A, Riera A, Tognetti S, Herrera MC, Samel S, Evrin C, Winkler C, Gardenal E, Uhle S, Speck C. 2013. An ORC/Cdc6/MCM2-7 complex is formed in a multistep reaction to serve as a platform for MCM double-hexamer assembly. Mol Cell. 50:577-88.

Finn KJ, Li JJ. 2013. Single-stranded annealing induced by re-initiation of replication origins provides a novel and efficient mechanism for generating copy number expansion via non-allelic homologous recombination. PLoS Genet 9: e1003192. doi: 10.1371/journal.pgen.1003192.

Fletcher RJ, Bishop BE, Leon RP, Sclafani RA, Ogata CM, Chen XS. 2003. The structure and function of MCM from archaeal M. Thermoautotrophicum. Nat Struct Biol. 10:160-7.

Fragkos M, Ganier O, Coulombe P, Méchali M. 2015. DNA replication origin activation in space and time. Nat Rev Mol Cell Biol. 16: 360-74.

Francis LI, Randell JC, Takara TJ, Uchima L, Bell SP. 2009. Incorporation into the prereplicative complex activates the Mcm2-7 helicase for Cdc7-Dbf4 phosphorylation. Genes Dev. 23:643-54.

Frigola J, Remus D, Mehanna A, Diffley JF. 2013. ATPase-dependent quality control of DNA replication origin licensing. Nature. 495:339-43.

Fu H, Maunakea AK, Martin MM, Huang L, Zhang Y, Ryan M, Kim R, Lin CM, Zhao K, Aladjem MI. 2013. Methylation of histone H3 on lysine 79 associates with a group of replication origins and helps limit DNA replication once per cell cycle. PLoS Genet. 9:e1003542.

Fugger K, Chu WK, Haahr P, Kousholt AN, Beck H, Payne MJ, Hanada K, Hickson ID, Sørensen CS. 2013. FBH1 co-operates with MUS81 in inducing DNA double-strand breaks and cell death following replication stress. Nat Commun. 4:1423. doi: 10.1038/ncomms2395.

Fugger K, Mistrik M, Danielsen JR, Dinant C, Falck J, Bartek J, Lukas J, Mailand N. 2009. Human Fbh1 helicase contributes to genome maintenance via pro- and anti-recombinase activities. J Cell Biol. 186:655-63.

Fugger K, Mistrik M, Neelsen KJ, Yao Q, Zellweger R et al. 2015. FBH1 catalyzes regression of stalled replication forks. Cell Rep 10:1749–1757.

Fujii-Yamamoto H, Kim JM, Arai K, Masai H. 2005. Cell cycle and developmental regulations of replication factors in mouse embryonic stem cells. J Biol Chem 280: 12976-12987.

Gaillard H, García-Muse T, Aguilera A. 2015. Replication stress and cancer. Nat Rev Cancer 15:276–289.

Galanos P, Vougas K, Walter D, Polyzos A, Maya-Mendoza A, Haagensen EJ, Kokkalis A, Roumelioti FM, Gagos S, Tzetis M et al. 2016. Chronic p53-independent p21 expression causes genomic instability by deregulating replication licensing. Nat Cell Biol 18: 777-89.

Gambus A, Jones RC, Sanchez-Diaz A, Kanemaki M, van Deursen F, Edmondson RD, Labib K. 2006. GINS maintains association of Cdc45 with MCM in replisome progression complexes at eukaryotic DNA replication forks Nat Cell Biol 8:358-66.

Gambus A, van Deursen F, Polychronopoulos D, Foltman M, Jones RC, Edmondson RD, Calzada A, Labib K. 2009. A key role for Ctf4 in coupling the MCM2-7 helicase to DNA polymerase alpha within the eukaryotic replisome. EMBO J 28:2992–3004.

Ge XQ, Blow JJ. 2010. Chk1 inhibits replication factory activation but allows dormant origin firing in existing factories. J Cell Biol. 191:1285-97.

Ge XQ, Jackson DA, Blow JJ. 2007. Dormant origins licensed by excess Mcm2-7 are required for human cells to survive replicative stress. Genes Dev 21:3331–3341.

Green BM, Li JJ. 2005. Loss of rereplication control in Saccharomyces cerevisiae results in extensive DNA damage. Mol Biol Cell. 16:421-32.

Green BM, Morreale RJ, Ozaydin B, Derisi JL, Li JJ. 2006. Genome-wide mapping of DNA synthesis in Saccharomyces cerevisiae reveals that mechanisms preventing reinitiation of DNA replication are not redundant. Mol Biol Cell. 17:2401-14.

Green BM, Finn KJ, Li JJ. 2010. Loss of DNA replication control is a potent inducer of gene amplification. Science. 329: 943-6.

Gómez M, Antequera F. 2008. Overreplication of short DNA regions during S phase in human cells. Genes Dev. 22:375-85.

Gonzalez MA, Tachibana KE, Adams DJ, van der Weyden L, Hemberger M, Coleman N, Bradley A, Laskey RA. 2006. Geminin is essential to prevent endoreduplication and to form pluripotent cells during mammalian development. Genes Dev. 20:1880-4.

Gonzalez S, Klatt P, Delgado S, Conde E, Lopez-Rios F, Sanchez-Cespedes M, Mendez J, Antequera F, Serrano M. 2006. Oncogenic activity of Cdc6 through repression of the INK4/ARF locus. Nature. 440:702-6.

Guillou E, Ibarra A, Coulon V, Casado-Vela J, Rico D, Casal I, Schwob E, Losada A, Méndez J. 2010. Cohesin organizes chromatin loops at DNA replication factories. Genes Dev 24:2812-22.

Guo C, Kumagai A, Schlacher K, Shevchenko A, Shevchenko A, Dunphy WG. 2015. Interaction of Chk1 with Treslin negatively regulates the initiation of chromosomal DNA replication. Mol Cell 57:492-505.

Guo ZP, Hu YC, Xie Y, Jin F, Song ZQ, Liu XD, Ma T, Zhou PK. 2017. MLN4924 suppresses the BRCA1 complex and synergizes with PARP inhibition in NSCLC cells. Biochem Biophys Res Commun. 483:223-229.

Halazonetis TD, Gorgoulis VG, Bartek J. 2008. An oncogene-induced DNA damage model for cancer development. Science 319:1352– 1355

Hall JR, Kow E, Nevis KR, Lu CK, Luce KS, Zhong Q, Cook JG. 2007. Cdc6 stability is regulated by the Huwe1 ubiquitin ligase after DNA damage. Mol Biol Cell. 18:3340-50.

Hall JR, Lee HO, Bunker BD, Dorn ES, Rogers GC, Duronio RJ, Cook JG. 2008. Cdt1 and Cdc6 are destabilized by rereplication-induced DNA damage. J Biol Chem. 283:25356-63.

Hanada K, Budzowska M, Davies SL, van Drunen E, Onizawa H, Beverloo HB, Maas A, Essers J, Hickson ID, Kanaar R. 2007. The structure-specific endonuclease Mus81 contributes to replication restart by generating double-strand DNA breaks. Nat Struct Mol Biol 14:1096-104.

Hanahan D, Weinberg RA. 2011. Hallmarks of cancer: the next generation. Cell. 144:646-74.

Hanlon SL, Li JJ. 2015. Re-replication of a centromere induces chromosomal instability and aneuploidy. PLoS Genet. 11:e1005039. doi: 10.1371/journal.pgen.1005039.

Hashimoto Y, Ray Chaudhuri A, Lopes M, Costanzo V. 2010. Rad51 protects nascent DNA from Mre11-dependent degradation and promotes continuous DNA synthesis. Nat Struct Mol Biol 17:1305-11.

Hendzel MJ, Wei Y, Mancini MA, Van Hooser A, Ranalli T, Brinkley BR, Bazett-Jones DP, Allis CD. 1997. Mitosis-specific phosphorylation of histone H3 initiates primarily within pericentromeric heterochromatin during G2 and spreads in an ordered fashion coincident with mitotic chromosome condensation. Chromosoma 106: 348-360.

Hesketh EL, Parker-Manuel RP, Chaban Y, Satti R, Coverley D, Orlova EV, Chong JP. 2015. DNA induces conformational changes in a recombinant human minichromosome maintenance complex. J Biol Chem. 290:7973-9.

Heyer WD, Ehmsen KT, Liu J. 2010. Regulation of homologous recombination in eukaryotes. Annu Rev Genet. 44:113-39.

Higa LA, Banks D, Wu M, Kobayashi R, Sun H, Zhang H. 2006. L2DTL/CDT2 interacts with the CUL4/DDB1 complex and PCNA and regulates CDT1 proteolysis in response to DNA damage. Cell Cycle. 5:1675-80.

Higgs MR, Reynolds JJ, Winczura A, Blackford AN, Borel V, Miller ES, Zlatanou A, Nieminuszczy J, Ryan EL, Davies NJ, Stankovic T, Boulton SJ, Niedzwiedz W, Stewart GS. 2015. BOD1L Is Required to Suppress Deleterious Resection of Stressed Replication Forks. Mol Cell. 59:462-77.

Hills SA, Diffley JF. 2014. DNA replication and oncogene-induced replicative stress. Curr Biol. 24: R435-44.

Hiom K. 2010. FANCJ: solving problems in DNA replication. DNA Repair (Amst). 9:250-6.

Hoshina S, Yura K, Teranishi H, Kiyasu N, Tominaga A, Kadoma H, Nakatsuka A, Kunichika T, Obuse C, Waga S. 2013. Human origin recognition complex binds preferentially to G-quadruplex-preferable RNA and single-stranded DNA. J Biol Chem. 288:30161-71.

Hu J, McCall CM, Ohta T, Xiong Y. 2004. Targeted ubiquitination of CDT1 by the DDB1-CUL4A-ROC1 ligase in response to DNA damage. Nat Cell Biol. 6:1003-9.

Hu Y, Raynard S, Sehorn MG, Lu X, Bussen W, Zheng L, Stark JM, Barnes EL, Chi P, Janscak P, Jasin M, Vogel H, Sung P, Luo G. 2007. RECQL5/Recql5 helicase regulates homologous recombination and suppresses tumor formation via disruption of Rad51 presynaptic filaments. Genes Dev 21:3073-84.

Huang M, Kim JM, Shiotani B, Yang K, Zou L, D'Andrea AD. The FANCM/FAAP24 complex is required for the DNA interstrand crosslink-induced checkpoint response. Mol Cell. 39:259-68.

Huang YY, Kaneko KJ, Pan H, DePamphilis ML. 2015. Geminin is Essential to Prevent DNA Re-Replication-Dependent Apoptosis in Pluripotent Cells, but not in Differentiated Cells. Stem Cells 33: 3239-3253.

Huberman JA, Riggs AD. 1968. On the mechanism of DNA replication in mammalian chromosomes. J Mol Biol. 32:327-41.

Ibarra A, Schwob E, Méndez J. 2008. Excess MCM proteins protect human cells from replicative stress by licensing backup origins of replication. Proc Natl Acad Sci U S A 105:8956–8961

Im JS, Ki SH, Farina A, Jung DS, Hurwitz J, Lee JK. 2009. Assembly of the Cdc45-Mcm2-7-GINS complex in human cells requires the Ctf4/And-1, RecQL4, and Mcm10 proteins. Proc Natl Acad Sci U S A 106:15628-32.

Jackson DA, Pombo A. 1998. Replicon clusters are stable units of chromosome structure: evidence that nuclear organization contributes to the efficient activation and propagation of S phase in human cells. J Cell Biol 140: 1285-1295.

Jayathilaka K, Sheridan SD, Bold TD, Bochenska K, Logan HL, Weichselbaum RR, Bishop DK, Connell PP. 2008. A chemical compound that stimulates the human homologous recombination protein RAD51. Proc Natl Acad Sci U S A. 105:15848-53.

Jiang W, Wells NJ, Hunter T. 1999. Multistep regulation of DNA replication by Cdk phosphorylation of HsCdc6. Proc Natl Acad Sci U S A. 96:6193-8.

Jones RM, Mortusewicz O, Afzal I, Lorvellec M, García P, Helleday T, Petermann E. 2013. Increased replication initiation and conflicts with transcription underlie Cyclin E-induced replication stress. Oncogene 32:3744–3753

Kang S, Warner MD, Bell SP. 2014. Multiple functions for Mcm2-7 ATPase motifs during replication initiation. Mol Cell. 55:655-65.

Kanke M, Kodama Y, Takahashi TS, Nakagawa T, Masukata H. 2012. Mcm10 plays an essential role in origin DNA unwinding after loading of the CMG components. EMBO J 31:2182-94.

Karakaidos P, Taraviras S, Vassiliou LV, Zacharatos P, Kastrinakis NG, Kougiou D, Kouloukoussa M, Nishitani H, Papavassiliou AG, Lygerou Z, Gorgoulis VG. 2004. Overexpression of the replication licensing regulators hCdt1 and hCdc6 characterizes a subset of non-small-cell lung carcinomas: synergistic effect with mutant p53 on tumor growth and chromosomal instability--evidence of E2F-1 transcriptional control over hCdt1. Am J Pathol. 165:1351-65.

Karamitros D, Patmanidi AL, Kotantaki P, Potocnik AJ, Bähr-Ivacevic T, Benes V, Lygerou Z, Kioussis D, Taraviras S. 2015. Geminin deletion increases the number of fetal hematopoietic stem cells by affecting the expression of key transcription factors. Development 142: 70-81.

Katou Y, Kanoh Y, Bando M, Noguchi H, Tanaka H, Ashikari T, Sugimoto K, Shirahige K. 2003. S-phase checkpoint proteins Tof1 and Mrc1 form a stable replication-pausing complex. Nature 424: 1078–1083

Kawabata T, Luebben SW, Yamaguchi S, Ilves I, Matise I, Buske T, Botchan MR, Shima N. 2011. Stalled fork rescue via dormant rep- lication origins in unchallenged S phase promotes proper chromo- some segregation and tumor suppression. Mol Cell 41:543–553.

Keller H, Kiosze K, Sachsenweger J, Haumann S, Ohlenschläger O, Nuutinen T, Syväoja JE, Görlach M, Grosse F, Pospiech H. 2014. The intrinsically disordered amino-terminal region of human RecQL4: multiple DNA-binding domains confer annealing, strand exchange and G4 DNA binding. Nucleic Acids Res. 42:12614-27.

Kim TM, Ko JH, Hu L, Kim SA, Bishop AJ, Vijg J, Montagna C, Hasty P. 2012. RAD51 mutants cause replication defects and chromosomal instability. Mol Cell Biol. 32:3663-80.

Kimura K, Hirano T. 2000. Dual roles of the 11S regulatory subcomplex in condensin functions. Proc Natl Acad Sci U S A. 97: 11972-7.

Kittler R, Pelletier L, Heninger AK, Slabicki M, Theis M, Miroslaw L, Poser I, Lawo S, Grabner H, Kozak K, Wagner J, Surendranath V, Richter C, Bowen W, Jackson AL, Habermann B, Hyman AA, Buchholz F. 2007. Genome-scale RNAi profiling of cell division in human tissue culture cells. Nat Cell Biol. 9:1401-12.

Klotz-Noack K, McIntosh D, Schurch N, Pratt N, Blow JJ. 2012. Re-replication induced by geminin depletion occurs from G2 and is enhanced by checkpoint activation. J Cell Sci 15: 2436-2445.

Kumagai A, Shevchenko A, Shevchenko A, Dunphy WG. 2010. Treslin collaborates with TopBP1 in triggering the initiation of DNA replication. Cell 140:349-59.

Kumagai A, Shevchenko A, Shevchenko A, Dunphy WG. 2011. Direct regulation of Treslin by cyclin-dependent kinase is essential for the onset of DNA replication. J Cell Biol. 193:995-1007.

Kunnev D, Rusiniak ME, Kudla A, Freeland A, Cady GK, Pruitt SC. 2010. DNA damage response and tumorigenesis in Mcm2-deficient mice. Oncogene 29: 3630-3638.

Lange SS, Takata K, Wood RD. 2011. DNA polymerases and cancer. Nat Rev Cancer 11:96-110.

Laulier C, Cheng A, Stark JM. 2011. The relative efficiency of homology-directed repair has distinct effects on proper anaphase chromosome separation. Nucleic Acids Res. 39:5935-44.

Lee CY, Johnson RL, Wichterman-Kouznetsova J, Guha R, Ferrer M, Tuzmen P, Martin SE, Zhu W, DePamphilis ML. 2012. High-throughput screening for genes that prevent excess DNA replication in human cells and for molecules that inhibit them. Methods. 57:234-48.

Leuzzi G, Marabitti V, Pichierri P, Franchitto A. 2016. WRNIP1 protects stalled forks from degradation and promotes fork restart after replication stress. EMBO J. 35:1437-51.

Li CJ, Vassilev A, DePamphilis ML. 2004. Role for Cdk1 (Cdc2)/cyclin A in preventing the mammalian origin recognition complex's largest subunit (Orc1) from binding to chromatin during mitosis. Mol Cell Biol 24:5875-86.

Li N, Zhai Y, Zhang Y, Li W, Yang M, Lei J, Tye BK, Gao N. 2015. Structure of the eukaryotic MCM complex at 3.8 Å. Nature. 524:186-91.

Liberi G, Maffioletti G, Lucca C, Chiolo I, Baryshnikova A, Cotta-Ramusino C, Lopes M, Pellicioli A, Haber JE, Foiani M. 2005. Rad51-dependent DNA structures accumulate at damaged replication forks in sgs1 mutants defective in the yeast ortholog of BLM RecQ helicase. Genes Dev 19:339-50.

Lin JJ, Dutta A. 2007. ATR pathway is the primary pathway for activating G2/M checkpoint induction after re-replication. J Biol Chem. 282:30357-62.

Lin JJ, Milhollen MA, Smith PG, Narayanan U, Dutta A. 2010. NEDD8-targeting drug MLN4924 elicits DNA rereplication by stabilizing Cdt1 in S phase, triggering checkpoint activation, apoptosis, and senescence in cancer cells. Cancer Res 70: 10310-10320.

Liontos M, Koutsami M, Sideridou M, Evangelou K, Kletsas D, Levy B, Kotsinas A, Nahum O, Zoumpourlis V, Kouloukoussa M et al. 2007. Deregulated overexpression of hCdt1 and hCdc6 promotes malignant behavior. Cancer Res 67: 10899-10909.

Liu E, Lee AY, Chiba T, Olson E, Sun P, Wu X. 2007. The ATR-mediated S phase checkpoint prevents rereplication in mammalian cells when licensing control is disrupted. J Cell Biol 179:643-57.

Liu E, Li X, Yan F, Zhao Q, Wu X. 2004. Cyclin-dependent kinases phosphorylate human Cdt1 and induce its degradation. J Biol Chem. 279:17283-8.

Liu Y, Nielsen CF, Yao Q, Hickson ID. 2014. The origins and processing of ultra fine anaphase DNA bridges. Curr Opin Genet Dev 26:1-5.

Lopes M, Cotta-Ramusino C, Pellicioli A, Liberi G, Plevani P, Muzi- Falconi M, Newlon CS, Foiani M. 2001. The DNA replication checkpoint response stabilizes stalled replication forks. Nature 412:557–561

Lopez-Mosqueda J, Maas NL, Jonsson ZO, Defazio-Eli LG, Wohlschlegel J, Toczyski DP. 2010. Damage-induced phosphorylation of Sld3 is important to block late origin firing. Nature 467:479-83.

Lovejoy CA, Lock K, Yenamandra A, Cortez D. 2006. DDB1 mantains genome integrity through regulation of Cdt1 Mol Cell Biol 26:7977-90.

Lydeard JR, Lipkin-Moore Z, Sheu YJ, Stillman B, Burgers PM, Haber JE. 2010. Break-induced replication requires all essential DNA replication factors except those specific for pre-RC assembly. Genes Dev 24:1133-44.

MacDougall CA, Byun TS, Van C, Yee MC, Cimprich KA. 2007. The structural determinants of checkpoint activation. Genes Dev 21:898-903.

Machida YJ, Dutta A. 2007. The APC/C inhibitor, Emi1, is essential for prevention of rereplication. Genes Dev. 21:184-94.

Machwe A, Lozada E, Wold MS, Li GM, Orren DK. 2011. Molecular cooperation between the Werner syndrome protein and replication protein A in relation to replication fork blockage. J Biol Chem. 286:3497-508.

Mailand N, Diffley JF. 2005. CDKs promote DNA replication origin licensing in human cells by protecting Cdc6 from APC/C-dependent proteolysis. Cell. 122:915-26.

Mailand N, Gibbs-Seymour I, Bekker-Jensen S. 2013. Regulation of PCNA-protein interactions for genome stability. Nat Rev Mol Cell Biol 14:269-82.

Mankouri HW, Hickson ID. 2006. Top3 processes recombination intermediates and modulates checkpoint activity after DNA damage. Mol Biol Cell 17:4473-83.

Matsuoka S, Ballif BA, Smogorzewska A, McDonald ER 3rd, Hurov KE, Luo J, Bakalarski CE, Zhao Z, Solimini N, Lerenthal Y, Shiloh Y, Gygi SP, Elledge SJ. 2007.

ATM and ATR substrate analysis reveals extensive protein networks responsive to DNA damage. Science. 316:1160-6.

Maya-Mendoza A, Petermann E, Gillespie DA, Caldecott KW, Jackson DA. 2007. Chk1 regulates the density of active replication origins during the vertebrate S phase. EMBO J 26:2719-31.

Melixetian M, Ballabeni A, Masiero L, Gasparini P, Zamponi R, Bartek J, Lukas J, Helin K. 2004. Loss of geminin induces rereplication in the presence of functional p53. J Cell Biol 165:473-82.

Méndez J, Stillman B. 2000. Chromatin association of human origin recognition complex, cdc6, and minichromosome maintenance proteins during the cell cycle: assembly of prereplication complexes in late mitosis. Mol Cell Biol. 20:8602-12.

Mendez J, Zou-Yang XH, Kim SY, Hidaka M, Tansey WP, Stillman B. 2002. Human origin recognition complex large subunit is degraded by ubiquitin-mediated proteolysis after initiation of DNA replication. Mol Cell 9:481-91.

Milhollen MA, Narayanan U, Soucy TA, Veiby PO, Smith PG, Amidon B. 2011. Inhibition of NEDD8-activating enzyme induces rereplication and apoptosis in human tumor cells consistent with deregulating CDT1 turnover. Cancer Res 71: 3042-3051.

Miotto B, Ji Z, Struhl K. 2016. Selectivity of ORC binding sites and the relation to replication timing, fragile sites, and deletions in cancers. Proc Natl Acad Sci U S A. 113:E4810-9.

Miotto B, Struhl K. 2010. HBO1 histone acetylase activity is essential for DNA replication licensing and inhibited by Geminin. Mol Cell. 37:57-66.

Mourón S, Rodriguez-Acebes S, Martínez-Jiménez MI, García-Gómez S, Chocrón S, Blanco L, Méndez J. 2013. Repriming of DNA synthesis at stalled replication forks by human PrimPol. Nat Struct Mol Biol 20:1383-9.

Mukherji M, Bell R, Supekova L, Wang Y, Orth AP, Batalov S, Miraglia L, Huesken D, Lange J, Martin C, Sahasrabudhe S, Reinhardt M, Natt F, Hall J, Mickanin C, Labow M, Chanda SK, Cho CY, Schultz PG. 2006. Genome-wide functional analysis of human cell-cycle regulators. Proc Natl Acad Sci U S A. 103:14819-24.

Muñoz S, Méndez J. 2016. DNA replication stress: from molecular mechanisms to human disease. Chromosoma. PMID: 26797216

Muramatsu S, Hirai K, Tak YS, Kamimura Y, Araki H. 2010. CDK-dependent complex formation between replication proteins Dpb11, Sld2, Pol (epsilon}, and GINS in budding yeast. Genes Dev 24(6):602-12.

Murphy N, Ring M, Heffron CC, Martin CM, McGuinness E, Sheils O, O'Leary JJ. 2005. Quantitation of CDC6 and MCM5 mRNA in cervical intraepithelial neoplasia and invasive squamous cell carcinoma of the cervix. Mod Pathol. 18:844-9.

Nakajima R, Masukata H. 2002. SpSld3 is required for loading and maintenance of SpCdc45 on chromatin in DNA replication in fission yeast. Mol Biol Cell. 13:1462-72.

Nakamura H, Morita T, Sato C. 1986. Structural organizations of replicon domains during DNA synthetic phase in the mammalian nucleus. Exp Cell Res. 165:291-7.

Neelsen KJ, Lopes M. 2015. Replication fork reversal in eukaryotes: from dead end to dynamic response. Nat Rev Mol Cell Biol 16: 207–220

Neelsen KJ, Zanini IM, Mijic S, Herrador R, Zellweger R, Ray Chaudhuri A, Creavin KD, Blow JJ, Lopes M. 2013. Deregulated origin licensing leads to chromosomal breaks by rereplication of a gapped DNA template. Genes Dev 27: 2537-2542.

Nguyen VQ, Co C, Li JJ. 2001. Cyclin-dependent kinases prevent DNA re-replication through multiple mechanisms. Nature. 411:1068-73.

Nishitani H, Sugimoto N, Roukos V, Nakanishi Y, Saijo M, Obuse C, Tsurimoto T, Nakayama KI, Nakayama K, Fujita M, Lygerou Z, Nishimoto T. 2006. Two E3 ubiquitin ligases, SCF-Skp2 and DDB1-Cul4, target human Cdt1 for proteolysis. EMBO J 25:1126-36.

Okuno Y, McNairn AJ, den Elzen N, Pines J, Gilbert DM. 2001. Stability, chromatin association and functional activity of mammalian pre-replication complex proteins during the cell cycle. EMBO J. 20:4263-77.

Ohta S, Koide M, Tokuyama T, Yokota N, Nishizawa S, Namba H. 2001. Cdc6 expression as a marker of proliferative activity in brain tumors. Oncol Rep. 8:1063-6.

Pan WW, Zhou JJ, Yu C, Xu Y, Guo LJ, Zhang HY, Zhou D, Song FZ, Fan HY. 2013. Ubiquitin E3 ligase CRL4(CDT2/DCAF2) as a potential chemotherapeutic target for ovarian surface epithelial cancer. J Biol Chem. 288:29680-91.

Peschiaroli A, Dorrello NV, Guardavaccaro D, Venere M, Halazonetis T, Sherman NE, Pagano M. 2006. SCFbetaTrCP-mediated degrada- tion of Claspin regulates recovery from the DNA replication check- point response. Mol Cell 23:319–329.

Petermann E, Helleday T. 2010. Pathways of mammalian replication fork restart. Nat Rev Mol Cell Biol 11:683–687.

Petermann E, Orta ML, Issaeva N, Schultz N, Helleday T. 2010. Hydroxyurea-stalled replication forks become progressively inactivated and require two different RAD51-mediated pathways for restart and repair. Mol Cell 37:492-502.

Petermann E, Woodcock M, Helleday T. 2010. Chk1 promotes replication fork progression by controlling replication initiation. Proc Natl Acad Sci U S A. 107:16090-5.

Petersen BO, Lukas J, Sørensen CS, Bartek J, Helin K. 1999. Phosphorylation of mammalian CDC6 by cyclin A/CDK2 regulates its subcellular localization. EMBO J. 18:396-410.

Petersen BO, Wagener C, Marinoni F, Kramer ER, Melixetian M, Lazzerini Denchi E, Gieffers C, Matteucci C, Peters JM, Helin K. 2000. Cell cycle- and cell growth-regulated proteolysis of mammalian CDC6 is dependent on APC-CDH1. Genes Dev. 14:2330-43.

Petrakis TG, Komseli ES, Papaioannou M, Vougas K, Polyzos A, Myrianthopoulos V, Mikros E, Trougakos IP, Thanos D, Branzei D, Townsend P, Gorgoulis VG. 2016. Exploring and exploiting the systemic effects of deregulated replication licensing. Semin Cancer Biol 38: 3-15.

Picard F, Cadoret JC, Audit B, Arneodo A, Alberti A, Battail C, Duret L, Prioleau MN. 2014. The spatiotemporal program of DNA replication is associated with specific combinations of chromatin marks in human cells. PLoS Genet. 10:e1004282.

Pinyol M, Salaverria I, Bea S, Fernández V, Colomo L, Campo E, Jares P. 2006. Unbalanced expression of licensing DNA replication factors occurs in a subset of mantle cell lymphomas with genomic instability. Int J Cancer. 119:2768-74.

Powell SK, MacAlpine HK, Prinz JA, Li Y, Belsky JA, MacAlpine DM. 2015.
Dynamic loading and redistribution of the Mcm2-7 helicase complex through the cell cycle. EMBO J. 34:531-43.

Prioleau MN, MacAlpine DM. 2016. DNA replication origins-where do we begin? Genes Dev. 30: 1683-97.

Pruitt SC, Bailey KJ, Freeland A. 2007. Reduced Mcm2 expression results in severe stem/progenitor cell deficiency and cancer. Stem Cells 25:3121–32

Quinlan AR, Hall IM. 2010. BEDTools: a flexible suite of utilities for comparing genomic features. Bioinformatics. 26:841-2.

Raderschall E, Stout K, Freier S, Suckow V, Schweiger S, Haaf T. 2002. Elevated levels of Rad51 recombination protein in tumor cells. Cancer Res. 62:219-25.

Randell JC, Bowers JL, Rodríguez HK, Bell SP. 2006. Sequential ATP hydrolysis by Cdc6 and ORC directs loading of the Mcm2-7 helicase. Mol Cell. 21:29-39.

Ray Chaudhuri A, Hashimoto Y, Herrador R, Neelsen KJ, Fachinetti D, Bermejo R, Cocito A, Costanzo V, Lopes M. 2012. Topoisomerase I poisoning results in PARP-mediated replication fork reversal. Nat Struct Mol Biol 19:417-23.

Raynard S, Bussen W, Sung P. 2006. A double Holliday junction dissolvasome comprising BLM, topoisomerase IIIalpha, and BLAP75. J Biol Chem 281:13861-4.

Remeseiro S, Cuadrado A, Carretero M, Martínez P, Drosopoulos WC, Cañamero M, Schildkraut CL, Blasco MA, Losada A. 2012. Cohesin-SA1 deficiency drives aneuploidy and tumourigenesis in mice due to impaired replication of telomeres. EMBO J. 31:2076-89.

Remus D, Beuron F, Tolun G, Griffith JD, Morris EP, Diffley JF. 2009. Concerted loading of Mcm2-7 double hexamers around DNA during DNA replication origin licensing. Cell 139:719-30.

de Renty C, Kaneko KJ, DePamphilis ML. 2014. The dual roles of geminin during trophoblast proliferation and differentiation. Dev Biol. 387:49-63.

Richardson CD, Li JJ. 2014. Regulatory mechanisms that prevent re-initiation of DNA replication can be locally modulated at origins by nearby sequence elements. PLoS Genet. 10:e1004358. doi: 10.1371/journal.pgen.1004358.

Rosado IV, Niedzwiedz W, Alpi AF, Patel KJ. 2009. The Walker B motif in avian FANCM is required to limit sister chromatid exchanges but is dispensable for DNA crosslink repair. Nucleic Acids Res 37:4360-70.

Saha P, Chen J, Thome KC, Lawlis SJ, Hou ZH, Hendricks M, Parvin JD, Dutta A. 1998. Human CDC6/Cdc18 associates with Orc1 and cyclin-cdk and is selectively eliminated from the nucleus at the onset of S phase. Mol Cell Biol. 18:2758-67.

Saini N, Ramakrishnan S, Elango R, Ayyar S, Zhang Y, Deem A, Ira G, Haber JE, Lobachev KS, Malkova A. 2013. Migrating bubble during break-induced replication drives conservative DNA synthesis. Nature 502:389-92.

Sakofsky CJ, Roberts SA, Malc E, Mieczkowski PA, Resnick MA, Gordenin DA, Malkova A. 2014. Break-induced replication is a source of mutation clusters underlying kataegis. Cell Rep 7:1640-8.

Sale JE. 2012. Competition, collaboration and coordination--determining how cells bypass DNA damage. J Cell Sci 125:1633-43.

Sale JE, Lehmann AR, Woodgate R. 2012. Y-family DNA polymerases and their role in tolerance of cellular DNA damage. Nat Rev Mol Cell Biol 13:141-52.

Samel SA, Fernández-Cid A, Sun J, Riera A, Tognetti S, Herrera MC, Li H, Speck C. 2014. A unique DNA entry gate serves for regulated loading of the eukaryotic replicative helicase MCM2-7 onto DNA. Genes Dev. 28:1653-66.

Sangrithi MN, Bernal JA, Madine M, Philpott A, Lee J, Dunphy WG, Venkitaraman AR. 2005. Initiation of DNA replication requires the RECQL4 protein mutated in Rothmund-Thomson syndrome. Cell. 121:887-98.
Schwab RA, Blackford AN, Niedzwiedz W. 2010. ATR activation and replication fork restart are defective in FANCM-deficient cells. EMBO J. 29:806-18.

Sato T, Clevers H. 2013. Primary mouse small intestinal epithelial cell cultures. Methods in Molecular Biology 945: 319-328.

Schlacher K, Christ N, Siaud N, Egashira A, Wu H, Jasin M. 2011. Double-strand break repair-independent role for BRCA2 in blocking stalled replication fork degradation by MRE11. Cell 145:529-42.

Schlacher K, Wu H, Jasin M. 2012. A distinct replication fork protection pathway connects Fanconi anemia tumor suppressors to RAD51-BRCA1/2. Cancer Cell 22:106-16.

Seiler JA, Conti C, Syed A, Aladjem MI, Pommier Y. 2007. The intra-S-phase checkpoint affects both DNA replication initiation and elongation: single-cell and -DNA fiber analyses. Mol Cell Biol. 27:5806-18.

Senga T, Sivaprasad U, Zhu W, Park JH, Arias EE, Walter JC, Dutta A. 2006. PCNA is a cofactor for Cdt1 degradation by CUL4/DDB1-mediated N-terminal ubiquitination. J Biol Chem. 281:6246-52.

Seo J, Chung YS, Sharma GG, Moon E, Burack WR, Pandita TK, Choi K. 2005. Cdt1 transgenic mice develop lymphoblastic lymphoma in the absence of p53. Oncogene. 24:8176-86.

Sequeira-Mendes J, Díaz-Uriarte R, Apedaile A, Huntley D, Brockdorff N, Gómez M. 2009. Transcription initiation activity sets replication origin efficiency in mammalian cells. PLoS Genet. 5:e1000446.

Shah PP, Zheng X, Epshtein A, Carey JN, Bishop DK, Klein HL. 2010. Swi2/Snf2-related translocases prevent accumulation of toxic Rad51 complexes during mitotic growth. Mol Cell. 39:862-72.

Sheu YJ, Stillman B. 2006. Cdc7-Dbf4 phosphorylates MCM proteins via a docking site-mediated mechanism to promote S phase progression. Mol Cell. 24:101-13.

Sheu YJ, Stillman B. 2010. The Dbf4-Cdc7 kinase promotes S phase by alleviating an inhibitory activity in Mcm4. Nature. 463:113-7.

Shima N, Alcaraz A, Liachko I, Buske TR, Andrews CA, Munroe RJ, Hartford SA, Tye BK, Schimenti JC. 2007. A viable allele of Mcm4 causes chromosome instability and mammary adenocarcinomas in mice. Nat Genet 39:93–98

Shinnick KM, Eklund EA, McGarry TJ. 2010. Geminin deletion from hematopoietic cells causes anemia and thrombocytosis in mice. J Clin Invest 120: 4303-4315.

Shukla A, Navadgi VM, Mallikarjuna K, Rao BJ. 2005. Interaction of hRad51 and hRad52 with MCM complex: a cross-talk between recombination and replication proteins. Biochem Biophys Res Commun. 329:1240-5.

Sideridou M, Zakopoulou R, Evangelou K, Liontos M, Kotsinas A, Rampakakis E, Gagos S, Kahata K, Grabusic K, et al. 2011. Cdc6 expression represses E-cadherin transcription and activates adjacent replication origins. J Cell Biol. 195:1123-40.

Sidorova JM, Li N, Folch A, Monnat RJ Jr. 2008. The RecQ helicase WRN is required for normal replication fork progression after DNA damage or replication fork arrest. Cell Cycle 7:796-807.

Simandlova J, Zagelbaum J, Payne MJ, et al. 2013. FBH1 helicase disrupts RAD51 filaments in vitro and modulates homologous recombination in mammalian cells. J Biol Chem 288:34168-80.

Smith CE, Llorente B, Symington LS. 2007. Template switching during break-induced replication. Nature 447:102-5.

Sogo JM, Lopes M, Foiani M. 2002. Fork reversal and ssDNA accumu- lation at stalled replication forks owing to checkpoint defects. Science 297:599–602

Solinger JA, Kiianitsa K, Heyer WD. 2002. Rad54, a Swi2/Snf2-like recombinational repair protein, disassembles Rad51:dsDNA filaments. Mol Cell. 10:1175-88.

Sommers JA, Rawtani N, Gupta R, Bugreev DV, Mazin AV, Cantor SB, Brosh RM Jr. 2009. FANCJ uses its motor ATPase to destabilize protein-DNA complexes, unwind triplexes, and inhibit RAD51 strand exchange. J Biol Chem 284:7505-17.

Somyajit K, Saxena S, Babu S, Mishra A, Nagaraju G. 2015. Mammalian RAD51 paralogs protect nascent DNA at stalled forks and mediate replication restart. Nucleic Acids Res. 43:9835-55.

Soucy TA, Smith PG, Milhollen MA, Berger AJ, Gavin JM, Adhikari S, Brownell JE, Burke KE, Cardin DP, et al. 2009. An inhibitor of NEDD8-activating enzyme as a new approach to treat cancer. Nature. 458(7239):732-6.

Speck C, Chen Z, Li H, Stillman B. 2005. ATPase-dependent cooperative binding of ORC and Cdc6 to origin DNA. Nat Struct Mol Biol. 12: 965-71.

Stark JM, Hu P, Pierce AJ, Moynahan ME, Ellis N, Jasin M. 2002. ATP hydrolysis by mammalian RAD51 has a key role during homology-directed DNA repair. J Biol Chem. 277:20185-94.

Stark JM, Pierce AJ, Oh J, Pastink A, Jasin M. 2004. Genetic steps of mammalian homologous repair with distinct mutagenic consequences. Mol Cell Biol. 24:9305-16.

Stubblefield E. 1975. Analysis of the replication pattern of Chinese hamster chromosomes using 5-bromodeoxyuridine suppression of 33258 Hoechst fluorescence. Chromosoma. 53:209-21.

Su F, Mukherjee S, Yang Y, Mori E, Bhattacharya S, Kobayashi J, Yannone SM, Chen DJ, Asaithamby A. 2014. Nonenzymatic role for WRN in preserving nascent DNA strands after replication stress. Cell Rep. 9:1387-401.

Sugimoto N, Kitabayashi I, Osano S, Tatsumi Y, Yugawa T, Narisawa-Saito M, Matsukage A, Kiyono T, Fujita M. 2008. Identification of novel human Cdt1-binding proteins by a proteomics approach: proteolytic regulation by APC/CCdh1. Mol Biol Cell. 19:1007-21.

Sugimoto N, Yoshida K, Tatsumi Y, Yugawa T, Narisawa-Saito M, Waga S, Kiyono T, Fujita M. 2009. Redundant and differential regulation of multiple licensing factors ensures prevention of re-replication in normal human cells. J Cell Sci 122:1184-91.

Syljuåsen RG, Sørensen CS, Hansen LT, Fugger K, Lundin C, Johansson F, Helleday T, Sehested M, Lukas J, Bartek J. 2005. Inhibition of human Chk1 causes increased initiation of DNA replication, phosphorylation of ATR targets, and DNA breakage. Mol Cell Biol 25:3553-62.

Takara TJ, Bell SP. 2011. Multiple Cdt1 molecules act at each origin to load replication-competent Mcm2-7 helicases. EMBO J. 30: 4885-96.

Takata K, Reh S, Tomida J, Person MD, Wood RD. 2013. Human DNA helicase HELQ participates in DNA interstrand crosslink tolerance with ATR and RAD51 paralogs. Nat Commun. 4:2338.

Takeda DY, Parvin JD, Dutta A. 2005. Degradation of Cdt1 during S phase is Skp2-independent and is required for efficient progression of mammalian cells through S phase. J Biol Chem 280: 23416-23.

Tanaka S, Umemori T, Hirai K, Muramatsu S, Kamimura Y, Araki H. 2007. CDK-dependent phosphorylation of Sld2 and Sld3 initiates DNA replication in budding yeast. Nature 445:328-32.

Tanaka T, Umemori T, Endo S, Muramatsu S, Kanemaki M, Kamimura Y, Obuse C, Araki H. 2011. Sld7, an Sld3-associated protein required for efficient chromosomal DNA replication in budding yeast. EMBO J. 30:2019-30.

Tanny RE, MacAlpine DM, Blitzblau HG, Bell SP. 2006. Genome-wide analysis of re-replication reveals inhibitory controls that target multiple stages of replication initiation. Mol Biol Cell. 17:2415-23.

Tardat M, Brustel J, Kirsh O, Lefevbre C, Callanan M, Sardet C, Julien E. 2010. The histone H4 Lys 20 methyltransferase PR-Set7 regulates replication origins in mammalian cells. Nat Cell Biol. 12:1086-93.

Tatsumi Y, Sugimoto N, Yugawa T, Narisawa-Saito M, Kiyono T, Fujita M. 2006. Deregulation of Cdt1 induces chromosomal damage without rereplication and leads to chromosomal instability. J Cell Sci. 119:3128-40.

Teer JK, Dutta A. 2008. Human Cdt1 lacking the evolutionarily conserved region that interacts with MCM2-7 is capable of inducing re-replication. J Biol Chem. 283:6817-25.

Tercero JA, Diffley JF. 2001. Regulation of DNA replication fork pro- gression through damaged DNA by the Mec1/Rad53 checkpoint. Nature 412:553–557

Thangavel S, Berti M, Levikova M, Pinto C, Gomathinayagam S et al. 2015. DNA2 drives processing and restart of reversed replication forks in human cells. J Cell Biol 208:545–562.

Thomer M, May NR, Aggarwal BD, Kwok G, Calvi BR. 2004. Drosophila double-parked is sufficient to induce re-replication during development and is regulated by cyclin E/CDK2. Development. 131:4807-18.

Ticau S, Friedman LJ, Ivica NA, Gelles J, Bell SP. 2015. Single-molecule studies of origin licensing reveal mechanisms ensuring bidirectional helicase loading. Cell. 161:513-25.

Tognetti S, Riera A, Speck C. 2015. Switch on the engine: how the eukaryotic replicative helicase MCM2-7 becomes activated. Chromosoma. 124:13-26.

Toledo LI, Altmeyer M, Rask MB, Lukas C, Larsen DH, Povlsen LK, Bekker-Jensen S, Mailand N, Bartek J, Lukas J. 2013. ATR pro- hibits replication catastrophe by preventing global exhaustion of RPA. Cell 155:1088–1103

Trenz K, Errico A, Costanzo V. 2008. Plx1 is required for chromosomal DNA replication under stressful conditions. EMBO J 27:876-85.

van Deursen F, Sengupta S, De Piccoli G, Sanchez-Diaz A, Labib K. 2012. Mcm10 associates with the loaded DNA helicase at replication origins and defines a novel step in its activation. EMBO J 31:2195-206.

Vassilev A, Lee CY, Vassilev B, Zhu W, Ormanoglu P, Martin SE, DePamphilis ML. 2016. Identification of genes that are essential to restrict genome duplication to once per cell division. Oncotarget. 7:34956-76.

Vaziri C, Saxena S, Jeon Y, Lee C, Murata K, Machida Y, Wagle N, Hwang DS, Dutta A. 2003. A p53-dependent checkpoint pathway prevents rereplication. Mol Cell 11:997-1008.

Vermeulen L, Snippert HJ. 2014. Stem cell dynamics in homeostasis and cancer of the intestine. Nat Rev Cancer. 14:468-80.

Walter D, Hoffmann S, Komseli ES, Rappsilber J, Gorgoulis V2, Sørensen CS. 2016. SCF(Cyclin F)-dependent degradation of CDC6 suppresses DNA re-replication. Nat Commun. 7:10530. doi: 10.1038/ncomms10530.

Watson LA, Goldberg H, Bérubé NG. 2015. Emerging roles of ATRX in cancer. Epigenomics. 7:1365-78.

Wiese C, Dray E, Groesser T, San Filippo J, Shi I, Collins DW, Tsai MS, Williams GJ, Rydberg B, Sung P, Schild D. 2007. Promotion of homologous recombination and genomic stability by RAD51AP1 via RAD51 recombinase enhancement. Mol Cell. 28:482-90.

Wilson MA, Kwon Y, Xu Y, Chung WH, Chi P, Niu H, Mayle R, Chen X, Malkova A, Sung P, Ira G. 2013. Pif1 helicase and Polδ promote recombination-coupled DNA synthesis via bubble migration. Nature 502:393-6.

Wohlschlegel JA, Dwyer BT, Dhar SK, Cvetic C, Walter JC, Dutta A. 2000. Inhibition of eukaryotic DNA replication by geminin binding to Cdt1. Science. 290:2309-12.

Wu L, Davies SL, Levitt NC, Hickson ID. 2001. Potential role for the BLM helicase in recombinational repair via a conserved interaction with RAD51. J Biol Chem 276:19375-81.

Wu C, Orozco C, Boyer J, Leglise M, Goodale J, Batalov S, Hodge CL, Haase J, Janes J, Huss JW 3rd, Su AI. 2009. BioGPS: an extensible and customizable portal for querying and organizing gene annotation resources. Genome Biol 10: R130.

Xouri G, Lygerou Z, Nishitani H, Pachnis V, Nurse P, Taraviras S. 2004. Cdt1 and geminin are down-regulated upon cell cycle exit and are over-expressed in cancer-derived cell lines. Eur J Biochem. 271:3368-78.

Yang VS, Carter SA, Hyland SJ, Tachibana-Konwalski K, Laskey RA, Gonzalez MA. 2011. Geminin escapes degradation in G1 of mouse pluripotent cells and mediates the expression of Oct4, Sox2, and Nanog. Curr Biol. 21:692-9.

Yeeles JT, Deegan TD, Janska A, Early A, Diffley JF. 2015. Regulated eukaryotic DNA replication origin firing with purified proteins. Nature. 519:431-5.

Yellajoshyula D, Patterson ES, Elitt MS, Kroll KL. 2011. Geminin promotes neural fate acquisition of embryonic stem cells by maintaining chromatin in an accessible and hyperacetylated state. Proc Natl Acad Sci U S A. 108:3294-9.

Yekezare M, Gómez-González B, Diffley JF. 2013. Controlling DNA replication origins in response to DNA damage - inhibit globally, activate locally. J Cell Sci. 126:1297-306.

Ying S, Hamdy FC, Helleday T. 2012. Mre11-dependent degradation of stalled DNA replication forks is prevented by BRCA2 and PARP1. Cancer Res. 72:2814-21.

Yuan J, Ghosal G, Chen J. 2009. The annealing helicase HARP protects stalled replication forks. Genes Dev 23:2394-9.

Zegerman P, Diffley JF. 2007. Phosphorylation of Sld2 and Sld3 by cyclin-dependent kinases promotes DNA replication in budding yeast. Nature 445:281-5.

Zegerman P, Diffley JF. 2010. Checkpoint-dependent inhibition of DNA replication initiation by Sld3 and Dbf4 phosphorylation. Nature 467:474-8.

Zeman MK, Cimprich KA. 2014. Causes and consequences of replica- tion stress. Nat Cell Biol 16:2–9

Zellweger R, Dalcher D, Mutreja K, Berti M, Schmid JA, Herrador R, Vindigni A, Lopes M. 2015. Rad51-mediated replication fork reversal is a global response to genotoxic treatments in human cells. J Cell Biol 208:563-79.

Zhang Y, Shi CC, Zhang HP, Li GQ, Li SS. 2016. MLN4924 suppresses neddylation and induces cell cycle arrest, senescence, and apoptosis in human osteosarcoma. Oncotarget. 7:45263-45274.

Zhong W, Feng H, Santiago FE, Kipreos ET. 2003. CUL-4 ubiquitin ligase maintains genome stability by restraining DNA-replication licensing. Nature. 423:885-9.

Zhong Y, Nellimoottil T, Peace JM, Knott SR, Villwock SK, Yee JM, Jancuska JM, Rege S, Tecklenburg M, Sclafani RA et al. 2013. The level of origin firing inversely affects the rate of replication fork progression. J Cell Biol 201: 373-383.

Zhu L, Skoultchi AI. 2001. Coordinating cell proliferation and differentiation. Curr Opin Genet Dev. 11:91-7.

Zhu W, Chen Y, Dutta A. 2004. Rereplication by depletion of geminin is seen regardless of p53 status and activates a G2/M checkpoint. Mol Cell Biol 24:7140-50.

Zhu W, DePamphilis ML. 2009. Selective killing of cancer cells by supression of geminin activity. Cancer Res 69:4870-7.

Zhu W, Dutta A. 2006. An ATR- and BRCA1-mediated Fanconi anemia pathway is required for activating the G2/M checkpoint and DNA damage repair upon rereplication. Mol Cell Biol. 26:4601-11.

Zhu W, Lee CY, Johnson RL, Wichterman J, Huang R, DePamphilis ML. 2011. An image-based, high-throughput screening assay for molecules that induce excess DNA replication in human cancer cells. Mol Cancer Res. 9:294-310.

Zielke N, Edgar BA, DePamphilis ML. 2013. Endoreplication. Cold Spring Harb Perspect Biol. 5:a012948.

ANNEX I

ANNEX I – PUBLICATIONS

Boskovic J, Bragado-Nilsson E, Saligram Prabhakar B, Yefimenko I, Martínez-Gago J, **Muñoz S**, Méndez J, Montoya G. 2016. Molecular architecture of the recombinant human MCM2-7 helicase in complex with nucleotides and DNA. Cell Cycle.15: 2431-40.

Muñoz S, Méndez J. 2017. DNA replication stress: from molecular mechanisms to human disease. Chromosoma. 126:1-15.

Muñoz S*, Búa S*, Rodríguez-Acebes S, Megías D, Ortega S, de Martino A, Méndez J. 2017. *In vivo* DNA re-replication elicits lethal tissue dysplasias. Cell Reports, *accepted for publication.*